60

ANALYSIS OF PLATINUM, PALLADIUM AND RHODIUM AT TRACE CONCENTRATIONS IN LEAD USING THE TIME RESOLVED SPARK EMISSION TECHNIQUE CALLED SAFT

A thesis submitted to the
UNIVERSITY OF CAPE TOWN
in fulfillment of the requirements for the degree of
MASTER OF SCIENCE
in
CHEMISTRY

by
L.P. SUNDQUIST (née HOWDEN),
B.Sc.
UNIVERSITY OF NATAL

Department of Chemistry
University of Cape Town
Rondebosch
7700
South Africa

March 2000

CONTENTS.

ACKNOWLEDGEMENTS.

The author would like to sincerely thank

- her supervisor, Prof. Klaus R. Koch, for his expert guidance, advice, encouragement, patience and support throughout the duration of this work which was done part-time under difficult circumstances,

- Mr. Dane Gerneke, for his willingness to give expert assistance for the electron microscope study,

- Dr. Candy Lang, for her willingness to assist in doing tests for hardness of samples,

- Angelique and Lize, for the many hours assisting with sample preparation and reading,

- the management of Impala Platinum Limited, not only for their financial backing, but their interest and continued confidence in the author's self-development.

This document was written and typed by the author.

ABSTRACT.

The fire assay technique may be used to extract noble metals from platinum bearing ores. It allows for the use of relatively large quantities of ore sample from which trace quantities of noble metals are concentrated. The fire assay with lead as the collector is one such procedure, where preconcentration of the noble metals allows for direct analysis of the noble metals in lead. The samples may be prepared by pyrochemically treating the ore sample with a litharge-based flux. These lead buttons require an homogenising remelt and rapid cast before direct determination of the noble metals can be made using a time resolved form of spectroscopy called SAFT, or *Spark Analysis for Traces*. The unique characteristics of this technique is that immediately after the electrical spark discharge has taken place radiation from atomic species continues and is termed *after-glow*. Special electronic techniques are required to observe this phenomenon as it takes place in microseconds. By studying the emission characteristics of various spectral wavelengths it is possible to determine the time at which the photomultiplier measures the atomic radiation, and not the background radiation. The atomic emission line to background ratio is thus improved and hence precision and limits of detection.

Initial investigations into the SAFT analysis of platinum, palladium and rhodium using synthetic standards prepared from pure noble metals and lead revealed an analytical method of great promise. However the method failed when applied to real ore samples for several reasons.

The SAFT analysis is particularly sensitive to the effects due to changes of the matrix of the lead depending on the type of sample used to prepare the lead buttons. Corrections for these effects could not be applied as preparation of matrix matched standards also failed.

Another serious problem experienced with the SAFT technique was the inherent insensitivity of the selected platinum wavelengths together with high background emissions. The platinum atomic emission to background ratio was thus poor, and hence scientifically inappropriate practice to measure platinum in lead under these circumstances. The most sensitive platinum emission wavelength could not be used because corrections for a spectral interference from nickel could not be applied. A certain portion of base metals are collected in the lead buttons along with the noble metals during the fusion process, and since nickel is present in all ore samples associated with platinum group metals the presence of nickel and platinum together in lead after collection is inevitable.

Because of the nature of the ore samples used in the investigations, the concentration range of platinum, palladium and rhodium in lead even after preconcentration using fire assay, was very limited, and attempts to create calibrations using only these samples proved unsuccessful. Additional standards prepared from different ore samples were used to extend the concentration ranges of the calibrations, however this also proved to be of no use as the different matrices of these samples detracted from any possibility of defining an accurate calibration curve.

The problem of creating a useful calibration was compounded because of less than ideal confidence limits for the concentration values of platinum, palladium and rhodium to be used for SAFT calibration standards. These values were determined by the alternative fire assay technique using nickel sulfide as the collector of the noble metals.

Although palladium and rhodium atomic emissions were found to be significantly more sensitive than platinum emissions, and the background emissions were close to zero, useful calibrations could not be achieved as these metals were also found to be sensitive to matrix changes of the lead.

Studies of the structure of the lead buttons using electron microscopy showed there was variability of the lead matrix from button to button. Inconclusive evidence was found regarding homogeneity of the lead matrix within any single button. Tests to show a relationship between the physical hardness of the lead buttons and the base metal content were also inconclusive. However, the hardness of a lead button was found to have a significant depressing effect on the emissions of platinum, palladium and rhodium.

A technique in which great interest was shown because initial testwork held promise of success of introducing a new rapid method of analysing noble metals in their absolute form has failed for the application of trace analysis of platinum, palladium and rhodium in lead. The reasons are mainly due to the inherent insensitvity of platinum, and the sensitivity of all three metals to matrix changes of the lead due to the nature of the ore samples.

The traditional and currently practiced classical methods are unlikely to disappear from laboratory manuals in the mining industry. These methods can be binding by government legislation and even economic restrictions. Another reason is that there is resistance to change. However no one analytical method can ever be relied upon as being universally applicable. Limitations due to optimum concentration range and susceptibility to interferences will always demand an alternative method of analysis. Instrumental methods are more cost effective, less liable to human error and more readily adaptable to on-line control of plant operation than the corresponding classical methods. On-line control is assuming greater importance as plant operation becomes more sophisticated, and as more strenuous efforts are made to improve efficiency.

1.2. Fire assay methods commonly used for platinum group metal analysis.

1.2.1. Fire assay using lead as the better collection medium.

The first operation in making an assay is to take ore samples that must be typical and representative in all respects of the ore being mined. The samples may be selected either by hand, or preferably, automatically. Each sample is assayed separately. If the assay determinations of the ore sample are within 10% (relative) agreement, the sampling is taken as correct and the average of the assays constitutes the final assay.

The fire-assay method utilizes heat and suitable fluxes to separate the metal from gangue (worthless material) in the ore. A sample is blended with a flux mixture containing varying amounts of litharge (lead monoxide), silica, soda ash, borax, and carbon usually in the form of flour or charcoal.[8] The blended material is fused at about 1200°C for approximately one hour during which time the flux combines with the gangue to form a fluid slag and the litharge in the flux is reduced to minute globules of lead. As the lead globules fall through the molten mass, they collect the particles of precious metal and coalesce into a button at the bottom of the crucible. The entire molten mass is poured into an iron mould and cooled. The mass settles into two distinct layers, a top layer of slag which when cooled can be chipped away, and a bottom layer consisting of a lead alloy "button". This button is assumed to contain all the platinum group metals and gold and silver originally present in the ore sample.[9] For effective collection the composition of the flux, the furnace temperature and its rate of increase must be optimised. The determination of the optimum flux composition requires some knowledge of the ore type and an understanding of the principles of pyrochemistry.[10, 11]

The process of removing the lead from the alloy button leaving the platinum group metals and gold in a pure state is termed *cupellation*. This step is based on the fact that when an alloy of these metals and lead is heated in the presence of air, lead monoxide or litharge is formed. The alloy button is placed in an open, porous container called a cupel, which absorbs the litharge that forms during the heating. Air is forced past the heated cupel at approximately 1050°C until all the litharge is absorbed, and the mass of metal remaining contains only the precious metals. The proportion of individual precious metals will depend on the type of sample, the interelement proportions of the metals in the ore and the pyrometallurgical conditions. Just before the last traces of lead are removed, the bead changes color, darkening and then finally brightening, thereby indicating the completion of the operation. The cupel is removed from the furnace and cooled, and the bead is cleaned of any foreign particles. In the case of gold the bead is weighed and treated by wet chemical methods to determine the gold content and hence the grade of the ore. For the determination of platinum group metals the beads, also known as *prills*, must be treated differently because of their different composition.

The platinum group metal prills are exposed to high temperature cupellation at 1350°C for several hours during which time pure lead is added in small quantites at regular intervals to wash out impurites such as silver. After cooling, the resultant prill containing platinum group metals and gold is available for measurement either by simply obtaining the prill mass, or by dissolving the prill and analysing the solution.[12]

The lead button, low temperature cupellation prill or high temperature cupellation prill may be analysed for platinum group metal content. The routine procedure is to measure the mass of the high temperature cupellation prill to report total platinum group metals and gold. This method is preferable because it is rapid and sensitive to low concentrations. However all the platinum group metals and gold are subject to varying degrees of losses. Such losses occur to the slag, to the crucible and cupel surfaces, and by volatilisation. The extent of the losses of the individual metals differs markedly such that 98 to 100%($^{m}/_{m}$) of the osmium and ruthenium are volatilised as tetroxides, and 50 to 60%($^{m}/_{m}$) of iridium and 0 to 10%($^{m}/_{m}$) of platinum, palladium, rhodium and gold are lost.[4] A number of factors influence the degree of loss such as the presence of base metals, ratios of the individual precious metals, quantity of silver, size of prill, cupellation temperature and time.

For most plant samples analysed within a laboratory, these factors can be assumed to be reasonably constant, so that it has been possible to apply a constant empirical correction factor to the mass measurement of the prill to obtain an accurate value of the total platinum group metals and gold. The correction factor can only accurately be established by relating a large number of uncorrected prill masses to known values in the original ore samples obtained by chemical analysis. Usually therefore these factors are applicable to routine plant samples in production laboratories only. Although constant over a period of time within a laboratory, they can vary between laboratories.

The reproducible formation of assay prills depends on the concentration of noble metal present in the lead button after fusion. If the content of noble metals in the lead button is kept approximately the same for every assay by adjusting the sample mass used for pre-concentration, then the cupellation stages where lead is separated from the noble metals can be kept reasonably constant and therefore also the losses of noble metals during prill formation. In practice there are small variations in the noble metal concentrations in samples of the same type. Certain sample types contain such low quantities of noble metals that the maximum amount of sample which can be tolerated by the pre-concentration step of fusion will not yield the desired prill mass.

Ideally if every assay could have the same metal content in the lead after fusion then the fire assay method could confidently be used to monitor trends in ore grades. In reality it is questionable as to the usefulness of the fire assay correction factors as they can easily become erroneous if there are changes either in the ore itself or its processing. Some of these problems are overcome in practice by the huge numbers of samples analysed. Since there is no other analytical method which can be used as a comparative technique to analyse the same large population of samples, there is some doubt as to the validity of the assay measurements.

1.2.2. Fire assay using nickel sulphide as the collection medium.

Because of the difficulty in determining the platinum group metals in lead buttons and because of losses during high temperature cupellation, an alternative method of fire assay collection is typically practiced. Noble metals are naturally associated with nickel and copper sulfides. Methods have successfully been developed where fusion of nickel carbonate in combination with borax, sulfur, silica and sodium carbonate has been used to obtain full collection of the noble metals.[13] The fusion takes place at 1100°C to 1300°C for about an hour after which the nickel sulfide melt is allowed to cool in a mould. The slag can be removed from the button either to be discarded or retained for a second fusion. Where losses could occur during the collection process, for instance due to high concentrations of noble metals in the sample, fusion of the slag obtained from the first fusion with a further quantity of nickel carbonate flux will recover possible losses.[14] The nickel sulfide buttons may be combined or treated separately. A fine powder is obtained after grinding the solid nickel sulfide buttons in a mill. This is then treated with a mixture of hydrochloric acid and ammonium chloride, so that the sample dissolves while the platinum group metal sulfides and gold remain insoluble which are then collected by filtration. The residue is dissolved under severe conditions using chlorine at high pressure and temperature. Measurement of individual metals can be obtained in the final solution using spectroscopic techniques.[15] The sample preparation can take several days depending on the availability of equipment and the number of samples to be analysed.

1.3. Development of the spectroscopic analysis technique known as *Spark Analysis For Traces.*

A modern approach to evaluate the individual platinum group metals, other than using fire assay and its correction factors, is to allow each metal to be determined independently using spectroscopic means. Modern technology such as inductively-coupled plasma atomic emission and atomic absorption require the sample to be in solution so that measurements can be obtained either simultaneously or sequentially.[16] The complexity of the many dissolution techniques and separation of the metals make the process of obtaining a solution suitable for measurement lengthy, difficult and sometimes hazardous, such as has been described for the nickel sulfide method. Emission measurements can be subject to errors such as spectral interferences from other elements present in the solution and are also dependent on the concentrations of analyte in solution which is determined by the effectiveness of noble metal pre-concentration in samples having low concentrations.

Other techniques such as X-ray fluorescence where no sample dissolution is necessary can be useful but is limited to samples having percentage levels of noble metal which would be sufficient to produce radiation which can be practically and meaningfully measured. Problems with this technique can also arise depending on other elements which may be present in the sample.[17]

Direct current arcs have been used for many years for atomic emission spectroscopy. A portion of the sample is evaporated and its high temperature causes atoms to be excited. Temperatures generated by direct current arc are in the order of 5000°C depending on the cathode material, current and gas medium. Because of the quantity of material consumed during excitation, the method is very sensitive and can even be used for solutions of precious metals which have been evaporated onto an inert discharge medium such as graphite. However precision was never very good because of the variability of each discharge.[18]

The spark was later developed by charging a capacitor to a certain voltage, then allowing it to discharge between two electrodes, one of which is the sample. The discharge characteristics are defined by the voltage, capacitor, the resistance and the inductance. This produced high oscillatory voltage. Depending on the discharge parameters, gas discharge temperatures of 5000°C to 7000°C were generated. However electron temperatures of 20K to 40K were common depending on capacitance, voltage, inductance and resistance. These high electron temperatures cause high backgrounds (bremsstrahlung) normally associated with spark emission spectroscopy. The analytical characteristics of these sparks give poorer sensitivity than arcs, but better precision because discharge parameters can be controlled. Interelement effects and poor line to backgound ratio are other disadvantages of spark emissions.[19, 20]

One of the recent developments technologically is the analysis of precious metals using an advanced electronically controlled spark emission source, called *SAFT*, an acronym for *Spark Analysis For Traces*.[21] The sample for analysis must be conductive in the form of a metal, making platinum group metals in the lead buttons obtained from the fire assay fusion possibly useful for this technique. Further research into the excitation characteristics of sparks and the emission of spectral lines related to time proved that background radiation due to electron effects follow the discharge closely. Radiation from ions which cause severe non-specific spark background also does. But most importantly, radiation from atomic species continued after the electrical discharge decayed, termed *after-glow*. This phenomenon which takes place in microseconds can be isolated and measured using a rapid switching technique whereby the photomultiplier only "sees" the afterglow radiation. This requires specialised electronic equipment. Thus the "SAFT" is essentially a time resolved form of spark emission spectroscopy. The advantages were to improve the line to background ratio significantly, with improved sensitivity and precision.

SAFT spectrometers were manufactured under direction of K. Slickers by *Spectro* in Germany. Initial calibration tests for low levels of platinum, palladium, rhodium, gold, ruthenium, iridium and silver in pure lead had shown that linear calibrations for platinum, palladium, rhodium, gold and silver were possible at levels of up to 100ppm($^{m}/_{m}$).[22] Ruthenium and iridium were found to migrate in the lead during the slow cooling stage

resulting in heterogeneous distribution of these metals in the analytical sample. Without access to real ore and fire assay laboratory facilities *Spectro* could not carry out further investigations. The first spectrometer was brought to South Africa in 1991. Various platinum producers were approached and motivated parties initiated investigations into appropriate sample preparation using their fire assay facilities and measurement of their samples using the SAFT. The possibility that the noble metals extracted from ores and collected in lead by fire assay could be measured directly for the individual noble metal content required investigation. This analytical procedure would provide a rapid technique of obtaining noble metal measurements that could surpass other analytical methods for these elements. The control of the mineral processing at a plant lies partly with analysis of daily samples taken at strategic sampling points in the process. The noble metal values of these samples indicate the performance of the processing. Action to rectify deviations from the norm can be implemented as soon as the grades are obtained. Hence analysis time is important from a process control point of view, while the actual grade of individual noble metals may be used for accounting across the plant to calculate process efficiency.

Prior to about 1992, there was little communication between different platinum producers for competitive business reasons. This was a distinct disadvantage when it came to validation of analytical measurements and resulted in each producer having its own validation systems using inhouse reference materials. Besides SARM7 international certified standard,[23] no other certified standards of low grade platinum group metal ore existed which could be analysed by different laboratories to establish the validity of their measurements. To certify a bulk material is not only costly but because portions of the sample must be distributed and analysed by different laboratories who usually specialise in platinum group metal analysis meant that competitor platinum producers would be aware of the originator's grade of ore. At that time it was felt that a breach of confidentiality regarding grades would be to the economic disadvantage of the originator of the standard. The immediate problem arising from this situation was that the accuracy of analytical measurements was questionable. Since each platinum producer uses its own methods of analysis and interchange of samples was not possible for business confidentiality, the problem could not easily be resolved.

Being a comparative technique, ie. relating intensity to concentration, the SAFT spectrometer must be "accurately" calibrated. A series of ore samples of known concentrations of platinum group metals must be obtained. The degree of calibration accuracy will depend to a large extent on the quality of the calibration standards. The concentrations must be obtained from an alternative reliable method of analysis. For this purpose the method of nickel sulfide collection for individual platinum group metal analysis was used since the method has been widely accepted as being the most reliable for individual platinum group metal analysis within the platinum industry.[14, 15] Unfortunately sample analysis time is lengthy and the quantity of specialised equipment available for sample preparation in any one laboratory limits the number of determinations that can be carried out at any one time. The collection and dissolution of the noble metals is also hazardous involving molten material at temperatures of over 1000°C, hot concentrated acids, chlorine gas, and hot pressure dissolution vessels. Individual metal measurements can be made simultaneously for each solution using inductively-coupled plasma atomic emission spectroscopy (ICP-AES). There can be considerable overall error of up to 10% (rel) on the determination of any single element, this error attributed in part to the nature of the sample itself, sample preparation and sample measurement. This can be a problem when these concentrations are intended for use in the calibration of the SAFT. In order to compensate for this error, a large number of calibration samples need to be obtained, which is further complicated by the tediousness of the nickel sulfide method, making the task of calibrating the SAFT and evaluating the data obtained from those calibrations more difficult.

The advantages of the SAFT analysis over the traditional fire assay is that individual noble metal concentrations in samples could be obtained in considerably less time. Since individual metal concentrations could be reported the need for fire assay correction factors becomes unnecessary. The opportunity to research these prospects was granted in order to assess the analytical potential of the SAFT from a scientific point of view bearing in mind its practical application. Due to the complexity of the project and the economic value of the different precious

metals, the investigation was limited to platinum, palladium and rhodium. Low concentrations of gold are present in platinum ores but pre-concentration in lead using fire assay did not yield sufficient levels such that gold emissions were below the detection limit of the SAFT and therefore could not be measured.

The specific objective of this study was to examine and evaluate the development and application of the SAFT technique as applicable to "real" samples for a production laboratory in the platinum mining industry, and to determine its advantages and disadvantages.

REFERENCES.

1. J. Moir and G.H. Stanley, "A Textbook of Rand Assay Practice", Chamber of Mines, Johannesburg, 1923.

2. V.S. Dillon, "Assay Practice on the Witwatersrand", Transvaal and Orange Free State Chamber of Mines, Cape Town, 1955.

3. R.J. Adamson, "Gold Metallurgy in South Africa", Chamber of Mines of South Africa, Cape Town, 1972.

4. W.C. Lenehan and R. de L. Murray-Smith, "Assay and Analytical Practice in the South African Mining Industry", The South African Institute of Mining and Metallurgy, Johannesburg, 1986.

5. J. Haffty, L.B. Riley and W.D. Goss, "A Manual on Fire Assaying and Determination of the Noble Metals in Geological materials", U.S. Geological Survey Bulletin 1445, U.S. Government Printing Office, Washington, 1977.

6. R.V.D. Robert, E. van Wyk, R. Palmer and T.W. Steele, *Journal of South African Chemical Institute*, Vol.25, No.3, 179, 1992.

7. G.H. Faye and W.R. Inman, *Analytical Chemist*, Vol.33, 278, 1961.

8. F.E. Beamish and J.C. Van Loon, "Analysis of Noble Metals", Academic Press, New York, 1977.

9. E.E. Bugbee, "A Textbook of Fire Assaying", John Wiley and Sons Inc., New York, 1940.

10. F.E. Beamish and J.C. Van Loon, "Analysis of Noble Metals - Overview and Selected Methods", Academic Press, New York, 1977.

11. J. Haffty, L.B. Riley and W.D. Goss, "A Manual on Fire Assaying and Determination of the Noble Metals in Geological Materials", US Geological Survey Bulletin 1445, US Government Printing Office, Washington, 1977.

12. E. van Wyk, "The determination of platinum, palladium, rhodium and gold in ores and concentrates by the fusion technique with lead as the collector", National Institute for Metallurgy, Report No.2068, Randburg, 1980.

13. R.V.D. Robert, E. van Wyk and R. Palmer, "Concentration of the noble metals by a fire assay technique with nickel sulfide as the collector", National Institute for Metallurgy, Report No.1371, Randburg, 1971.

14. R. Palmer and J.I.W. Watterson, "The recovery of noble metals for analysis. A radiotracer investigation of losses", National Institute for Metallurgy, Report No. 1186, Randburg, 1971.

15. F.M. Russel and A.E. Watson, " The use of an inductively-coupled plasma source in the determination of the precious metals by emission spectroscopy", The South African Institute of Assayers and Analysts, Diamond Jubilee Publication of the Symposium on Assaying and Analytical Techniques for the Determination of Noble Metals, Johannesburg, August, 1979.

16. R.V.D. Robert, E. van Wyk and T.W. Steele, "The effects of various matrix elements on the efficiency of the fire-assay procedure using nickel sulfide as the collector", National Institute for Metallurgy, Report No. 1705, Randburg, 1975.

17. F.E. Beamish, C.L. Lewis and J.C. van Loon, "A critical review of atomic absorption, spectrochemical and X-ray fluorescence methods for the determination of the noble metals"" Talanta, Vol.16, 1969.

18. K. Dixon and T.W. Steele, "Spectrographic analysis for the noble metals present in solutions", National Institute for Metallurgy, Report No. 1219, Randburg, 1971.

19. K.A. Slickers, "Constructive and analytical possibilities of OE-Spectrometers of type Spectrolab and Spectroflame-ICP using fibre optics", Application report 27, *Spectro*, Germany.

20. G. Roberts, "The analysis of precious metals via spark emission spectrometry - an update", International Precious Metals Institute, Johannesburg, 1992.

21. K.A. Slickers, "Automatic Atomic-Emission Spectroscopy", second edition, Giessen, Germany, 1993.

22. *SPECTROGOLD* Operation Manual, *Spectro* Analytical Instruments, Kleve, Germany, 1991.

23. T.W. Steele et al, "Preparation and certification of a reference sample of a precious metal ore", Report No. 1696, National Institute for Metallugy, Randburg, 1975.

CHAPTER 2.

MINERALOGY AND MINERAL PROCESSING OF PLATINUM ORE.

2.1. Mineralogy.

The source of platinum group *metals* (PGM) produced in South Africa is the Bushveld Complex which is a very large layered igneous rock complex. Radiometric dating estimate the complex to be about 1400 million years old. It extends east west from Mpumalanga to the North West Province into Botswana, and north towards Zimbabwe. It is composed of intrusive, layered magma at shallow depths. The magma erupts from the earth's centre due to heat and pressure resulting in mobilisation of elements and their reassembly in concentrated form as new minerals. Sedimentary processes concentrate valuable metals and non-metals according to their specific gravity. In the case of the platinum bearing minerals, the main pipe-like tube separates into different connecting feeders which can be mined as they are close to the surface of the earth.

The mining area around Rustenburg in the North West Province is known as the Pilanesberg Complex. The Merensky Reef which is part of this complex is estimated to contain sixteen million kilograms of noble metals.[1] The noble metals are recovered by the process involving flotation of the base metal and associated noble metal sulfides to produce a low grade concentrate. The concentrate is smelted to remove the iron to form matte which is refined to the final metals using various chemical-winning processes. For the past sixty years or so, most of the platinum produced in South Africa has come from the Merensky Reef.

Below the Merensky Reef (1200m deep) and running roughly parallel to it lie several chromitite seams (1300m deep). In geological terms chromitite is chromite with inclusions of varying amounts of silicates. Chromite has the empirical composition $FeO.Cr_2O_3$, which is a complex spinel where chromium may be substituted with aluminium and iron with magnesium. One of the chromitite seams is the Upper Chromitite layer or UG2 layer of the Complex. The estimated reserves in this seam are about 24 million kilograms of PGM. Exploitation of this ore only began recently in the early 1980's because generally, although not always, the UG2 contains less PGM, copper and nickel, but more chromite than Merensky Reef. Chromite could be a problem with smelting the PGM but it could also provide a valuable by-product to offset the loss of revenue that might accrue from the recovery of copper and nickel in Merensky ore. Also, UG2 ore is easy to mine on existing mines as the shafts are already sunk so further development is relatively inexpensive.

Quantitative data on the types, volume distribution and mode of occurrence of the platinum group *minerals* present in the Merensky Reef, and the UG2 chromitite layer has been recorded.[2, 3] The generalised platinum group mineralogy at mines in the Rustenburg area is given in Table 2.1 where the distribution by volume (as percent) of each mineral determined by electron microprobe analysis is shown.

Table 2.1. The percentage volume distribution of discrete platinum group mineral categories for Merensky and UG2 Reefs at Rustenburg.

Mineral name	%(v/v) Distribution of Reef type	
	Merensky*	UG2
Pt_3Fe alloys and intergrowths	1.7	0.2
Electrum AuAg	3.3	
PtPd sulfides	80.9	84.9
Laurite $Ru(Os,Ir)S_2$	5.2	10.2
Sperrylite $PtAs_2$	6.0	1.2
PtPd tellurides	2.6	0.2
Rh sulfides		3.3

*There is no account of the remaining 0.3%(v/v) of the total distribution for the Merensky Reef.

Platinum group minerals are either enclosed or attached to base metal sufides or chromites. If they are enclosed they are non-recoverable, but if attached they may be recovered. The estimated platinum group mineral associations for Merensky and UG2 Reef are shown in Table 2.2.

Table 2.2. Platinum group mineral associations as volume (percent) distribution for Merensky and UG2 Reefs.

Platinum group mineral associations	%(v/v) Distribution of Reef type	
	Merensky	UG2
Association with base metal sulfides	97	84
Association with silicates	3	11
Association with chromite	0	5

Therefore for mines in the Rustenburg area 97%(v/v) of the platinum group minerals of the Merensky Reef, and 89%(v/v) of the same minerals of UG2 Reef are probably recoverable.

If one depicts the cross-section of a magma feeder (Fig.2.1), the platinum which is extractable is that which is sulfidic. Platinum in alloys with iron cannot be extracted using conventional means.

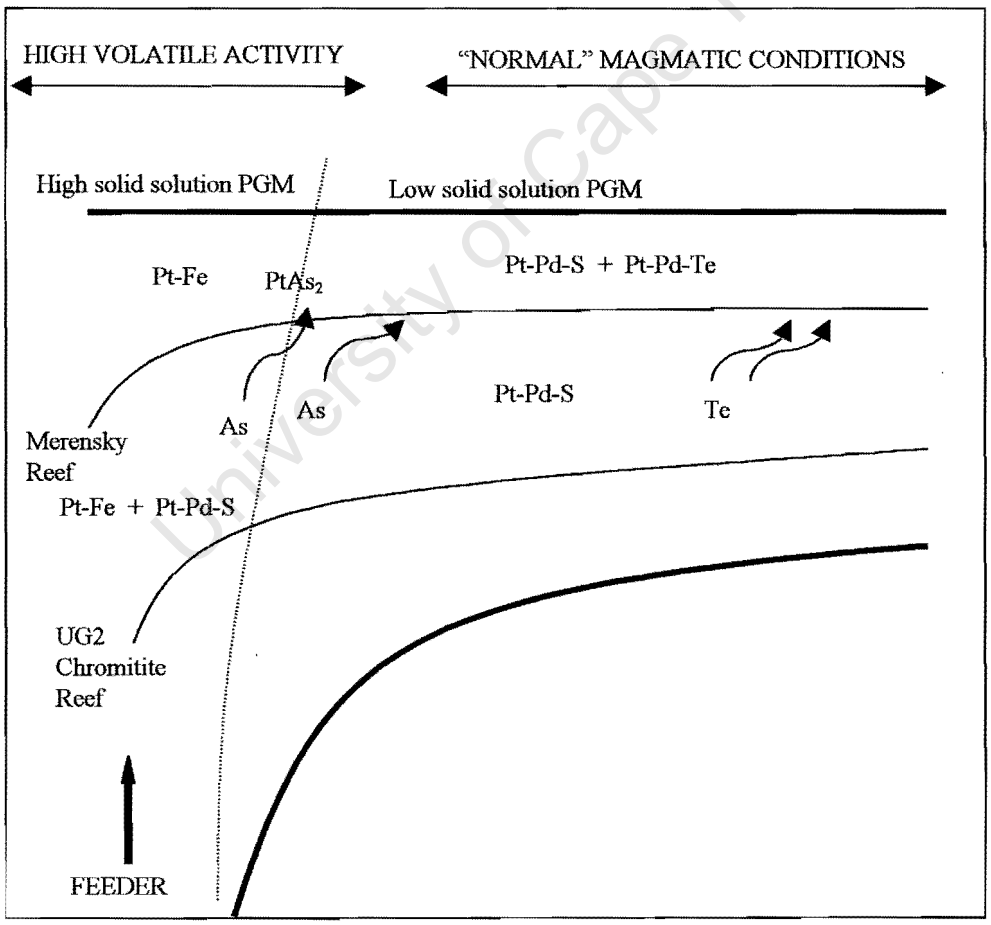

Fig.2.1. Diagram showing the distribution of platinum group minerals in a cross-section of a magma feeder.[2]

Arsenides and tellurides are associated with reef disturbances (includes potholes). These are also avoided during mining. Their mineralogy changes to such an extent that platinum sulfides are minimally present and platinum-iron alloys predominate.

All these features are important from an analytical perspective, since it is the Merensky and UG2 Reef ores which are processed by chemical flotation in order to pre-concentrate the valuable sulfidic platinum group minerals. The feed ore and products of the flotation process must be sampled and chemically analysed for the PGM, copper and nickel content. Because of the unavoidable changes in the mineralogy of the ore which is mined, one can expect there to be changes to the composition of the material treated by the flotation process from time to time. Very little information has been documented on the composition of Merensky and UG2 ores. The Pilanesburg Complex has unique mineralogy and if research work has been carried out, it probably would not have been published because of confidentiality restrictions within the different platinum mining companies. Technologically there has been limited and outdated equipment to speciate these minerals. However recent extensive work carried out at Gencor Process Research Laboratories has shown the speciation of Merensky ore from the Pilanesberg Complex to be as presented in Table 2.3. The mineral species were determined using an x-ray scanning device combined with a magnification system called *Quantitative Evaluation of Minerals by Scanning Electron Microscope* (QEM*SEM).[4,5]

Table 2.3. Mineral speciation of Merensky ore mined at the Pilanesberg Complex, and the expected mineral migration during the pre-concentration process of flotation.

Mineral content	Composition (approx.)	Minerals contributing to final products
Pyrrhotite	FeS	Sulfidic noble and base metals report to the final concentrate. Relatively small quantities go to the flotation tailings.
Pyrite	FeS_2	
Pentlandite	(FeNi)S	
Chalcopyrite	$CuFeS_2$	
PGM		
Other sulfides		
Feldspar	K, Na, Ca, Ba substituting in $(KAlSi_3O_8)$ or $(CaAl_2Si_2O_8)$	Most of the alumino silicate based minerals will report to the flotation tailings. Some pyroxene, talc and feldspar goes to the concentrate.
Orthopyroxene	Ca, Mg, Fe, Na, Li silicates	
Clinopyroxene	Ca, Mg, Fe, Na, Li silicates	
Talc	$H_2Mg_3(SiO_3)_4$	
Olivine	$(MgFe)_2SiO_4$	
Serpentine	$Mg_3Si_2O_5(OH)_4$	
Chlorite	$(MgFe)_5Al(Si_3Al)O_{10}(OH)_8$	
Micas	K, Li substituting in $K_2O.Al_2O_3.6MgO.6SiO_2.2H_2O$	
Quartz	SiO_2	
Other silicates	$FeCr_2O_4$	
Chromite and other metallic oxides		Chromite mostly reports to the flotation tailings. This is controlled carefully to prevent build-up in the smelter hearths.

The separation of the valuable platinum group minerals and associated base metal sulfides from the waste gangue takes place by chemical flotation. Hence the sulfides will be collected by the froth which floats at the surface of the reagent tank and may be separated as the *concentrate*, while most of the alumino silica based minerals will be chemically depressed and remain unaffected by the frother to be discarded as the waste product termed *flotation tailing*.

In our own laboratory the ore and products from the flotation were analysed by wet chemical means to determine the metal content. The individual platinum group metals were determined using the nickel sulfide collection and pressure dissolution method (Chapter 1, Section 1.2 and Appendix 1, Section 1.4), the resultant solutions being analysed by ICP-AES. The base metal and others were determined using sodium peroxide fusion and acid leach to dissolve the samples, and ICP-AES to measure the metals present in the sample solutions. Typical concentration of some noble metals and base metals are shown in Table 2.4.

Table 2.4. Typical metal content of ore feed, concentrate and tailing samples of Merensky and UG2 ores from the Rustenburg area.

Sample type	ppm ($^m/_m$)				% ($^m/_m$)		
	PGM	Pt	Pd	Rh	Ni	Cu	Cr_2O_3
Merensky ore feed	4.6	2.9	1.3	0.3	0.125	0.062	2.6
Merensky ore concentrate	103	70	31	5	2.58	1.59	0.4
Merensky ore tailing	0.79	0.51	0.26	0.07	0.020	0.008	2.5
UG2 ore feed	3.9	2.4	1.4	0.47	0.029	0.008	19
UG2 ore concentrate	250	150	78	24	0.47	0.15	2.5
UG2 ore tailing	1.01	0.67	0.39	0.14	0.019	0.004	18

2.2. Method of separation and concentration of valuable ore from the gangue.

Metallurgical processes consist of two operations where firstly there is concentration or separation of a metal or metallic compound from the useless waste rock material, or gangue. This is followed by the refining where the metal is produced in a pure or nearly pure state suitable for use.

The waste sample material obtained from the flotation of the ore is the basis on which the research into the assessment of the SAFT as an analytical tool to analyse samples containing low concentrations of platinum group metals was made.

There are two fundamental operations in mineral processing of ore extracted from underground. The valuable minerals are released or liberated from their waste gangue minerals, hence the separation of these values from the gangue as concentrate.

Liberation of the valuable minerals from the gangue is accomplished by *comminution* which involves crushing and if necessary grinding to such a particle size that the product is a mixture of relatively clean particles of mineral and gangue. Fine grinding can lead to the production of very fine untreatable "slime" particles which may be lost to the tailings. Grinding therefore becomes a compromise between high grade concentrates and losses of fine minerals.[6] Therefore an intimate knowledge of the mineralogical assembly of the ore is essential if efficient processing is to be carried out.

The physical method which is used to process platinum ores to concentrate ores is separation using the different surface properties of the minerals.[7, 8] Froth flotation is effected by the degree of affinity of the minerals for air bubbles within the agitated pulp. By adjusting the conditions of the pulp by adding various reagents it is possible to make the valuable minerals aerophilic and the gangue minerals aerophobic. This results in separation by transfer of the valuable minerals to the air bubbles which form the froth floating on the surface of the pulp. The air bubbles can only stick to the mineral particles if they can displace water from the mineral surface, which can only happen if the mineral is to some extent water repellent or hydrophobic. Having reached the surface, the air bubbles can only continue to support the mineral particles if they can form a stable froth, otherwise they will burst and drop the mineral particles. To achieve these conditions it is necessary to use flotation reagents. Collectors (for example xanthates) adsorb on mineral surfaces which render them hydrophobic or aerophyllic and facilitate bubble attachment. Frothers such as cresylic acid maintain a

reasonably stable froth. Copper sulphate as a solution is a regulator and is used to control the flotation process whereby it can either activate or depress mineral attachment to air bubbles and is also used to control the pH of the system.

In practice complete liberation is seldom achieved even if the ore is ground down to the grain size of the desired mineral particles. This happens because the particle containing the mineral sometimes contains a portion of gangue. The particles of "locked" mineral and gangue called *middlings* can only be liberated by further comminution. The degree of liberation refers to the percentage of the mineral occurring as free particles in the ore, in relation to the total content. Ores are ground to an optimum mesh of grind determined by a laboratory to produce an economical degree of liberation. The concentration process is then designed to produce a concentrate consisting predominantly of valuable minerals with an accepted degree of locking with the gangue minerals, and a middlings fraction which may require further grinding to promote optimum release of the minerals. The tailings should be composed mainly of gangue minerals.

Fine liberated valuable mineral particles often report in the middlings and tailings. The technology for treating fine sized minerals is poorly developed. The recovery in the case of the concentration of a metallic ore is the percentage of the total metal contained in the ore that is recovered in the concentrate. A recovery of 80%($^{m}/_{m}$) can be interpreted as 80%($^{m}/_{m}$) of the metal in the ore is recovered in the concentrate and 20% is lost in the tailings. The grade or assay usually refers to the content of the marketable end product in the material. Thus in the case of low grade platinum ores the metal content may be expressed as parts per million (ppm($^{m}/_{m}$))or its equivalent grams per tonne (g/t).

2.3. Sampling.

Metallurgical accounting is an essential feature of all efficient metallurgical operations. Not only is it used to determine the distribution of the various products of a mill, and the values contained in them, but it is also used to control the operations, since the values of recovery and grade obtained from the accounting procedure are indications of process efficiency.

The essential requirements of a good accounting and control system are efficient and representative sampling of the process streams, upon which accurate analyses of the valuable components can be undertaken, and reliable and accurate measurement of the mass flowrate of important flowstreams. Sampling is the means where a small amount of material is taken from the main bulk in such a manner that it is representative of that larger amount. In practice the material is sampled while it is in motion at a point of free fall discharge making a cut at right angles to the stream so that particle size variation or settling out of particles in a pulp can be minimised. When a sample cutter moves continuously across the stream at uniform speed the sample taken represents a small portion of the entire stream. If the cutter moves through the stream at regular intervals it produces incremental samples that are considered representative of the stream at the time the sample was taken. Sampling is dependent on probability, and the more frequently the incremental sample is taken the more accurate the final sample will be. The sampling method devised by Gy[9] is often used to calculate the size of the sample necessary to give the required degree of accuracy. The method takes into account the particle size of the material, the content and degree of liberation of the minerals, and the particle shape. Gy's basic equiprobable sampling model can be written as

$$\frac{M L}{L - M} = \frac{C d^3}{\sigma^2}$$

where M is the minimum weight of sample required (g).
L is the gross weight of material to be sampled (g).
C is the sampling constant characterising the material to be sampled (g cm^{-3}).
d is the dimension of the coarsest fragment in the material to be sampled (cm).
σ^2 is the variance of tolerated sampling error.

In most cases M is small in relation to L and the equation approximates to

$$M = \frac{C d^3}{\sigma^2}$$

The term σ is used to obtain a measure of confidence in the results of the sampling procedure. The relative standard deviation of a normal distribution curve representing the random assay frequency data for a large number of samples taken from the ore is σ and the relative variance is σ^2. The actual variance determined by Gy's equation may differ from that obtained in practice because it is usually necessary to carry out a number of sampling steps in order to obtain the assay sample, and there are also errors in assaying. The practical variance would therefore be the sum of all the other variances.

Overall estimation error = total sampling error + analytical error

$$\sigma^2 = \sigma^2_{\text{sampling}} + \sigma^2_{\text{assay}}$$

The values of $\sigma^2_{\text{sampling}}$ and σ^2_{assay} would normally be small, but could be determined by assaying a large number of portions of the same sample to give σ^2_{assay}, and by cutting a similar number of samples in an identical manner and assaying each one to give $[\sigma^2_{\text{sampling}} + \sigma^2_{\text{assay}}]$.

Gy's equation gives the minimum theoretical weight of sample that must be taken but does not state how the sample is taken. The size of each increment taken in the case of stream sampling and the increment between successive cuts must be such that sufficient weight is recovered to be representative.

REFERENCES.

1. J. Lurie, "South African Geology for Mining, Metallurgical, Hydrological and Civil Engineering", 4th edition, McGraw-Hill, Johannesburg, 1984.

2. E.D. Kinloch, "Regional trends in the platinum group mineralogy of the critical zone of the Bushveld Complex, South Africa", Economic Geology, 1982, Vol. 77, 1328-1347.

3. C.H. McLaren and J.P.R. de Villiers, "The Platinum-Group Chemistry and Mineralogy of the UG-2 Chromitite Layer of the Bushveld Complex", Economic Geology, 1982, Vol. 77, 1348-1366.

4. Confidential report, "Metallurgical data from a QEM*SEM study of Merensky Reef flotation samples, MF2a configuration", Report R08/96-IMR.06, Gencor Laboratories, Mineralogical Services, Johannesburg, 1996.

5. Confidential report, "QEM*SEM characterisation of section 6 Merensky Reef samples, MF1 configuration", Report R23/95-IMR.36, Gencor Laboratories, Mineralogical Services, Johannesburg, 1996.

6. P.W. Overbeek, J.P. Loo and R.C. Dunne, "The development of a concentration procedure for the platinum group metals and chromite from the UG2 Reef of the Bushveld Complex", in proceedings First International Symposium of Precious Metals Recovery, Reno, 1984.

7. K.S. Liddel, L.B. McRae and R.C. Dunne, "Process routes for beneficiation of noble metals from Merensky and UG2 ores", Council for Mineral Technology, Randburg, South Africa, 1985.

8. B.A. Wills, "Mineral Processing Technology", 4th edition, Oxford, New York, etc., Pergamon, 1988.

9. P.M. Gy, "Sampling of Particulate Materials, Theory and Practice", Elsevier, Amsterdam, 1979.

CHAPTER 3.

GENERAL PRINCIPLE OF SPARK EMISSION AND SAFT.

3.1. Atomisation and atomic spectra.

Energy must be supplied to the sample material such that a representative portion may be vaporised at high temperatures and atom excitation can take place. Photons that are released when the excited atoms return to a lower or ground state appear as radiation. This radiation is then examined to determine its spectrum type and characteristics.[1] A selection of spectral lines is made so that the least amount of spectral interference and interelement effects are present.

3.1.1. Atom excitation.

When energy is applied to solid matter it passes through the solid to liquid to gaseous to plasma states. For example, hydrogen is present as the gaseous molecule. When energy is applied to the gas with increasing temperature some molecules are dissociated to atoms ($H_2 \rightarrow 2H$) where the equilibrium is displaced to the right of the equation as the temperature increases.

At higher temperatures an atom may lose an electron as a result of a collision with another atom. Therefore $H \rightarrow H^+ + e^-$ giving rise to a positively charged atom and an electron. With increasing temperature more hydrogen atoms will be ionised. A gas, which in addition to neutral or charged molecules has atoms, ions and electrons such that it is electrically conductive and is known as a plasma. The plasma as a whole is electrically neutral. A conductive gas may be considered a plasma when more than 3% of the particles are electrons or ions.

At 2000K a large number of molecules are dissociated into atoms. At 4000K the proportion of molecules is already low. Positively charged ions and free electrons appear. At 6000K no more molecules are present and the proportion of neutral atoms is already low. From 8000K, not even neutral atoms are present. The gas is completely ionised. Multiple charged ions appear, for example, N^+, N^{++}, N^{+++}. [2]

As the temperature of a gas increases the number of collisions between the constituent particles per unit of time increases. These collisions may be elastic or in-elastic. Electrons having a much lower mass than ions move faster and consequently have more collisions. The temperature is defined as the number of collisions per unit time, so that electrons have a higher temperature than ions or neutral particles. Plasmas thus have two temperatures, namely electron and gas temperature. The lower the temperature, the closer these two temperatures, but the higher, especially where there is an electric potential or a lower total pressure, the further the two temperature deviate. Thermal equilibrium describes the state when electron and gas temperatures are similar.

An atom consists of a positive charged nucleus surrounded by negatively charged electrons moving in fixed orbits. When energy is supplied to an atom the electrons can be raised to a higher orbit and the atom is said to go from the ground state to an excited state. Only fixed excited states are allowed as the atom can take up fixed amounts of energy. When the atom returns to a lower excitation state or the ground state, a fixed amount of energy is released. This energy appears as radiation particles called photons with a fixed wavelength.[3]

Excitation can occur when a material is supplied with thermal, electrical and light energy. The relationship of energy of a photon to wavelength and temperature is [4]

$$E = \frac{h \times c}{\ell}$$

where E = energy of 1 photon (eV)
h = Planck's constant (6.624×10^{-34} Js)
ℓ = wavelength (nm)
c = velocity of electromagnetic radiation in a vacuum (2.99×10^{8} ms^{-1}).

3.1.2. Excitation sources.

3.1.2.1. Excitation using thermal energy.

When an electrical discharge heats the gases in the discharge path a plasma is formed comprising neutral and ionised particles, electrons and photons. Depending on the amount of kinetic energy these particles have, then dissociation, excitation, ionisation and recombination occurs. Since the interacting particles have a wide energy distribution and that any magnitude of excitation energy may be transmitted on impact, the spectra thus generated consist of numerous lines of discrete wavelengths and backgrounds.

3.1.2.2. Excitation using electrical energy.

Electrons are emitted from an incandescent electrode (cathode) and accelerated by an adjustable voltage (0 to 50V) towards a grid and pass through it to move against a low voltage (1V) at the anode. If their energy is sufficient to reach the anode, a current is set up. If this system is in an evacuated glass flask filled with gas, as the voltage is increased at the cathode, the greater the measured current. At a certain voltage depending on the type of gas the current falls again with further increase in electron energy. At a certain voltage the energy of an electron is sufficient to excite an atom on impact so that the electrical energy is converted to electromagnetic radiation so that the electron has no more energy to move against the decelerating voltage.

3.1.2.3. Excitation using light energy.

Energy at specific wavelengths in white light cause excitation that corresponds to discrete differences in permitted energy states in the atomic shell. An absorption spectrum appears at these wavelengths which are absorbed by the atom. Substances can only absorb light at the same wavelength as they are capable of emitting. If a portion of the white light absorbed by a gas is scattered in all directions, then atomic fluorescence occurs. When some substances are irradiated the excited atoms return to the ground state through intermediate energy states so that a fluorescence spectrum is emitted.

3.1.3. Types of spectra.

There are four kinds of spectra which are distinguished by their appearance. These are line, band, absorption and continuous spectra. Line spectra are emitted by atoms or ions. Band spectra are emitted by molecules. Absorption spectra are caused by the absorption of radiation by atoms or molecules. They appear as dark regions in spectral lines or in continuous spectra. Continuous spectra may be unresolved bands of molecular spectra or non-discreet radiation due to recombination processes These spectra are not atom or molecule specific and are produced by free electrons in a plasma which results in continuous radiation with free-free transitions (bremsstrahlung) and with free-bound transitions (combination radiation). In addition to the continuous background spectra there are other forms of specific radiation such as those from molecules, radicals and incandescent particles. The spectral background therefore consists of all these types of radiation as well as unresolved spectral lines.

3.1.3.1. Atomic or line spectra.

Historically the spectra of neutral atoms were called "arc spectra" because they could be emitted in electric arcs. Spectra of ions were called "spark spectra" because spark discharges at high temperatures are necessary for their excitation. Depending on the degree of ionisation a distinction is made between the first, second and so on spark spectrum. The terms arc and spark arose historically based on the excitation sources then known, the

discharge atmosphere being air. Spark discharges with the same energy lead to higher temperatures and under argon metastable states may occur. Hence spark spectra can be excited with arc-like discharges.

3.1.3.2. Molecule or band spectra.

Spectra of molecules consist of groups of many lines lying close together. When observed by low resolution spectrographs luminous bands of unresolved broad lines appear. Grating spectrographs with high dispersion are able to resolve the fine structure of the bands from continuous spectra.

With diatomic molecules there are two types, rotational and vibrational spectra. Rotational bands occur when a molecule with a specific energy rotates. Each time it rotates it loses some energy which being quantified gives out radiation at a specific wavelength. Vibration spectra give these rotational bands at different wavelengths.

Band spectra are present in emission sources at lower temperatures such as arcs and flames. In particular the bands of diatomic molecules give rise to background spectra especially in the visible and ultraviolet range of the spectrum. These contribute undesirable effects in the spectral analysis.

3.1.3.3. Continuous spectra.

Plasma continuous spectra are mainly attributed to recombination of electrons and ions to form atoms and bremsstrahlung, ie. electrons at any energy level losing this energy through non-discreet processes. Hot glowing particles may radiate according to Plank's law to also contribute to a continuum. Intensity increases with rising temperature and is not element or molecule specific. Optically unresolved atomic and molecular spectra, continuous spectra and radiation of incandescent particles determine the spectral background that is responsible for the limit of detection. If the spectral equipment does not give adequate optical resolution, atomic spectra lead to a structured spectral background. Continuous spectra generally lead to an unstructured spectral background.

3.1.4. Spectral characteristics.

3.1.4.1. Width and displacement of spectral lines.

Spectral lines are composed of a range of finite wavelengths resulting from radiation of atoms and molecules in various stages of excitation. The distribution of these wavelengths follows a Gaussian profile and is called a line profile. The width of the spectral line is defined as that width at half the peak or maximum intensity as shown in Fig.3.1. The line shape is characteristic for both emission and absorption and is determined by the following:

i) The motion of the atoms as a result of thermal activity, also known as Doppler broadening.

ii) A shift of the peak maximum known as Doppler shift because of a change in relative velocities such as when the detector moves relative to the radiation source.

iii) Collisions of atoms in the excited state with other particles causing broadening and shifting of the line profile called pressure broadening.

iv) The dispersive and imaging components in a spectrometer which may cause widening of a spectral line such that exit slits are usually set wider than entrance slits.

v) The finite lifetime of the excited state not being the same for all radiating atoms. In practice this effect is negligible.

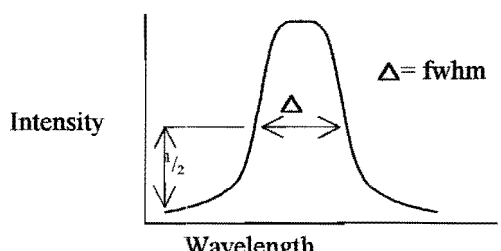

Fig.3.1. Representation of full width at half maximum; Δ= fwhm.

3.1.4.2. Self absorption and self reversal.

If the excited and unexcited atoms around the source of radiation are moving randomly, the radiation propagates freely and the relationship between intensity and concentration is linear.

If groups of unexcited atoms are present between the radiation source and the detector, for example due to temperature gradients at the source resulting in higher concentrations of unexcited atoms in the cooler regions, then the radiation is partly absorbed by these atoms because absorption and emission profiles show the same curve. Absorption is greatest at the centre of the wavelength. Because of the reduced intensity of the central wavelength, the line profile changes and an apparent line broadening of the full width half maximum appears which constitutes self absorption. As the concentration of the element in the sample increases the number of vaporised and unexcited atoms also increases, as well as the number of atoms emerging from the plasma after excitation so that the probability of absorption increases. Intensity and concentration no longer grow linearly with each other and the gradient of the slope gradually decreases. The effect of self absorption on the gradient of a calibration curve is shown in Fig.3.2.

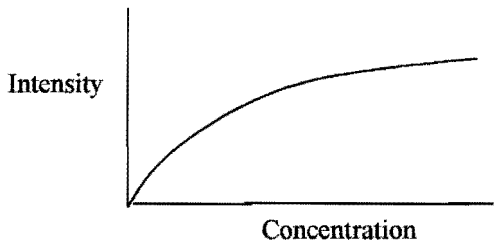

Fig.3.2. Effect of self absorption on the shape of the calibration curve.

With spark discharges in argon, temperatures of many thousands of degrees are reached so the number of ions exceeds that of atoms. The ion lines and atom lines show curved concentrations. Self absorption increases as the particle density of the discharge atmosphere increases.

Self reversal occurs when the intensity of the central wavelength becomes smaller than the intensity to right and left of it, as shown in Fig.3.3. Lines with self absorption characteristics are usually the most sensitive and are generally used only for determining low concentrations.

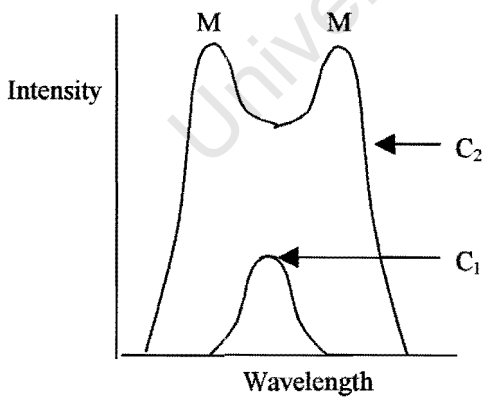

Fig.3.3. Self reversal and apparent increase in full width half maximum. Concentration of $C_2 >> C_1$ and M indicates the self reversal peaks.

3.1.4.3. Spectral interferences, interelement effects, and interferences associated with the sample in the plasma.

Interferences with the analyte lines lead to changes in intensity that must be corrected for before evaluation takes place with the calibration curve.

a) Spectral interferences can arise from the following:

i) Line overlaps causing enhanced intensities.
ii) Changes to the spectral background causing enhanced or reduced intensities.
iii) Stray light causing enhanced intensities.

b) Interelement effects can arise from the sample itself, and the sample and the discharge atmosphere. The effects associated with the *sample* are as follows:
i) Precipitates present in the sample that can change.
ii) Changes may occur in the form of solidification due to differences in vaporisation rate.
iii) Other elements may be present in the base material which may be dissolved or partly or completely precipitated.
iv) Changes due to elements with high vaporisation temperatures which are present in a low vaporisation temperature base material.
v) There may be changes in the vaporisation rate due to changes in vaporisation enthalpy. Due to lowering of the melting point by alloy elements, the energy necessary for vaporisation is reduced. Therefore for a given energy conversion in the discharge gap the quantity of sample material vaporised per discharge is increased which results in increased intensities.
vi) There may be changes in the vaporisation rate due to changes in thermal conductivity. Alloy constituents affect thermal conductivity in different ways. Low thermal conductivity leads to greater localised heating in the burn spot and therefore increased vaporisation of material and increased intensities.

When the analytical line is ratioed to a reference line the effects of changes in vaporisation rates due to changes in enthalpy and thermal conductivity mostly lose their effect on spectrochemical results. This is because the changes in vaporisation rate affect the dissolved analyte to the same extent as the reference.

The effects associated with the *sample and the discharge atmosphere* are as follows:
i) Changes in the type of discharge, that is, diffuse or concentrated, may occur due to presence of oxides in the sample.
ii) Changes in type of discharge due to constituents of the sample and discharge atmosphere other than oxides may occur.

c) Interferences associated with the sample in the plasma.
i) Changes in location of optimum excitation of an atomic emission line in the plasma may occur due to other elements and differences in the imaging of this location in the optics. This is responsible for discrepancies among interelement effects stated in various texts for the same analysis program. Interference in the plasma must present a maximum at some point between the electrodes since it is zero at the electrodes. This effect is lost during analysis where there is uniform radiation from the entire radiation source. Fig.3.4 serves to illustrate this.

ii) Changes in plasma temperature due to other elements with varying ionisation temperatures and resultant changes in excitation probability may also occur. In the presence of elements with low ionisation energy compared to the base element, the plasma temperature drops so that spectral lines with high excitation energy become weaker and those with low excitation energy become stronger. When elements with high ionisation energy compared with the base element are present together, the plasma temperature increases so that the spectral lines with high excitation energy become stronger and those with low excitation energy become weaker. This interference loses its effect on spectrometric results if homologous lines are used as analytical and reference lines.

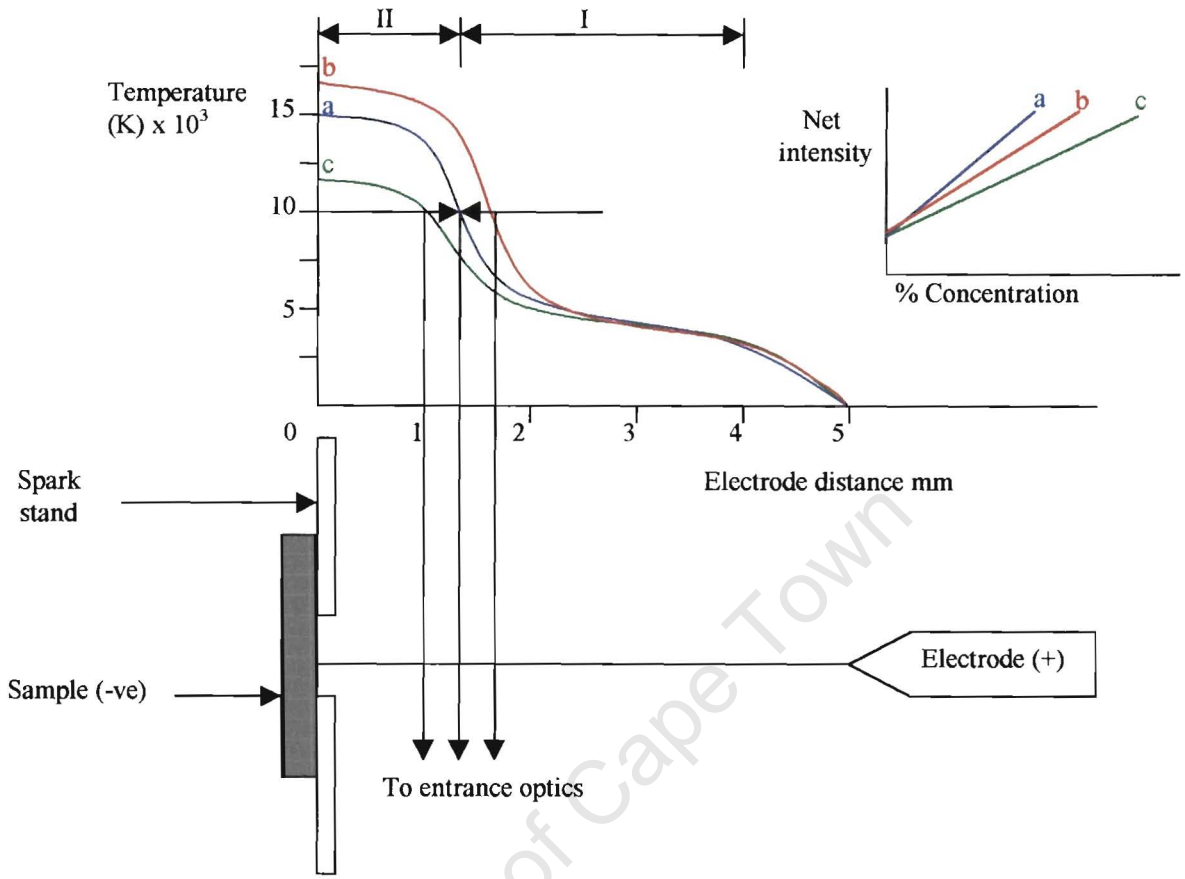

Fig.3.4. Displacement of location of optimum excitation.[4,5] 1=atom lines; 11=ion lines.

3.2. Spark emission.

K. Slickers has described the generation of arcs and sparks in some detail.[6] For ease of reference a summary of the information that is relevant to this research has been presented.

3.2.1. Principle of spark generator with external ignition.

The spark generator is selected for the purposes of
i) elimination of electrical defects;
ii) remelting the sample in the burn spot and establishing homogeneity ending in the steady state;
iii) vaporisation, dissociation, ionisation and excitation in the plasma in order to produce radiation.

Sparks may be generated using an external source of energy such as the mains power supply. Ignition of the spark is achieved by a high voltage low current spark which ionises the distance between the sample and electrode thus making it conductive. A direct current arc can then flow heating the sample such that a radiating metal vapour is created. This process of discharging a direct current arc occurs one hundred to four hundred times a second (100 to 400Hz). The shape of the discharge is said to be "arc like" or "spark like" depending on the peak current amplitude and duration. High amplitude and short duration is described as spark-like, while low amplitude and long duration is arc-like. With spark discharges plasma electron temperatures are higher

than in arc discharges because the power converted in the analysis gap per discharge is greater for spark than arc discharges. Spark discharges give line rich spectra including ion lines, but poorer limits of detection than for arc discharges.

It is primarily the current through the analytical gap that is critical for the efficiency of a spark generator, and to a lesser extent the electrical components by which the current is obtained. It is important that the energy available for each discharge is stabilised.

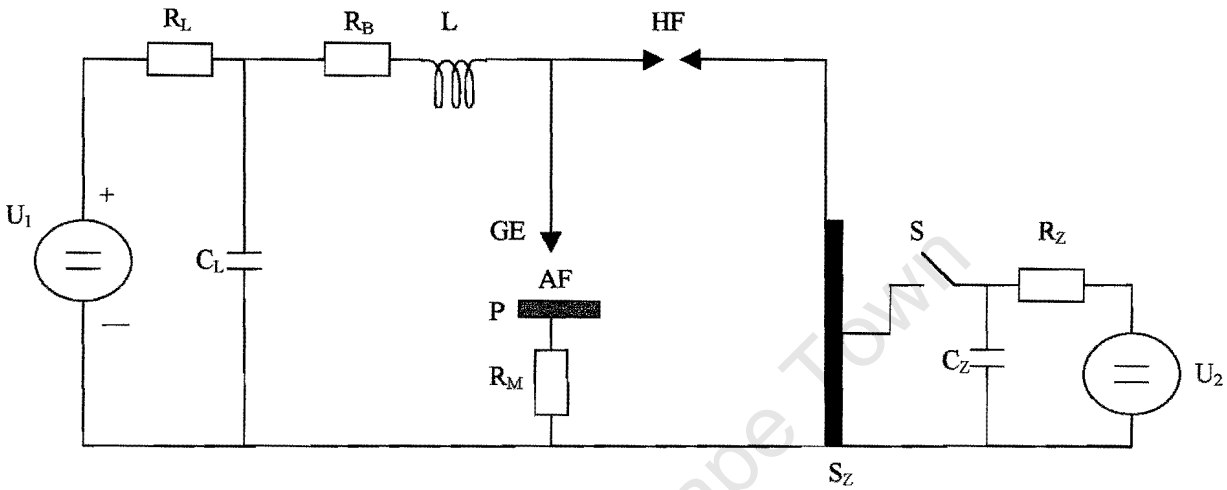

Fig.3.5. Principle of the spark generator with external ignition.
P=sample; GE=counterelectrode; AF=analytical gap; R_M=measuring resistor; C_L=capacitor; U_1 and U_2 = direct current sources; R_L=charging resistor; R_B=discharge resistor; L=inductance; R_Z=ignition resistor; C_Z=ignition capacitor; S=switch; S_Z=ignition coil (Tesla); HF=auxiliary gap.

The principle of the spark generator with external ignition is shown in Fig.3.5. The electrically conductive sample P is placed opposite a counter electrode GE at a distance of about 3mm from the latter. Both electrodes are connected by an induction coil L and resistances R_B and R_L to a direct current source U_1. Another direct current source U_2 charges the capacitor C_Z through the resistance R_Z. As soon as the switch S is closed, C_Z discharges itself through the primary coil of the high voltage ignition coil S_Z. The high voltage (20kV) thus induced on the secondary side of the coil passes through the auxillary gap HF and the analysis gap AF. A capacitor C_L (1 to 20µF) is charged by U_1 at 400 to 1000V through the charging resistor R_L. C_L then discharges itself through R_B, L and AF. The brief ignition spark produces in the analysis gap a small quantity of charged particles so that the latter becomes electrically conductive and thus passes between the two electrodes. Sample material is melted and vaporised.

3.2.2. Characteristics of spark discharge.

An oscillating spark discharge is a spectrochemical radiation source where energy is converted during the spark for a specific time. The energy determines the quantity of electrode material vaporised and thus the total intensity of the spectrum. The spark duration determines the spectral character. The shorter the discharge with constant energy, the more spark-like the spectrum. It is possible to produce arc-like spark discharges with different electrical parameters provided the energy and the duration are constant. Voltage has been varied from 18000V to 700V, and capacitors from 4600µF to 1µF. Continuation downward is limited by the aperiodic limit resistor. Soft spark discharges of long duration can be produced with a high degree of similarity.

The spark characteristic is determined by the supply voltage U and the parameters C_L, R_B, L and AF (refer to Fig.3.5). The lower the R_B and L values selected, the higher the spark current density. Peak current intensities of several hundred amps can be reached. With high values of R_B and L, weak current or soft arc-like sparks are obtained.

The parameters of the oscillating circuit are usually selected so that only half an oscillation appears for an individual spark. The oscillating circuit is aperiodically damped using critical discharge conditions to remove the oscillatory characteristics of the spark, which means that a single pulse of high energy takes place between the counter electrode and the sample and only sample material is evaporated as the full energy of the discharge meets the sample. This is called a uni-polar spark or arc discharge.

Using low voltage sources (at mains voltage) R_B should not be less than a few ohms during the intensity measurement so that it is this and not other resistors in the discharge circuit such as sample size and temperature which determine the current curve.

The working voltages of spark discharge are about 50V and are established by the internal mechanism of the discharge. Spark discharge voltages are current dependent and are only slightly dependent on electrode material. They are dependent on the length of the discharge path (not the same as the electrode gap) and on the working gas.

Hence excitation conditions for specific spectrometric tasks can be indicated by stating the spark energy and duration of the spark discharges. Power converted in the analysis gap per spark discharge is greater than with arc discharge so that plasma temperatures are for a short time higher resulting in spectra are rich in atomic and ionic lines. The precision of spark discharges is considerably improved over arc discharges, but unfortunately spark discharges have poorer detection limits than arc discharges as shown in Table 3.1.

Table 3.1. Analytical characteristics of arc and spark discharges.

Type of discharge	Limit of detection µg/g	Precision %RSD
Arc	0.1 – 1	5 - 10
Low voltage spark	1 – 10	2 – 4
High voltage spark	10 – 100	1 - 2

3.2.2.1. Evaluation of the burn spot.

A spark discharge creates a plasma which contains elements representative of the whole sample. The sample surface is micro-melted in an argon atmosphere during the high energy prespark and before the photomultiplier tubes start measuring radiation. Cooling and recrystallisation occurs rapidly and the surface is uniformly reformed. Thus any crystalline effects caused by the metallurgical history are partially overcome. The discharge is divided into prespark time and sparking. The prespark time is further divided into initial sparking and homogenising time. Mostly inclusions in the sample are attacked during the initial sparking. This leads to diffuse discharges causing low plasma temperatures. They are indicated by white burn spots, no craters in the surface, and very low intensities for the elements.

When all inclusions are eliminated, the intensities of the individual elements increase to the maximum. The time needed to achieve this state varies according to type and quality.

During homogenising a concentrated discharge occurs. The burn spot surface is refined to produce a metallic shiny surface with homogenous distribution of craters, and a deposit of black condensate on the edge of the burn spot. When the homogenising phase is complete the sample is in the stationary spark condition.

Vaporised material is replaced by material originating from deeper areas of the sample. There is a balance between evaporated and replacing material. The homogenous layer is thicker than the dimensions of the inclusions. When homogenising is finished the measurement time begins. The excitation source condition with minimum prespark time is selected. The presence of oxygen in the sample or in the spark area causes oxide formation and has a similar effect as inclusions on the vaporisation of material during the spark process.

The temperature of the plasma is about 5000K to 8000K at the point where the fibre optics are directed to transmit the atomic radiation. Closer to the sample where the temperature is above 10 000K, ionic radiation is emitted.

The intensities of all elements are increased by heating in the burn spot, particularly sulfur. By delaying the start of measurements for one second after switching over the high energy prespark discharge to the low energy measurement discharge, the effect of local heating can be eliminated for all elements except sulfur. Heat dissipation by means of a copper block placed on the reverse side of the sheet does not lead to localised heating which affects the intensities.

There are two types of burn spots derived from diffuse and concentrated discharges. A comparison can be seen in Fig.3.6.

If a metal contains no precipitates there are no preferred points of attack of the spark discharge. Concentrated discharges can be obtained with high purity metal.

In the case of diffuse discharges, the energy is distributed through numerous discharge channels. The cathode attack points are distributed over a wide area, so that numerous small craters less than 1μm deep are produced. Because of the low plasma temperature, the intensity is low.

In the case of concentrated discharges, the energy passes through one discharge channel, so that high temperatures are attained in the plasma and a crater 10μm to 20μm diameter is produced.

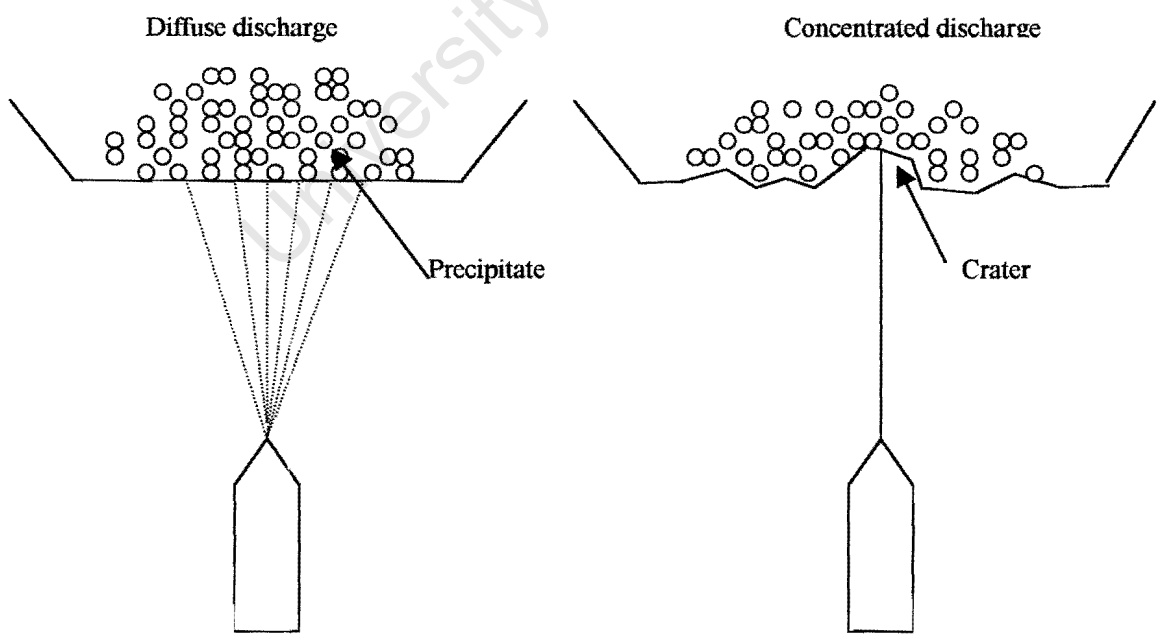

Fig.3.6. Characteristics of diffuse and concentrated discharges.

The characteristics of diffuse and concentrated discharges can be summarised as follows.

Diffuse.	Concentrated.
· Have a number of cathode attacks per discharge (approximately 100 000).	· Has a single cathode attack per discharge.
· Cathode region is attacked by individual discharges (approximately 2mm).	· Cathode region is attacked by individual discharges (approximately 0.02mm).
· Crater diameter approximately 1μm.	· Crater diameter approximately 20μm.
· Quantity of sample vaporised approximately 10ng.	· Quantity of sample vaporised approximately 100ng.

3.2.2.2. Characteristics of burn-off curves.

Atomic emission methods are based on the assumption that vaporisation of the sample constituents is proportional to the average chemical composition. In other words, the plasma composition is proportional to the sample composition. In reality this is not always the case.

Burn-off curves of elements are determined from the beginning of the sparking process by the mechanisms of material removal. Examples of such curves which depend on sample composition are given in Fig.3.7, 3.8 and 3.9.[7]

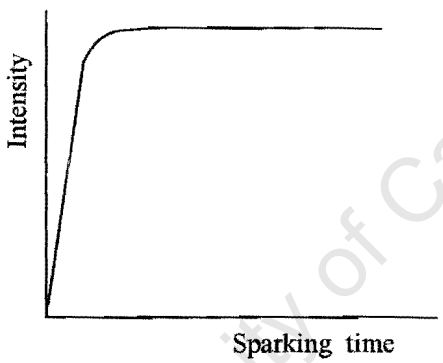

Fig.3.7. Burn-off curve for elements with high vaporisation temperatures in an easily vaporised base, such as nickel in an iron base.

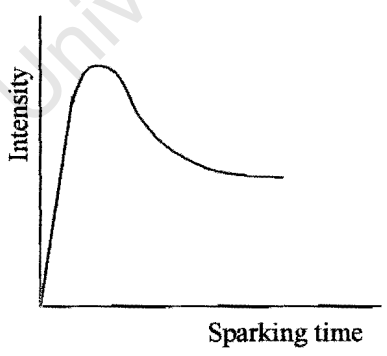

Fig.3.8. Burn-off curve for precipitated elements or compounds such as lead in iron base.

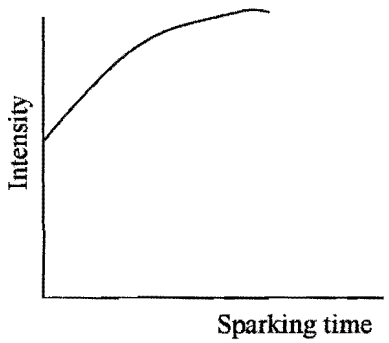

Fig.3.9. Burn-off curve for dissolved elements in a base with a high vaporisation temperature and base metal, such as iron in a zinc base or platinum in a lead base.

In most cases the intensities of the precipitates increase during sparking-in more rapidly than those of the base metals and of the elements dissolved in it. As sparking-in progresses, if the proportion of concentrated discharge exceeds that of diffuse discharges, the intensity passes through the maximum. This is followed by homogenisation, during which concentrated discharges melt and homogenise the sample in the burn spot region. During this process one area after another is melted in the burn spot. After each discharge ceases, the minute liquid region round the vaporised crater solidifies on the solid sample. In the melt, the precipitates are present in a finely dispersed distribution, or are brought into forced solid solutions. Because of rapid cooling at 1000°C between two discharges in 10ms sequence, the liquid phase freezes.

Sparking-in and homogenisation processes merge continuously. Each area of the sample in the burn spot has been remelted and homogenised by at least one discharge. Only this region supplies material for intensity measurements. Homogenisation ends in the steady state.

The sparking-in time increases with quantity and size of precipitate. It declines with the energy converted per discharge, and is completed when all precipitates and electrical defects in the sample have been removed. The remelted structureless layer grows with sparking time up to the steady state. In the steady state there is a structureless layer present which moves into the interior of the sample with constant thickness. The composition of the sample in the steady state is proportional to the average composition of the sample. The intensities of the base metals and the elements dissolved in it rise continuously after the start of the burn-off curve to become constant at the end of sparking-in.

3.3. SAFT: Measurement of spark intensity and time.

The emission of spectra with respect to time showed that background effects due to electron radiation and ionic radiation followed the electrical discharge closely. However, once the electrical discharge had decayed, radiation from atomic species continued afterwards. This phenomenon was termed *after-glow*. It takes place in microseconds and therefore special electronic techniques are required to observe it. The photomultiplier tube only reads the emission energy for the time period of the afterglow. Hence the background radiation has largely decayed at this stage. Therefore the line to background ratio is enhanced by orders of magnitude and serves to improve the sensitivity and limits of detection.

The intensity curve against time is basically determined by the excitation energy, and not the vaporisation or atomisation temperature. Elements of different atomisation temperature may differ considerably but their atomisation due to spark discharge is very similar against time. Because of the temperatures involved at the sample surface during discharge (up to 15000K) the vaporisation process is more physical atomisation than thermal vaporisation. With the correct electrical masking of the spectral background using time resolved

electronics, an improvement in the background equivalent concentration and thus the limit of detection can be obtained. The SAFT can also reduce spectral interferences from ion lines.

For spectrometric analysis with spark discharge in argon, unipolar low voltage discharges with sparking rates up to 600 per second are used. The time interval between two successive discharges must be such that
i) during recharging of the power capacitor there is no self ignition of subsequent discharges. The analytical gap must be deionised before the next discharge takes place, and
ii) all discharges must deliver statistically identical intensity, there being no mutual interference. This is determined by the time taken for the crater formed by the removal of sample material during a discharge to cool sufficiently before the next discharge takes place. If this time is not long enough, then a melt will form because of thermal electron emission and easily vaporised elements will undergo fractional vaporisation.

The average intensity per discharge must remain constant. The discharge is initiated by external ignition in parallel or in series with greater than 10kV and less than 5μs. This is followed by the discharge of the power capacitor, lasting approximately 100μs, and a current maximum occurs after about 35μs. If variations in the photomultiplier tube anode current against time are measured with an oscilloscope at, for example 50kΩ, then the intensity curves would be seen as shown in Fig.3.10.

When a pure sample is sparked, a background signal is obtained which is synchronous with the discharge current curve.

When sparking a sample with concentrations well above the background equivalent concentration, the intensity curves of the atom and ion lines differ. The intensity of the ion lines are also synchronous with the current and thus with the spectral background. This is because high temperatures are necessary for excitation of ion lines (approximately 15eV). These only exist with high currents, and the number of ions is also proportional to temperature. The intensities of atom lines appear with a time lag. Optimum excitation occurs during the afterglow.

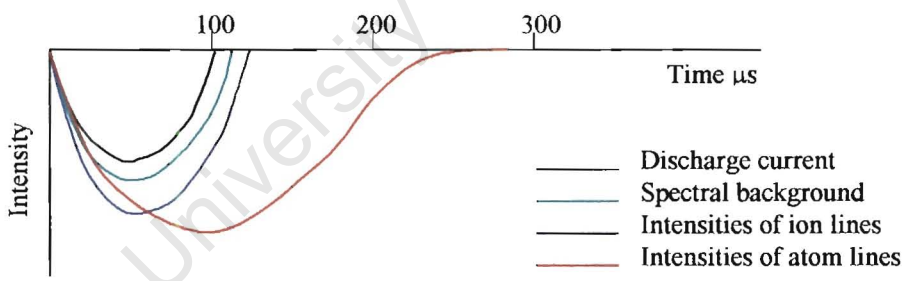

Fig.3.10. Intensity curve showing the principle of the SAFT technique.[8]

The intensity curve versus time is essentially determined by the excitation energy and not by the vaporisation temperature. The example is given where the temperature curve for iron (371.9nm, 3.3eV) and for cadmium (228.8nm, 5.4eV) in a copper base are very similar against time, although the vaporisation temperatures differ considerably.[9]

With spark discharge the vaporisation process is less thermal and is more correctly termed atomisation. The current increase from 0 to 100amps within 35μs leads to a temperature increase up to 15 000K in the region directly in front of the sample surface.

It is reported that the SAFT technique can be used to reduce spectral interference from ion lines or using sensitive lines which because of spectral interference from ion lines are unusable, for example, antimony 287.7nm in a copper base.[10] The intensity of the antimony atom line at 1000ppm is only slightly greater than

the copper ion line. With SAFT the copper ion line is largely eliminated so that the antimony line appears clearly above the background. The same applies to the emissions of the noble metals when present in lead. Brief mention of the analysis of noble metals using SAFT could be found,[11] and tables which are presented in this reference show limits of detection, background equivalent concentrations, and concentration ranges for noble metals in lead. The data for platinum, palladium and rhodium is shown in Table 3.2.

Table 3.2. Limits of detection (LOD), background equivalent concentration (BEC) and concentration ranges for platinum, palladium and rhodium in lead.

Element	LOD (μg/g)	BEC (μg/g)	Concentration range (μg/g)
Platinum	0.1	5	1 – 250
Palladium	0.01	0.2	1 – 10
Rhodium	0.002	0.04	0.1 – 1*

*with nickel correction.

REFERENCES.

1. H. De Lafffolie, "Optical emission spectral analysis. A short introduction and a historical survey", Kleve, Germany, 1991.

2. K.A. Slickers, "Automatic Atomic-Emission Spectroscopy", second edition, p35, Giessen, Germany, 1993.

3. J.R. Dean, "Atomic Absorption and Plasma Spectroscopy", second edition, John Wiley and Sons, England, 1997.

4. K.A. Slickers, "Automatic Atomic-Emission Spectroscopy", second edition, p38, Giessen, Germany, 1993.

5. K.A. Slickers, "Automatic Atomic-Emission Spectroscopy", second edition, p354, Giessen, Germany, 1993.

6. K.A. Slickers, "Automatic Atomic-Emission Spectroscopy", second edition, p132-141, Giessen, Germany, 1993.

7. K.A. Slickers, "Automatic Atomic-Emission Spectroscopy", second edition, p328, Giessen, Germany, 1993.

8. K.A. Slickers, "Automatic Atomic-Emission Spectroscopy", second edition, p359, Giessen, Germany, 1993.

9. K.A. Slickers, "Automatic Atomic-Emission Spectroscopy", second edition, p359, Giessen, Germany, 1993.

10. K.A. Slickers, "Automatic Atomic-Emission Spectroscopy", second edition, p361, Giessen, Germany, 1993.

11. K.A. Slickers, "Automatic Atomic-Emission Spectroscopy", second edition, p360-364, Giessen, Germany, 1993.

CHAPTER 4.

SPECTROMETER DESIGN AND ELECTRICAL DISCHARGE OPTIMISATION IN THE SAFT TECHNIQUE.

4.1. Spectrometer design.

The radiation produced at the spark source is passed to the entrance slit of the spectrometer optics to be split into its component wavelengths. The dispersed radiation passes through the exit slit to photomultiplier tubes where it is measured. The radiation pathway is shown in Fig.4.1. Radiation measurements are converted to concentrations using calibration coefficients.

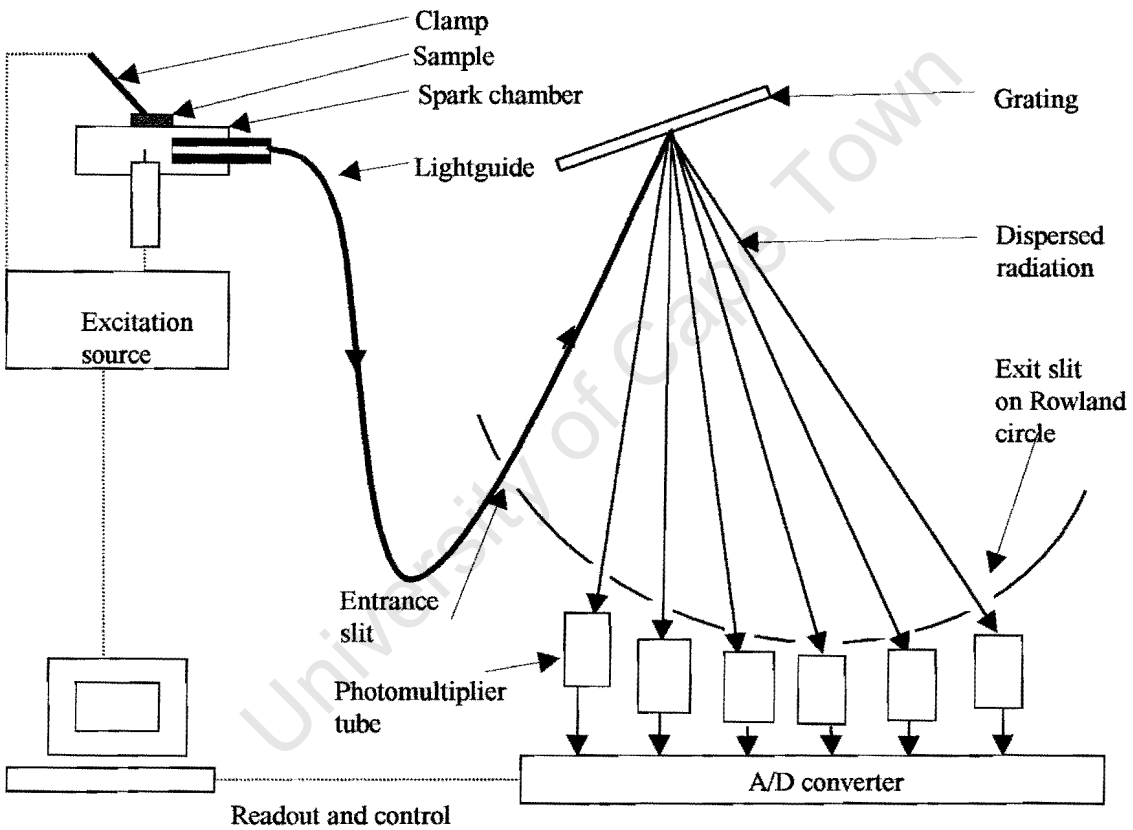

Fig.4.1. Path of radiation.

Two versions of SAFT spectrometer were used for this study, the older M5 and the upgraded M7 spectrometers. Similarities and differences are described in the following sections.

4.1.1. The sample stand.

The sample table slopes at about 10° to the optical axis. As shown in Fig.4.2 the lens axis is fixed in one position at an angle to the optical axis. This position is set to obtain good limits of detection and minimal calibration errors. The position of the lens axis cannot be adjusted once this has been fixed by the manufacturers. The assumption is made therefore that energy measurements taken for platinum, palladium,

rhodium and lead are best taken at the same height in the radiation. If this was not the case, then an adjustable lens position would be required to measure energy at different levels in the plasma.

The stand is coupled to the optical system in air. Because of the intense ultraviolet radiation between the optical plane and the entrance slit, ozone and nitrogen oxides form which alter transparency. This problem can be eliminated using a small pump to circulate air. This environment is suitable for measurement of platinum group metals and lead since it is only necessary to measure wavelengths shorter than 220nm under vacuum because of the reduced emission transparency.

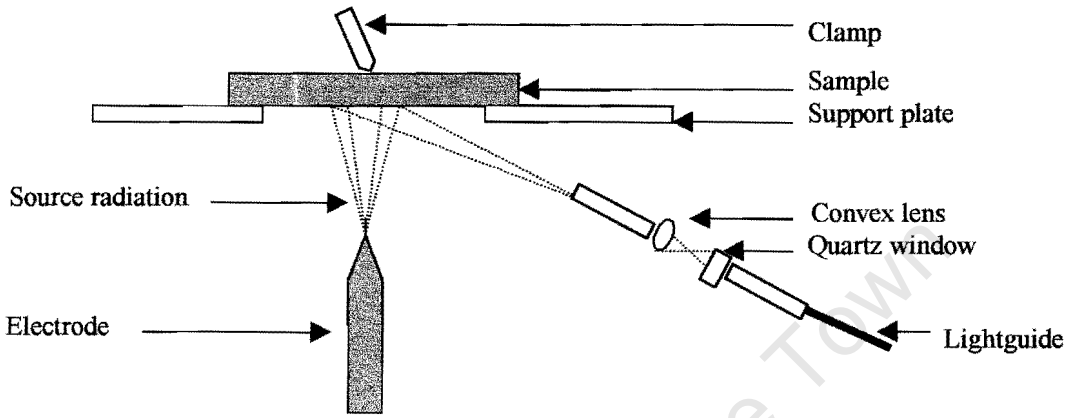

Fig.4.2. Lightguide setting in relation to the stand and plasma.

The spark is discharged in argon to reduce optical interference of the radiation. The stand is flushed with argon at a rate that is controlled carefully. It enters in the front of the side facing the radiation source and is exhausted through the back of the stand behind the plasma through a short pipe to bubble into a water trap. The argon carries with it any condensed vapour and fumes generated by the sparking of the sample. It is important that there are no gas leaks and that the water level of the trap is kept constant to ensure constant gas pressure, thereby maintaining unchanging conditions at the spark.

The sample table is usually made of brass and is chromium plated to reduce wear. The electrode pin is usually made of tungsten with 3%($^{m}/_{m}$) thorium to make it a better electron emitter. The electrode gap was set to 3mm for all measurements taken for the purpose of this research study. Under these conditions the temperatures generated at the spark are estimated to be between 5000K and 10 000K as shown in Fig.4.3.[1]

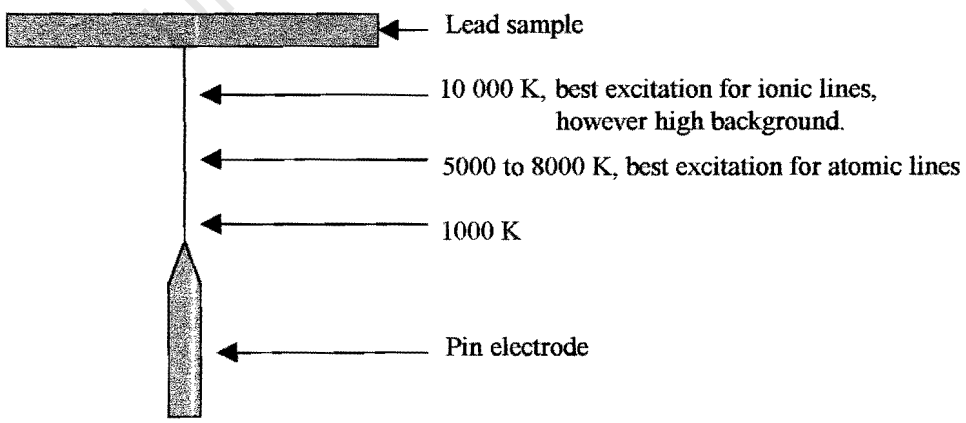

Fig.4.3. Temperature and intensity distribution at the spark source.

4.1.2. Radiation transfer from the source to the entrance slit.

The radiation generated by the spark is transmitted at the end of a lightguide through a lens at the entrance of the entrance slit to focus the image onto the grating. The lightguide is a quartz fibre which transmits the light by total reflection with little loss of intensity due to absorption over a short distance of about a meter. The construction of a lightguide is shown in Fig.4.4.

The lightguide consists of a core surrounded by cladding, and a protective plastic film on the outside. The core has a higher refractive index than the cladding, and the quartz has a transparency range to allow transmission of radiation from 190nm to 5μm.

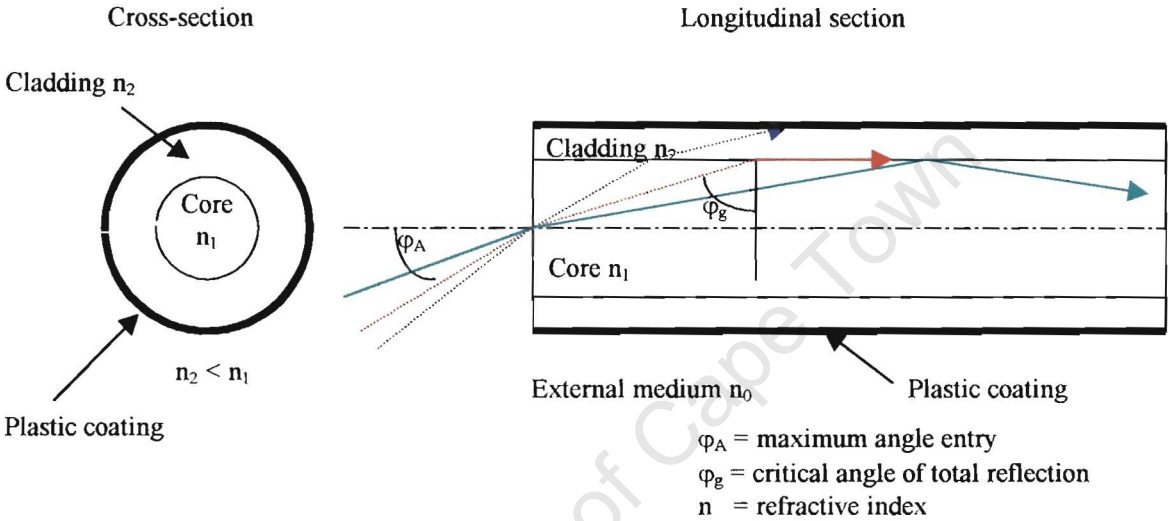

Fig.4.4. Cross-section of a lightguide, and the light pathway in longitudinal section.

In the diagram above angle A (φ_A) is the wavelength dependent aperture angle at which the incoming radiation, because of the total reflection on the interface between the core (refractive index n_1) and the cladding (refractive index n_2), is passed along inside the core emerging at the end of the lightguide and not through the cladding. The aperture angle is calculated from the refractive indices of the core and the cladding.[2,3]

$$\sin \varphi_A = \sqrt{n_1^2 - n_2^2}$$

Rays which enter at an angle larger than A are not totally reflected and emerge through the cladding. This dependence on the angle also explains the emergence of rays if the lightguide is bent, which is important when the lightguide is installed in the spectrometer.

It is necessary to optimise the distance of the entrance to the lightguide in the focal plane relative to the plasma to allow the maximum amount of light to pass through the lightguide to the grating. The distance between the convex lens and the face end of the lightguide may be adjusted in order to do this. A sample is sparked at each new distance to obtain intensities which are representative of emissions at the plasma and the optimum position is derived from the position at which the maximum intensities are obtained. An example is shown in Fig.4.5 where the intensities of lead and platinum at different wavelengths peak at about 4.5 points along the scale. The lightguide would then be fixed at this position along the focal plane of light (which has already been fixed as described in Section 4.1.1) and all wavelengths are then optimised simultaneously for maximum light transmission to the grating.

The transmission of rays entering the lightguide, particularly for the shorter wavelengths, depends on the smoothness of its end face. This is produced by abrading the surface very carefully using a 4000 grit abrasive paper and is usually done by a service engineer trained to perform this task.

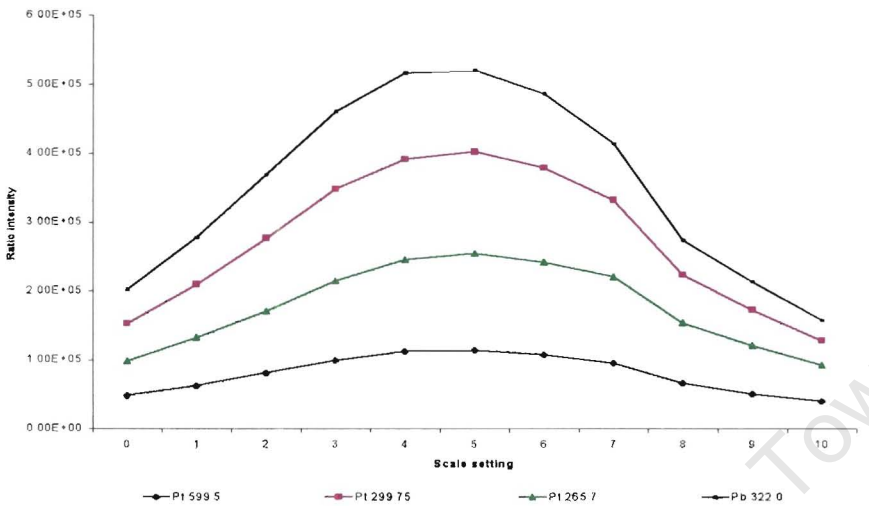

Fig.4.5. Emission profile for optimum setting of lightguide position.

4.1.3. Polychromator.

Spectral line selection is fixed by the design of the optical system. All lines are measured simultaneously as the radiation dispersed by the grating is directed to strategically positioned exit slits and photomultiplier tubes. Optimum setting of the wavelength peaks is done by profiling, where the grating is adjusted fractionally and corresponding analyte intensities are measured. The average line peak can be obtained by calculating the maximum of at least three central points of the Gaussian distribution for each element. Since the position of the exit slits and photomultiplier tubes are not moved once the spectrometer optic alignment has been set up, there should always be corresponding profile setting of peak maxima for all analytes.

Unfortunately it is not possible to run a wavelength scan using a spectrometer fitted with a polychromator. This can only be done where a monochromator is present which allows sequential element measurements to be made.

It is possible to adjust the position of the entrance slits to optimise the line maxima by profiling. Behind the entrance slit is a thin quartz parallel-sided refractor plate. When this plate is rotated the radiation passing through the plate moves laterally thus giving the effect of moving the slit. As it moves in one direction, the spectrum moves in the opposite direction. The wavelength displacements are up to 1nm which allows measuring the wider region of a spectral line. In order to set the correct position for the exit slits, the slits are mounted between cams which are used to adjust the slit positions to accommodate the transmission of wavelengths required for measurement.

The actual process of profiling adjusts the position of the entrance slit relative to all exit slits. This is done by turning the profile scanner manually in one direction across a selected spectral line of an element and recording the intensity at each position using a measuring spectrometer. The positions of the full width at half maximum for the line can be ascertained and the mean line maximum found and set by turning the profile scanner to this point. By always turning the scanner in the same direction the mechanical movement of the scanner is overcome.

In practice, when the spectral optics are set up on a symmetrical A-frame, the exit slits are adjusted for all the spectral lines to be measured at approximately their line maxima. Thereafter when profiling is carried out on the spectral line of one element, the others will automatically be set correctly. These would be measured and calculated to ensure that all measuring lines are reading at their maxima and serves to check that light is being correctly dispersed and transmitted to the photomultiplier tubes. Two optical spectrometers were coupled to the plasma in the M7 spectrometer. Four platinum channels and a lead channel were placed in one optical system, the light being transferred from the plasma to the entrance slit via one lightguide. Palladium, rhodium, nickel, copper, iron and lead channels were set up in the other spectrometer, the light being transferred from the plasma to a second entrance slit via a second lightguide. A specially blazed grating was used to obtain first and second order platinum wavelengths, while the other element wavelengths were dispersed using another grating. SAFT emissions were measured as intensities and were taken simultaneously for all the channels, the radiation from the plasma being transferred to the measuring devices simultaneously. When calculating the ratio of the raw intensity of each wavelength to the lead intensity, the lead intensity obtained from a particular radiation path could only be applied to the analyte intensity obtained from the same path. Hence the platinum intensities were ratioed to the lead intensities obtained from the same optical system, while the other analyte intensities were ratioed to the lead intensities obtained from the optical system used for measuring these elements.

Each radiation pathway for the analytes of interest was optimised by profiling to match the radiation path with the entrance slits to the exit slits and the phototmultiplier tubes. The profile position was checked at regular intervals during the eighteen month investigation period and no change to its position was found.

4.1.4. Gratings.

The means used to disperse radiation into its component wavelengths is the diffraction grating. The grating equation is defined as [4,5]

$$n \times \ell = d (\sin \alpha + \sin \beta)$$

where n = diffraction order
ℓ = wavelength
α = angle of incident ray
β = angle of reflected ray
d = grating constant.

The M5 SAFT spectrometer was fitted with a holographic grating on a symmetrical A frame with a focal length of 750mm. This type of grating has 3600 grooves/mm ruled onto a concave mirror that disperses light into its individual wavelengths from 200nm to 410nm and also images the slit.

The M7 SAFT spectrometer was fitted with a special grating blazed to the second order to improve the resolution such that spectral wavelength measurements can be made in the second diffraction order. It was thus possible for the second order of platinum 299.967nm to be measured at the 598.81nm first order position.

The grating efficiency in a higher order is critically dependent on the blaze angle and or the associated wavelength. The blaze angle is known as angle θ, where $\theta = (\alpha + \beta) / 2$ and since the angle of incidence is equal to the angle of reflection ($\alpha = \beta$), then

$$n \times \ell = 2d \sin \alpha.$$

4.1.5. Exit slits.

The photomultiplier tubes are mounted directly behind the exit slits. The positioning of the exit slit must be within less than 0.1mm of the focal plane of the light path. Directly behind the focal and the exit slits, the

image widens out so that at a distance corresponding to the distance to the grating it has the size of the illuminated area of the grating.

To reduce stray light, masks are fitted on either side of each exit slit. This is to reduce stray light or spectral lines of other elements reaching the photomultiplier tubes.

4.1.6. Photomultiplier tubes.

Photoelectric radiation measurement is done using photomultiplier tubes. These are radiation receivers in which the incident radiation releases electrons from the photocathode to the surrounding vacuum or gas and after amplification using dynodes are collected by the anode. The photocathode is coated with a special electron emitting material which determines spectral sensitivity, useable wavelength range and quantum yield. The electrons released are accelerated towards the adjacent more positive electrode (dynode) where they release secondary electrons. This process is repeated by a number of subsequent dynodes and can amplify the current by 10^6 to 10^8 times. The electron current is taken off at the anode. It is linear over large ranges of the incident radiation output.

The special electron emitting materials are usually bialkali photocathodes because they have low dark current even without cooling. Dark current is the sum of all the noise currents and possibly contains fluctuating currents due to surface leakages and discharges where there is no useful incident radiation. Electrons released from bialkali materials do not generate thermal energy which with other materials could be sufficient to raise the photocathode temperature.

Photomultiplier tubes have response times of 1 to 2ns at 50Ω. Operation requires stabilised voltages of 500V to 1000V at 0.1V variation, and is usually drawn from the high voltage supply.

4.1.7. Measurements of photoelectric current using an integrator and a converter.

The anode current from the photomultiplier tube is integrated in a capacitance before being passed to the analogue/digital converter. Negative photomultiplier tube currents are converted to positive voltages.

$$\frac{I_e \times t}{C} = U_a$$

I_e = integrator input current
C = integrator capacitor
U_a = positive voltages
t = time

The voltages are converted by the analogue/digital circuit to pulses registering as digital counts and finally to the computer microprocessor. Data transmission from the computer to an external computer is possible.

4.2. Pre-SAFT measurement time.

When a measurement is about to be made there is initially relatively intense ionic and background radiation included with atomic radiation. As time progresses and the spark stops, this complex radiation dies off and the atomic radiation remains. This is the mechanism of SAFT where time related electronics are activated to read the atomic radiation emission and has been described in detail in Chapter 3, Section 3.3. The SAFT measurement time is different to the pre-SAFT measurement time, the former being fixed to 40μs and is the time period measured from initiation during which spectral emissions are measured. The latter is the time delay before the window opens to allow light to be transmitted to the optical system so that spectral measurement of the residual emission can take place. Ideally this time delay should be optimised so as to allow as little background emission as possible to be present during the measurement time of the atomic emission. The time

that passes after the spark switches off could be varied from 96μs to 192μs in steps of 24μs using the software control on the M7 spectrometer. The manufacturer had selected this time to be 144μs for the simultaneous analysis of platinum group metals.

Pure lead containing platinum, palladium and rhodium was used to obtain the ratio intensites of emissions for the latter three elements. Pure lead containing no noble metals was used to obtain the intensities of background emissions for each of platinum, palladium and rhodium. Our investigations showed (Fig.4.6) that as the pre-SAFT measurement time was lengthened, the ratio intensity of platinum dropped off indicating that platinum emissions were reduced as the time delay lengthened, and correspondingly the background emissions. In contrast, the behaviour of palladium and rhodium emissions proved to be very different. The sensitivity of palladium and rhodium improved slightly as the pre-SAFT measurement time lengthened as there was an increase in their atomic emissions while their background emissions remained unchanged and close to zero at all the selected times. Therefore, selection of 144μs to 168μs as the pre-SAFT measurement time could be chosen in order to achieve the best situation for palladium and rhodium, while platinum is probably also best read at these times since the background emissions are the least even though the sensitivity is reduced.

Precision of emissions for platinum, palladium, rhodium and lead were below 3% relative standard deviation (RSD), hence could not be used to show preferential pre-SAFT measurement times.

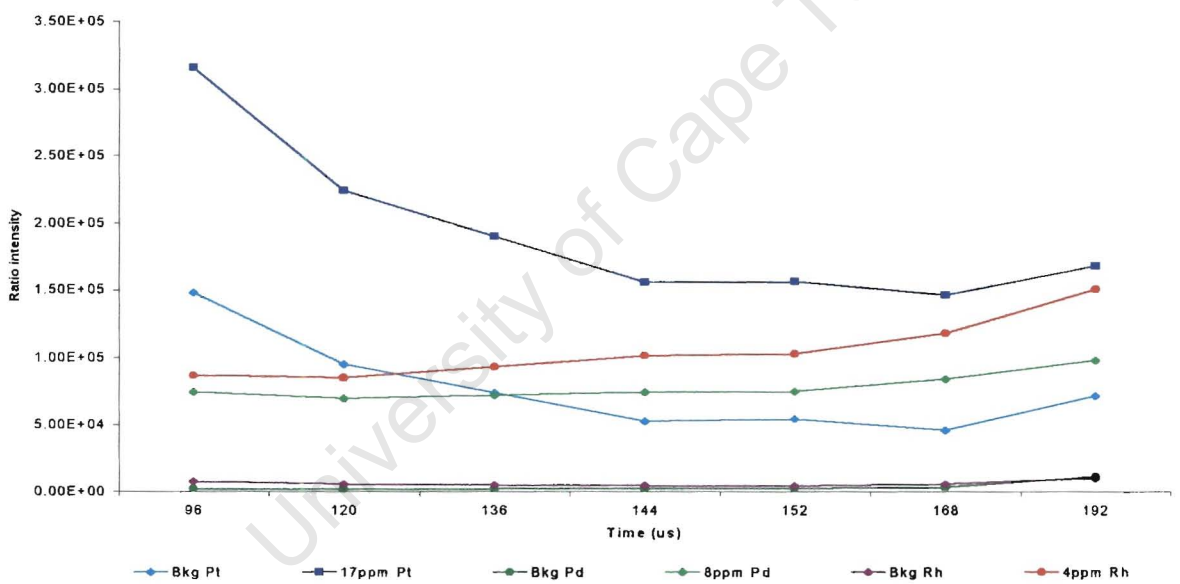

Fig.4.6. Emissions of Pt, Pd and Rh as ratio intensities measured at various pre-SAFT measurement times.

4.3. Optimisation of the spark discharge parameters.

The spark characteristics are determined by the electrical discharge parameters of the supply voltage, capacitance, resistance, inductance, and the distance between the sample and the electrode. The optional parameter settings available for the M7 spectrometer were limited to soft arc-like sparks of low voltage and current. (The electrical discharge parameters of the M5 spectrometers were set by the manufacturer and could not be changed once installed at our laboratory.) In practice the supply voltage was kept constant at 220V and the analysis gap at 3mm for all testwork. The parameter settings were adjusted for different capacitance, resistance and inductance in order to determine their effect on the SAFT measurement of platinum, palladium and rhodium in lead based samples. To do this each parameter was changed independently of the others, the

settings being conveniently selected via the software. The principle of the spark generator and the function of the variable parameters controlling spark discharges can be found in Chapter 3, Section 3.2.1.

The optional parameter settings available were as follows. (All measurements were taken at a pre-SAFT measurement time of 144μs.)
Capacitance (μF) 2.2, **4.7**, 6.9, 10.0, 12.2, 14.7.
Resistance (Ω) **1**, 2, 15, 16.
Inductance (mH) 30, **130**.

The settings could be applied independently to both the prespark and SAFT stages of the discharge. When applied to the *prespark* only, it was found as expected that little effect was seen on the *SAFT* measurements indicating that the homogenising process was taking place effectively and was not sensitive to changes to the discharge settings. The manufacturer selected prespark capacitance at 12.2μF, resistance at 1Ω, and inductance at 30mH for a 3s period. These prespark parameter settings were kept constant for the testwork carried out where variable parameter settings for the SAFT discharge were applied.

The effects on the precision of measurements, the sensitivity of the analysis channels as determined by the slope, and the background equivalent concentrations of each metal analyte which is representative of the y-axis intercept were monitored. The parameter settings selected by the manufacturer for the spark discharge prior to the SAFT measurement is typed in boldface in the list of optional settings above. In our investigation, the different options for one variable were selected while the other two variables were kept constant at the manufacturer's recommended setting. SAFT intensity measurements ratioed to the lead intensity were recorded to enable the effect on the SAFT emission due to the changed variable to be monitored.

4.3.1. Effect on SAFT emissions with variable capacitance at the spark discharge.

Table 4.1. Variable capacitance discharge and its effect on the precision of SAFT measurements, the slope and the background equivalent concentration for platinum, palladium and rhodium.

Capacitance μF	Precision as %RSD	Slope	BEC ppm ($^{m}/_{m}$)	Precision as %RSD	Slope	BEC ppm ($^{m}/_{m}$)	Precision as %RSD	Slope	BEC ppm ($^{m}/_{m}$)
	Pt	Pt	Pt	Pd	Pd	Pd	Rh	Rh	Rh
2.2	4.35	5132	8.4	3.56	26181	0.43	5.21	94498	0.18
4.7	1.98	5596	9.0	2.02	23378	0.27	2.72	77953	0.19
6.9	1.36	6304	10.8	1.48	23116	0.25	1.92	73602	0.22
10.0	1.15	7373	13.1	1.35	23787	0.31	1.53	70642	0.31
12.2	0.99	8075	14.8	1.52	24640	0.29	1.18	71451	0.32
14.7	0.88	9091	16.8	0.86	25730	0.33	1.41	72435	0.39

As shown in Table 4.1, when capacitor charges were increased from 2.2μF to 14.7μF, it was found that the precision of measurements (as %RSD) improved from 4% to less than 1% for platinum, with palladium and rhodium following similar trends. The sensitivity of the platinum channel improved significantly at larger capacitor discharges, while there was relatively little effect in general to the slopes of palladium and rhodium. The background equivalent concentration for platinum became progressively worse from 8ppm($^{m}/_{m}$) to 17ppm($^{m}/_{m}$) with increasing capacitance. Although a similar effect was seen on rhodium where there was an increase of 0.18ppm($^{m}/_{m}$) to 0.39ppm($^{m}/_{m}$), this was not considered to be significant as the background equivalent concentrations for both rhodium and palladium were below 0.5ppm($^{m}/_{m}$). The importance of this is that as the background emissions become less, so do the background equivalent concentrations. This measurement is represented on a calibration by the intercept on the y-axis and ideally should be as close to zero as possible.

The dilemma that arises from these tests is that for platinum the sensitivity and precision of measurements improved with increasing capacitance, while background emissions and hence equivalent concentrations became much larger and therefore worse. If the capacitance setting were to be selected at, for example 14.7μF, then precision and sensitivity would be good but the background equivalent concentration would be poor. If the capacitance were selected at, for example 4.7μF, then there would be poorer precision and a loss in sensitivity, but a significant lowering of the background equivalent concentration. Since the background equivalent concentration would have the most significant negative effect on the quality of calibration and analysis in this instance, the lower capacitance discharge would be a better selection for platinum analysis. As platinum was shown to be the "most difficult" element to analyse, to be able to read palladium and rhodium simultaneously with platinum would require some compromise to the analysis of these two elements. At lower capacitance discharges there was significant loss in precision for both palladium and rhodium, although there was a small improvement in the background equivalent concentration for rhodium which at these levels is probably not significant. Hence our selection of 4.7μF was in agreement with the manufacturer's selection for the capacitance discharge of the spark.

4.3.2. Effect on SAFT emissions with variable resistance at the spark discharge.

As shown in Table 4.2 SAFT measurements at different resistance settings resulted in all three elements showing better precision at 1Ω. The sensitivity as indicated by the slope for platinum improved at 1Ω, however palladium and rhodium were more sensitive at 2Ω. The background equivalent concentrations were most reduced at 2Ω for all elements. As a result of these tests, the resistance to the spark discharge for the SAFT emission by our testing should probably be set at 2Ω. The manufacturer's selection was at 1Ω. The effect of this difference is probably negligible.

Table 4.2. Variable resistance at the spark discharge and its effect on the precision of SAFT measurements, the slope and the background equivalent concentration for platinum, palladium and rhodium.

Resistance Ω	Precision as %RSD	Slope	BEC ppm ($^m/_m$)	Precision as %RSD	Slope	BEC ppm ($^m/_m$)	Precision as %RSD	Slope	BEC ppm ($^m/_m$)
	Pt	Pt	Pt	Pd	Pd	Pd	Rh	Rh	Rh
1	1.27	7134	13.8	2.03	19458	0.30	2.66	57857	0.29
2	2.14	5904	8.6	2.51	23178	0.26	3.85	76735	0.17
15	2.41	4980	15.2	3.24	18717	0.40	3.25	59358	0.29
16	2.80	5004	15.1	2.57	18565	0.36	3.84	59609	0.24

4.3.3. Effect on SAFT emissions with variable inductance at the spark discharge.

Table 4.3. Variable inductance at the spark discharge and its effect on the precision of SAFT measurements, the slope and the background equivalent concentration for platinum, palladium and rhodium.

Inductance mH	Precision as %RSD	Slope	BEC ppm ($^m/_m$)	Precision as %RSD	Slope	BEC ppm ($^m/_m$)	Precision as %RSD	Slope	BEC ppm ($^m/_m$)
	Pt	Pt	Pt	Pd	Pd	Pd	Rh	Rh	Rh
30	1.82	6579	7.4	1.84	28924	0.24	2.33	96432	0.19
130	2.28	6239	7.8	2.32	28094	0.26	2.93	94520	0.17

There were no major effects seen in the intensity measurements of platinum, palladium or rhodium when different inductance settings were investigated (Table 4.3). However, at 30mH, all three elements showed slightly improved precision and sensitivity. The differences in background equivalent concentrations were not thought to be of any significance. Hence the selection for this parameter on the basis of these findings is that inductance should be set to 30mH. This is contrary to the 130mH that was selected by the manufacturer.

4.4. SAFT spectrometer stability tests.

To obtain a measure of the long-term stability of the SAFT spectrometers, tests were conducted where the precision of emissions as ratio intensities for platinum, palladium and rhodium was monitored with respect to time.

Pure lead (blank) and three lead samples (Sample 1,2 and 3) containing increasing concentrations of platinum, palladium and rhodium were sparked by SAFT every hour for 8 hours per day, for 6 continuous days. The spark chamber was cleaned only at the beginning of each day and at no other time. No other samples were analysed during the test period. The ratio intensities for each SAFT measurement were recorded, and at the same time a reading taken using a voltmeter at the mains power supply to the spectrometer.

The stability of the spectrometer can be described by the relative standard deviation of the SAFT ratio intensity measurements for a total of 48 measurements taken during the 6 day test period. The results are shown in Tables 4.4 and 4.5 for the M7 and M5 spectrometers respectively.

Table 4.4. Overall precision of the ratio intensities of SAFT sparks, and precision of power supply voltage to the spectrometer expressed as %RSD for a 6 day test period using the M7 spectrometer.

M7 spectrometer	%RSD			
	Pt	Pd	Rh	Voltage (V)
Pure lead (blank)	5.0	8.4	12.6	1.5
Sample 1	3.8	8.7	9.6	
Sample 2	3.1	8.2	9.2	
Sample 3	4.1	8.0	10.4	

Table 4.5. Overall precision of the ratio intensities of SAFT sparks, and precision of power supply voltage to the spectrometer expressed as %RSD for a 6 day test period using the M5 spectrometer.

M5 spectrometer	%RSD			
	Pt	Pd	Rh	Voltage (V)
Pure lead (blank)	3.3	2.1	1.7	0.3
Sample 1	3.4	2.9	2.1	
Sample 2	3.3	3.0	2.3	
Sample 3	3.7	2.8	2.3	

Clearly the stability of the M7 spectrometer over the entire 6 day measurement period was much worse than the M5 spectrometer. When the precision (%RSD) was calculated for ratio intensities obtained on a *daily* basis, as shown in Table 4.6, there was a significant influence from day to day which could be attributed only to the setup at the spark stand since no other parameters changed. Poor sample homogeneity could be disregarded as a reason for the poor precision as there was little variation in the precision of each element *between* samples.

Table 4.6. Precision of ratio intensities of SAFT sparks calculated on a daily basis.

	%RSD					
	Pure lead (blank)			Sample 3		
	Pt	Pd	Rh	Pt	Pd	Rh
Day 1	1.9	3.7	3.9	1.5	3.5	3.5
Day 2	3.3	4.5	6.8	2.2	4.6	4.8
Day3	6.2	3.3	5.7	1.6	2.3	2.6
Day4	3.0	5.7	6.8	2.5	5.4	5.9
Day5	5.7	6.0	6.8	2.3	4.6	4.0
Day6	2.8	6.6	6.3	2.4	5.3	5.5

The overall stability of the M5 spectrometer for the 6 day period was far better than the M7 and less sensitive to the spark stand setup. A successful calibration curve using the M7 would therefore depend largely on all calibration standards being sparked without changing any spark chamber conditions, such as cleaning and resetting the electrode pin distance from the sample.

REFERENCES.

1. K.A. Slickers, "Automatic Atomic-Emission Spectroscopy", second edition, p156, Giessen, Germany, 1993.

2. D.A Skoog, D.M. West, "Principles of Instrumental Analysis", second edition, Holt-Saunders International, 1981, Japan.

3. K.A. Slickers, "Automatic Atomic-Emission Spectroscopy", second edition, p153, Giessen, Germany, 1993.

4. J.R. Dean, "Atomic Absorption and Plasma Spectroscopy", second edition, John Wiley and Sons, University of Greenwich, 1997, UK.

5. K.A. Slickers, "Automatic Atomic-Emission Spectroscopy", second edition, p169, Giessen, Germany, 1993.

CHAPTER 5.

MEASUREMENT AND EVALUATION OF SAFT EMISSIONS FOR PLATINUM, PALLADIUM AND RHODIUM AT TRACE LEVELS IN LEAD.

5.1. Creating and evaluating a calibration.

Since the SAFT analytical method is based on an electro-optical instrument response to an analyte concentration in lead, the accuracy of the final concentration of an unknown analyte is critically dependent on the calibration of the instrument.[1,2,3]

The success of a working calibration depends on the selection of the standards and the quality of their preparation, high quality concentration data for these standards, and the response of the spectrometer used for generating and measuring emissions of the required elements.

5.1.1. Evaluation of a calibration curve.

When the emission data (y_1, y_2, ... y_n) is paired with the concentrations (x_1, x_2, ... x_n) of each standard in a calibration, a regression analysis may be performed to evaluate the relationship of these bivariate characteristics for n observation pairs (x_1, y_1), (x_2, y_2), ... (x_n, y_n). The relationship between these two characteristics can be described by a mathematical equation $\hat{y} = f(x)$, the least squares curve. This is obtained by minimising the sum of squares of the vertical distances between the observed points and the corresponding points on the curve. Assuming a linear relationship of the form $\hat{y} = a + bx$, the least squares values of the intercept and slope are respectively a and b for which $\Sigma(y - \hat{y})^2$ is a minimum. The least squares values of a and b are

$$a = \bar{y} - b\bar{x} \qquad \text{and} \qquad b = \frac{\Sigma xy - 1/n(\Sigma x \Sigma y)}{\Sigma x^2 - 1/n(\Sigma x)^2}.$$

Therefore two equations may be used to fit a straight line to the observed (x, y) points in a scientific manner. The degree of strength of the linear relationship can be determined by the correlation. Linear correlation means that the relationship between x and y is linear. A scatter diagram may be used to indicate the strength of linear correlation. The correlation coefficient r is the square root of the coefficient of determination R^2 that describes how well the least squares curve fits the observed data and is defined as

$$r = \frac{b\sqrt{\Sigma x^2 - 1/n(\Sigma x)^2}}{\sqrt{\Sigma y^2 - 1/n(\Sigma y)^2}}$$

where r is a number between –1 and +1.

If a straight line gives a good description of the relationship between x and y this curve can confidently be used for interpolation purposes. If $\hat{y} = f(x)$ provides a perfect fit, then R^2 and r = 1.

5.1.2. Selection and preparation of samples.

Merensky ore and UG2 ore tailing samples were used to prepare the standards for calibration of the SAFT. The details of sample and standard preparation have been described in Sections 1.1 and 1.2 of Appendix 1. As the preparation was adapted from the PGM fire assay technique, the weighing of the sample and flux, and fusion was accepted as being correct. The SAFT preparation deviates from the PGM method at the transformation of the lead button into a suitable sample for spark analysis by remelting and rapidly casting it into a flat button.

This remelting step was investigated and conditions were selected for the best method to prepare good analytical samples by measuring concentrations and precision of noble metals in lead. The details of this testwork may be found in Appendix 2. It is worth commenting that the homogeneity of a solid sample may not be as good as that of a liquid solution. Therefore the error due to sample preparation cannot be considered negligible for SAFT analysis as it would be for the analysis of a liquid solution of wet chemically dissolved sample. The errors due to sample preparation for the SAFT determination of platinum, palladium and rhodium has been estimated by our testwork to be about 2% to 5% (rel) of the overall analytical error of the ore tailing sample. There is some doubt as to how accurate these figures are as it is difficult to separate the sample preparation errors from the instrument response errors and the errors due to the nature of the sample itself since the SAFT analytical technique is so complex. Other analytical techniques which may be used to analyse the platinum group metals as PGM (Appendix 1, Section 1.3) or as the individual noble metals using nickel sulfide pressure dissolution (Appendix 1, Section 1.4) are equally complex, so it is extremely difficult to quantify these type of errors.

Because of the complexity of the chemical reactions which take place in a lead collection, there is some variability within each collection process, with the result that different masses of lead are obtained even after fusion is carried out for the same sample under nominally similar conditions. Because the measured sample is a solid, each spark is unique. Since there may be some doubt as to the homogeneity of the lead buttons, problems are experienced with this type of analysis which would not normally occur when a solution, by comparison, is used for measurement.

5.1.3. Concentration of analytes in SAFT calibration standards.

The SAFT analysis is not an absolute technique because the concentrations of platinum, palladium and rhodium in the standards must be obtained from an alternative method of analysis. For noble metals the generally accepted technique is nickel sulfide collection where nickel sulfide is used to preconcentrate the noble metals which are then dissolved using chlorine to obtain a solution which may be analysed usually by optical emission spectroscopy (Appendix 1, Section 1.3). The error in the noble metal concentrations obtained from the nickel sulfide method was estimated at no greater than 10%(rel) for each of platinum, palladium and rhodium. The concentrations of each noble metal in the lead buttons for SAFT analysis were calculated using the data obtained from the nickel sulfide method.

5.1.4. Spectrometer response.

The spectrometer response is critical to the accuracy of future analyses. The error associated with its performance is difficult to estimate as a separate entity for reasons already discussed. The inherent emissions of platinum atoms in the spark plasma are much lower than that of palladium and rhodium which makes platinum analysis more difficult. There are no instrument scanning facilities to enable a full wavelength range investigation of spectral lines. Fixed spectral wavelengths were selected by the manufacturer for simultaneous measurement which limited investigations of other possible useful wavelengths. There may have been advantages to making use of a monochromatic system whereby each metal may be analysed independently of the others. From a scientific point of view this situation would have been ideal to obtain optimum wavelength selection and hence analysis. However in practical terms in a production environment the simultaneous measurement of the noble metals is preferred to a sequential measurement system in order to save time and money, often with a loss in accuracy of analytical values.

A measure of the instrument response may be made using the limit of detection and the background equivalent concentration for each analyte. Definition of these and other terms relating to calibration can be found in Appendix 3, Sections 1, 2 and 3.

5.2. Preliminary SAFT calibration studies carried out at the *Council for Mineral Technology.*

Preliminary work was carried out at the *Council for Mineral Technology* (Mintek) when the SAFT was initially introduced to the mining industry in South Africa in 1991. Their investigations involved calibrating trace levels of platinum, palladium, rhodium, gold, ruthenium, iridium and silver present in lead by adding ore samples to a litharge based flux to preconcentrate and collect the noble metals in lead using the fire assay fusion technique. The M5 spectrometer was available at that time for evaluation. The results they obtained for platinum, palladium and rhodium are shown in Fig.5.1 to 5.4.

The platinum emission line at 306.4nm has an atomic emission overlap with nickel. The outliers, shown as enhanced emission intensities in Fig.5.1 as red data points, are due to apparent emissions of platinum and are actually due to emissions of nickel together with platinum in the lead. A correction was applied which subtracted the nickel contribution to the total emission and reassigned the data points to be congruent with the rest of the platinum calibration. Details of how this correction was achieved were not documented.

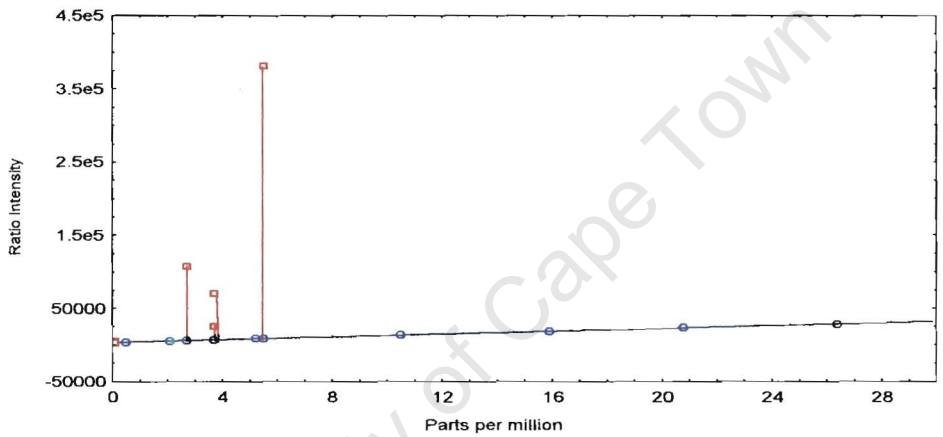

Fig.5.1. Calibration of platinum emissions at 306.4nm in pure lead as determined at Mintek, 1991. Enhancement of emissions due to nickel spectral overlap is evident.

The calibrations for the alternative platinum wavelength at 299.967nm is shown in Fig.5.2, palladium at 340.46nm in Fig.5.3, and rhodium at 343.49nm in Fig.5.4. Certainly these calibrations having wide concentration ranges looked promising.

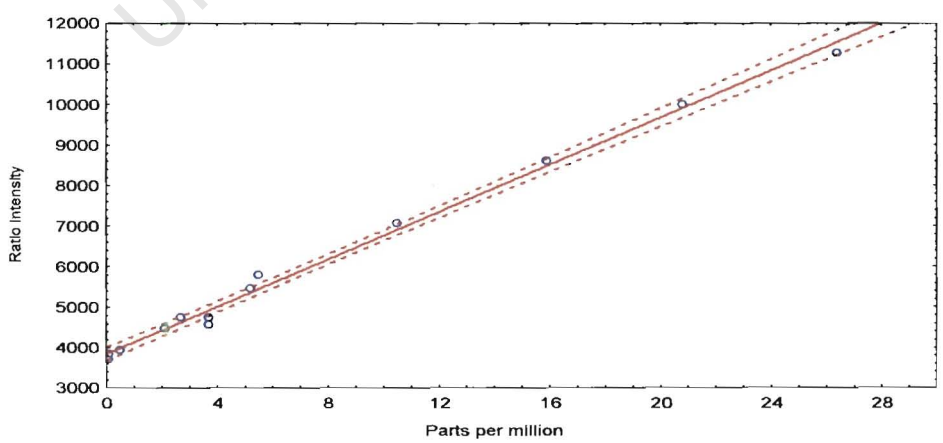

Fig.5.2. Calibration of platinum emissions at 299.967nm in pure lead as determined at Mintek, 1991.

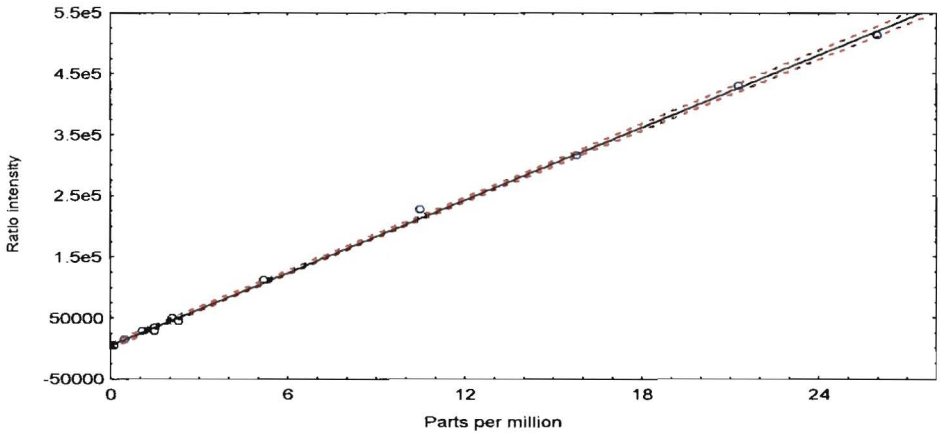

Fig.5.3. Calibration of palladium emissions at 340.46nm in pure lead as determined at Mintek, 1991.

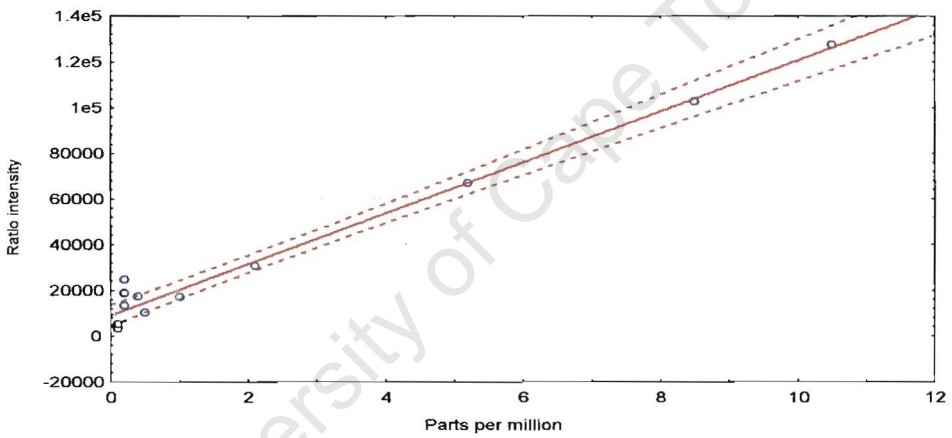

Fig.5.4. Calibration of rhodium emissions at 343.49nm in pure lead as determined at Mintek, 1991.

Taken from the Mintek work are the background equivalent concentrations and limits of detection for each of the SAFT measuring channels (Table 5.1).

Table 5.1. BEC and LOD for platinum, palladium and rhodium in lead using an M5 SAFT spectrometer, during 1991.

Element	BEC (ppm)	LOD (ppm)
Pt 306.47nm	3.0	0.10
Pt 299.8nm	12.5	0.42
Pd 340.4nm	0.17	0.006
Rh 343.5nm	0.22	0.007

It was reported at the International Conference on Applied Mineralogy, 1991,[4] that results obtained for the internationally certified standard SARM7 were very encouraging. Comparisons of the SAFT results with recommended values were unfortunately not documented in the ICAM91 report. A comment was made, however, that more attention should be given to the preparation of the lead button with regard to homogeneity.

5.3. Initial SAFT calibration studies to motivate the research recorded in this dissertation.

In view of the preliminary work carried out it was recommended that the spectrometer be taken into a mining environment. There, a thorough investigation into quality sample preparation and testing of the instrument could be done. This was subsequently arranged.

Initial calibrations were set up using synthetically prepared standards. Accurately weighed noble metals were added to litharge flux and then fused. The resultant lead buttons were transformed into discs suitable for sparking by remelting and rapidly recasting. The background equivalent concentrations (BEC) and limits of detection (LOD) for each SAFT measuring channel determined in these standards were found to be as shown in Table 5.2.

Table 5.2. BEC and LOD for platinum, palladium and rhodium in lead using an M5 SAFT spectrometer in 1995.

Element	BEC(ppm($^m/_m$))	LOD(ppm($^m/_m$))
Pt 306.47nm	5.1	0.17
Pt 299.967nm	7.6	0.25
Pd 340.46	0.42	0.014
Rh 343.49	0.20	0.007

Fig.5.5 shows the relationship of intensities to calculated concentrations of platinum, palladium and rhodium in the lead. Note that the analyte intensity is ratioed to the lead intensity obtained from simultaneous emissions, which serves the purpose of an internal standard to compensate for variations occurring from button to button, such as slight irregularities in the surface quality of the buttons.

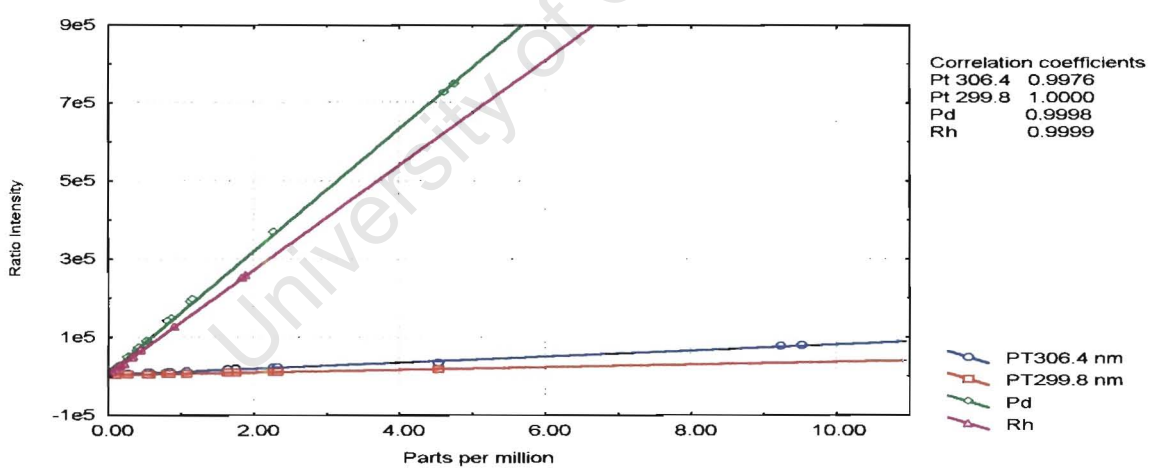

Fig.5.5. Calibration of noble metals in lead using pure metal "solutions" to prepare standards.

For concentration ranges up to 10ppm($^m/_m$) platinum, 5ppm($^m/_m$) palladium and 2ppm($^m/_m$) rhodium, the expected calibrations were linear or close to being linear as indicated by the correlation coefficient. The expected concentration range of the ore tailing sample was about 0.4 to 0.8ppm($^m/_m$) platinum, which preconcentrates to approximately 2 to 4ppm($^m/_m$) after it has been collected in lead by fire assay, at which levels analytical measurements are taken. Real ore samples were prepared and analysed using these calibrations (where the calibration standards were prepared from pure metals in lead). A comparison of the noble metal concentrations by SAFT and the concentrations determined using the nickel sulfide method showed that the SAFT calibration was giving incorrect concentrations. It was speculated that instrument drift, which had not

been included in the setup for practical reasons, could be responsible for the bias in concentrations. Alternatively, because real ore samples had low concentrations of noble metals in lead, measurements would therefore be near the limit of quantification and leave doubt as to precision of intensities, and therefore accuracy.

The sensitivity of the SAFT technique for platinum is very poor compared to palladium and rhodium. See Fig.5.6. This means that small changes in intensity occur for large concentration changes. For any calibration curve the sensitivity of the instrument response at a particular wavelength can be considered equivalent to the slope of the calibration curve. Hence a high sensitivity indicates a sharp positive slope, and low sensitvity indicates that small changes in instrument response (low slope) correspond to large changes in concentration.

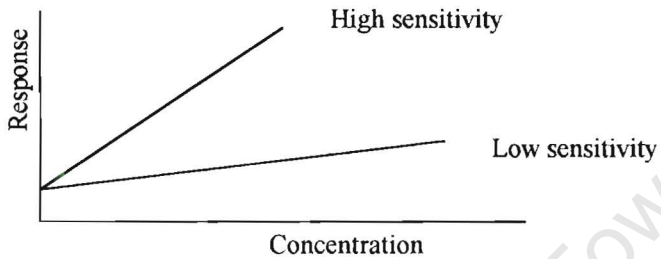

Fig.5.6. Low and high sensitivity due to instrument response.

Because of the poor sensitivity of platinum, standard addition was used to extend concentration ranges. The usual approach is to add known amounts of analyte to aliquots of the sample itself. A plot is drawn of the emission of atoms as a measured signal versus the amount of analyte added. The importance of the standard addition procedure is that matrices are kept constant between the sample and the standards. The concentration of the test sample is given by the intercept on the x axis and its standard deviation and an estimation of the confidence interval made. Hence we can obtain a single sample calibration value from its calibration line.

The motivation for using the standard addition method for collection of noble metals in lead was, not to establish the concentration of the working sample, but to use the preparation technique of standard addition to extend the calibration curves of the noble metals to beyond the restricted concentration range inherent of the ore samples, but at the same time maintain a constant matrix within the lead standards. The predicted difficulty lay in the selection of material containing PGM to be added to the ore sample. Two methods were considered.

i) Addition of known amounts of pure precious metal solutions to the ore tailing sample (referred to as PURE SA in the following sections).

ii) Addition of known amounts of PGM concentrate (referred to as CONC SA in the following sections) which contained about 60ppm($^{m}/_{m}$) platinum, 30ppm($^{m}/_{m}$) palladium and 5ppm($^{m}/_{m}$) rhodium. This concentrate also contained about 5%($^{m}/_{m}$) in total of the base metals nickel and copper.

Details of the methods of preparation by standard addition are described in Appendix 1, Section 1.2.

5.4. Evaluation of SAFT calibrations.

The following samples were used to prepare lead buttons as standards for the calibration containing platinum, palladium and rhodium by SAFT using both the M5 and M7 spectrometer versions. (The sample names in parentheses are referred to in the following sections.)

Merensky ore and UG2 ore tailing samples (MERENSKY and UG2); a mixture of Merensky ore and UG2 ore tailing samples (MF); standard addition samples (CONC SA and PURE SA) prepared as discussed in Section 5.3, i) and ii); no ore sample was added to the flux to produce a lead sample containing no PGM (BLANK).

All standards were prepared using the fire assay fusion procedure to preconcentrate the PGM in lead buttons. Each standard sample was sparked three times and the SAFT emission data obtained was paired with the calculated concentrations of platinum, palladium and rhodium in each lead standard. Scatter plots were drawn of the ratio intensity as a measure of the atomic emission of each element on the y-axis versus concentration on the x-axis. The slope and intercept are used to describe the calibrations and are denoted as b and a respectively. The correlation coefficient for the regression of each element was calculated and is denoted as r.

Details of statistical calculations performed for the purpose of this dissertation for regression analysis is described in Appendix 3, Section 4.1. The regression analysis performed using the operating software of the SAFT spectrometer supplied by *Spectro* has been described in Appendix 3, Section 4.2.

5.4.1. Calibrations for platinum.

The wavelengths available for measuring emissions of platinum were at 306.47nm and 299.967nm using the M5 spectrometer; 299.967nm in the first order and 598.81nm in the second order, 265.87nm in the first order and 531.93nm in the second order using the M7 spectrometer. Scatter diagrams were constructed for the SAFT emissions of platinum at each wavelength which were recorded as ratio intensities and the corresponding platinum concentrations.

5.4.1.1. Calibration of platinum using the M5 SAFT spectrometer.

At the wavelength 306.47nm, the distribution of data pairs for all the standards is shown in Fig.5.7.

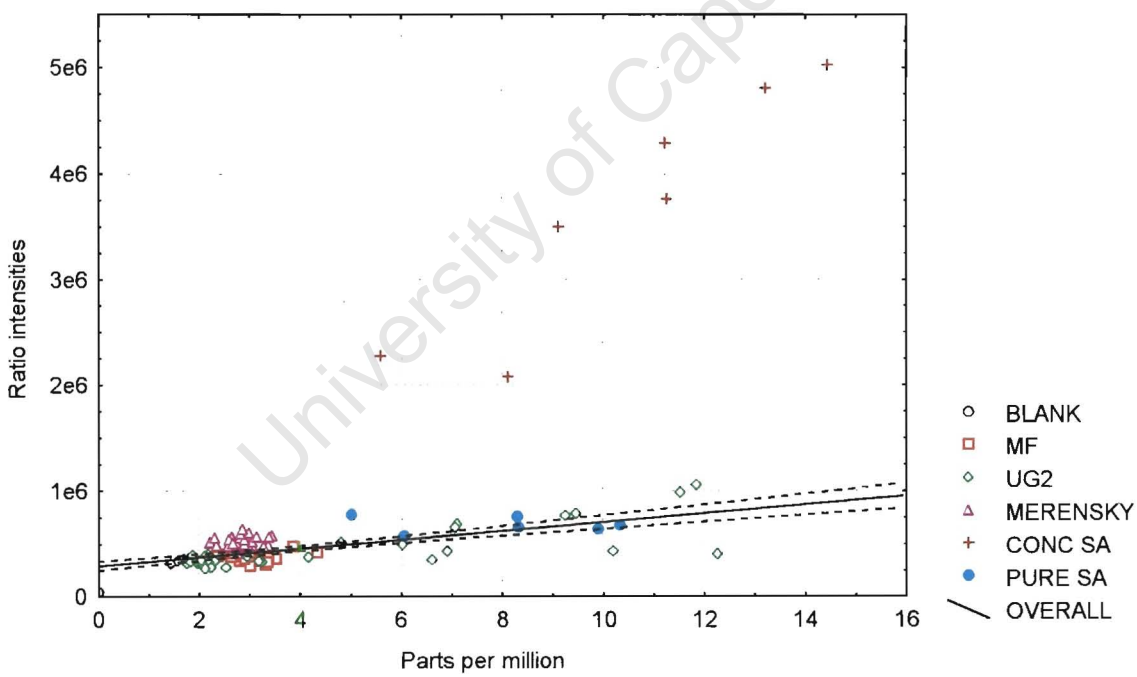

Fig 5.7. Calibration of Pt 306.47nm using the M5 spectrometer using real ore tailing samples (MERENSKY, UG2, MF) and standard addition materials (CONC SA and PURE SA). The regression analysis used to describe the curve excluding CONC SA data pairs is r = 0.68, b = 36506, a = 3.337E05.

The data pairs for the standards CONC SA were excluded from the calibration as they clearly did not "fit" with the other standards. The emissions for platinum at this wavelength were enhanced significantly, which was probably due to an element originating from the added PGM concentrate material being collected in the lead. If these outliers are excluded from the curve fit, there is still large scatter as indicated by r at 0.68. The platinum emissions of the blank lead sample were very close to zero, but well removed from the least squares line. It was

assumed that the platinum emissions for the blank lead were different to the emissions of the ore samples because the matrix of the blank lead would be "cleaner", and hence would incorrectly influence the curve fit.

If a curve is fitted to only the ore samples, then the scatter diagram is as shown in Fig.5.8.

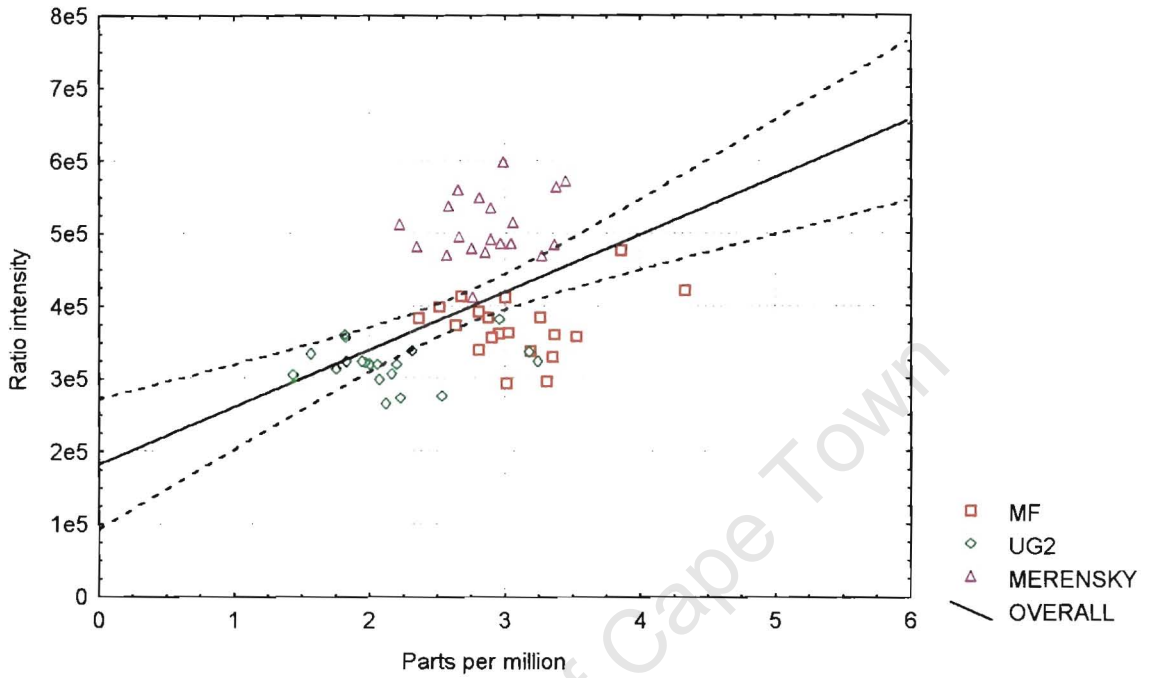

Fig 5.8. Calibration of Pt 306.47nm using the M5 spectrometer for ore tailing samples (MERENSKY, UG2 and MF) only. The regression analysis used to describe the curve is r = 0.39, b = 79175, a = 1.819E05.

The observed emissions for the platinum at 306.47nm using the M5 spectrometer could not be fitted to a straight line when paired to concentrations. The Merensky, UG2 and MF ore samples formed uniquely identifiable groups of data. A curve fit gave an unacceptable correlation coefficient (r = 0.39) indicating that the calibration was unacceptable.

The platinum emissions for the PGM concentrate calibration standards shown in Fig.5.7 were clearly outliers. An investigation into a possible cause of the enhanced emissions revealed that nickel emissions occurred at 306.46nm which would affect the platinum emissions at this wavelength, the resulting emissions being a combination of both platinum and nickel. Since there was 3%($^{m}/_{m}$) nickel in the PGM concentrate which was added in increasing proportions to the ore sample used to improve the range of noble metals in the lead calibration standards, it was possible that some nickel also collected in the lead. This was confirmed by the ratio intensities for nickel in the lead CONC SA calibration standards that were found to be considerably higher than the nickel ratio intensities for ore calibration standards.

In order to correct for spectral interferences such as nickel on platinum at 306.47nm, a calibration for nickel needed to be created. Hence, in theory, the contribution of the total emission due to nickel could be calculated and subtracted from the total apparent platinum emission to obtain the real platinum intensity. In practice, however, the preparation of suitable lead calibration standards containing known amounts of nickel without PGM also being present was not possible. Several attempts were made to prepare standards by adding pure nickel to the flux followed by fusion. Nickel was also added directly to pure lead and melted together in an induction furnace. Drillings of the buttons were taken for a wet chemical analysis to quantify the nickel. Unfortunately, it was found that the nickel was not homogeneous in the lead and buttons containing exactly the

same quantities of nickel could not be produced. These two characteristics are essential for long-term means to accurately correct for the nickel spectral overlap with platinum. Hence we found no practical means of determining platinum at 306.47nm in the presence of nickel which is a contaminant in lead collected during the fusion and originates from the ore samples.

Several sources of error could be contributing to the large scatter of data pairs and hence poor correlation coefficients of the calibrations. Possible reasons lie in the lead button preparation, the assigned concentrations determined by the nickel sulfide method, and the actual emission response at a particular wavelength.

i) The concentration errors have been minimised as far as possible by analysing the samples themselves exhaustively using the nickel sulfide technique. It is known that it is possible that an error of up to 10%(rel) can exist for platinum, palladium and rhodium in ore tailings samples, and this must be accepted since no other reliable method of analysis can improve on this. To minimise the overall error due to the error of individual concentration values, as many nickel sulfide values as practically possible should be represented on the x-axis.

ii) In order to obtain the ideal number of SAFT measurements (sparks) per button by establishing the effect of different numbers of sparks on the precision (as standard deviation) of an x value, a plot of the x value error (s_{x0}) for up to ten sparks per button was prepared. An example is given in Fig.5.9. for platinum at 299.5nm using the M7 spectrometer.

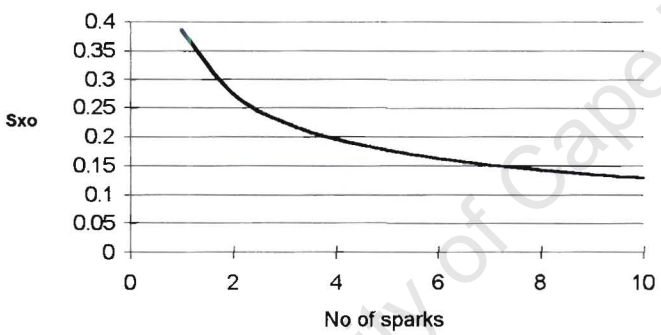

Fig.5.9. Changes in precision (indicated by s_{x0}) of platinum depending on the number of SAFT measurements.

Ideally not fewer than eight sparks per button should be obtained to achieve a precision where there is no further real improvement. However the diameter of the button and the time taken for measurements are practical limitations. The length of time of calibration was of concern because of possible instrument drift that could occur due to changing conditions such as the cleanliness of the spark chamber and the distance of the electrode from the button which will increase gradually as it is worn away by spark action.

A second attempt at calibrating platinum was set up using ninety lead buttons prepared from forty-five samples with good quality nickel sulfide values. Taking into account the handling time, the total measurement period of this second calibration attempt was six hours. Each button was sparked three times which meant that a compromise had to be made to precision to keep the calibration process practical with respect to time and instrument stability. The spark chamber was cleaned and the electrode distance from the sample reset twice during the entire reading period. The procedure was followed in a similar manner using both the M5 and M7 spectrometers.

The preparation of the samples for SAFT was carried out using the utmost care and optimum working conditions to have the best chance of obtaining homogenous lead samples. Even so, the second platinum calibration using 306.47nm where only the real samples were sparked was not successful. There could have

been interference from nickel to a small extent, since large aliquots of the ore samples used to preconcentrate the noble metals contain small quantities of nickel that may also be collected in the lead. It was also possible that some of the error may originate from the instrument response to platinum atomic emissions that are measured close to the detection limit. Since the different sample types were grouped, it could also be possible that the lead matrix played a role in disturbing emission responses. If the concentration of copper and nickel in both the lead calibration standards and analytical samples was fairly constant, then there was a possibility that their effects could, in theory, be canceled out. It was shown in other investigations (discussed in Chapter 6) however that there were different levels of copper and nickel in lead collected from different sample types. There was also evidence that there was a certain amount of base metal segregation in the lead. There was no clear evidence that the platinum was not homogeneously distributed in the lead. This information tended to indicate that a single calibration for all types of sample would not work even though the levels of noble metals in lead exist at trace levels for all the different ore tailing samples. This was confirmed by the emission data obtained for the calibration of platinum at 306.47nm. In Fig.5.8 the concentration range of platinum is small from 1.5 to 4.5ppm($^{m}/_{m}$) in lead and the matrices of the three different gangue types are sufficiently different to cause the apparent platinum concentrations to separate uniquely according to sample type.

Hence platinum at 306.47nm was found to be totally unsuitable for the calibration and measurement of platinum in lead samples prepared by fusion of ore tailings samples.

It was possible to observe the platinum atomic emissions by SAFT using the M5 spectrometer at 299.797nm. At this wavelength there are no spectral effects on platinum due to base metals that may be present in the lead samples. A scatter plot of platinum emissions and concentrations was prepared and can be seen in Fig.5.10.

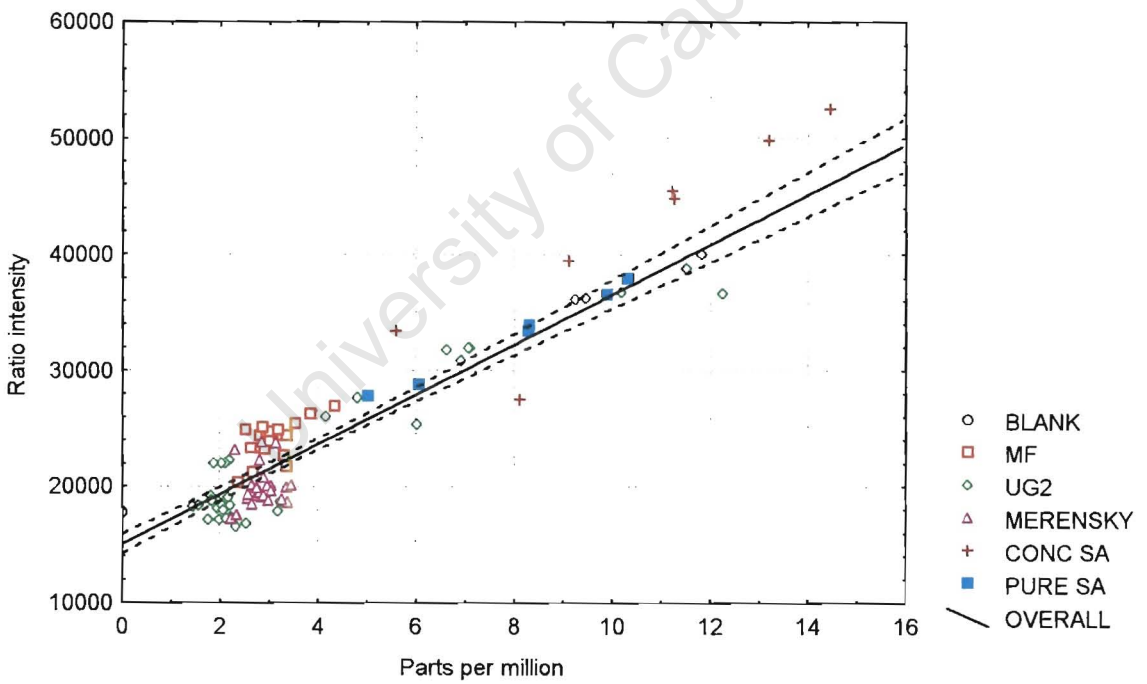

Fig 5.10. Calibration of Pt 299.797nm using the M5 spectrometer with ore tailing samples (MERENSKY, UG2 MF) and standard addition materials (CONC SA AND PURE SA). The regression analysis to describe the curve excluding CONC SA data pairs is r = 0.97, b = 2134, a = 15090; r (including all standards) = 0.95.

Platinum concentrations at 299.797nm in calibration standards where PGM concentrate (CONC SA) was added to the ore samples were outliers to the best fit curve (Fig.5.10). Since the concentrations of platinum in lead were assumed to be correctly assigned from the nickel sulfide method of analysis, the error therefore lay in the

y-axis as ratio intensities. The raised intensities or emissions could not be attributed to spectral interferences, therefore the enhancement could be the result of changes in the lead matrix with the addition of concentrate to the ore tailing sample. The different matrix composition such as density of the lead and the formation of the atomic plasma during the spark process could affect the emission response of platinum, in this case by enhancement of emissions. It was found that when pure platinum was added to the calibration sample the platinum emission response was normal since the assigned platinum concentration lay on the "best fit curve". This supports the idea that the lead matrix plays a critical role in the response of SAFT emissions and ultimately this affects the accuracy of calibration. The correlation coefficient for the calibration excluding the CONC SA standards was 0.97. However there is cause for concern about the insensitivity of platinum emissions at 299.797nm and the intercept on the y-axis which translates into a background equivalent concentration of 7ppm($^{m}/_{m}$) platinum. The consequences of a larger background equivalent concentration is that the ratio of the analyte to background intensities is smaller and hence relatively small changes in the background emission will have a major effect on the measured concentrations. This can be shown in changes to precision of platinum SAFT concentrations depending on the background equivalent concentration. For example, if the background equivalent concentration is 2ppm($^{m}/_{m}$) platinum, then the precision of platinum concentrations can be expected at about 2%RSD, whereas if the background equivalent concentration is 10ppm($^{m}/_{m}$) platinum, the precision becomes 7%RSD. Hence the calibration in question having a low slope and a high background equivalent concentration would therefore be of poor quality and would not be desirable for accurate analytical work.

Besides these problems, the question whether the pure platinum calibration standards are biased in comparison to the tailing calibration standards remains. The scatter plot clearly identifies the CONC SA standards as being biased, however it is not clear whether the PURE SA standards also created a bias. A means by which a bias may be identified in a set of data pairs for calibration is a plot of the y-axis residuals. When a plot of the y residuals was examined as shown in Fig.5.11, it was found that a bias was introduced by two sets of calibration standards where platinum was added as pure metal or as PGM concentrate. By deleting each set from the data population, the effect on the line of least squares and the y residuals could be investigated. It was found that both methods of adding platinum to the standards caused biases and therefore any form of standard addition should not be considered for the purpose of extending the calibration range.

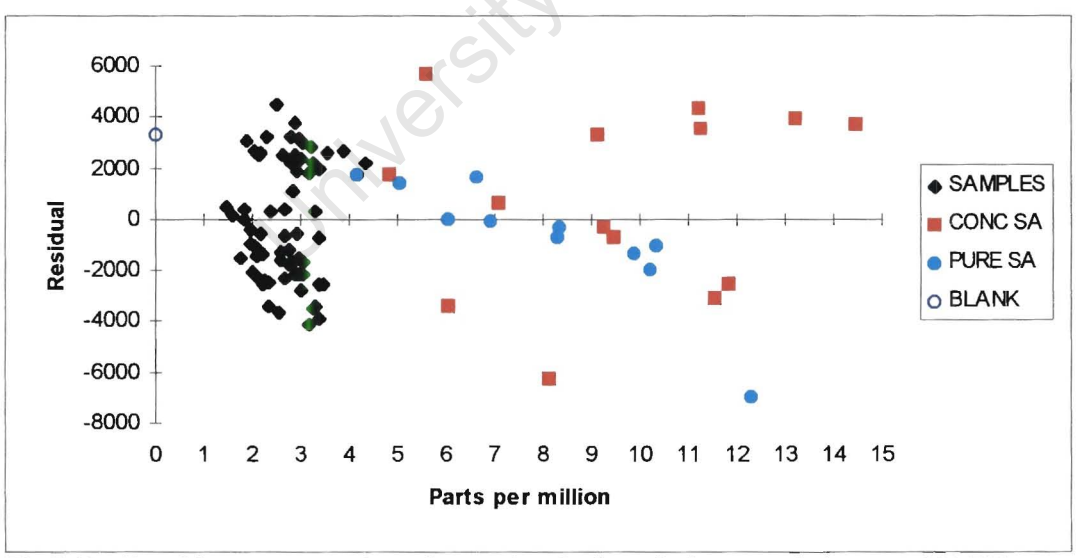

Fig.5.11. Graphic representation of y residuals for platinum emissions at 299.797nm using the M5 spectrometer. "SAMPLES" are all of MERENSKY, UG2 AND MF ore tailing samples.

If the calibration contained only the ore tailing samples to ensure constant lead matrix, as shown in Fig 5.12, and a regression analysis is carried out, the outcome is that there is unacceptably large scatter around the best fit curve (r = 0.62), and therefore this calibration is also unacceptable.

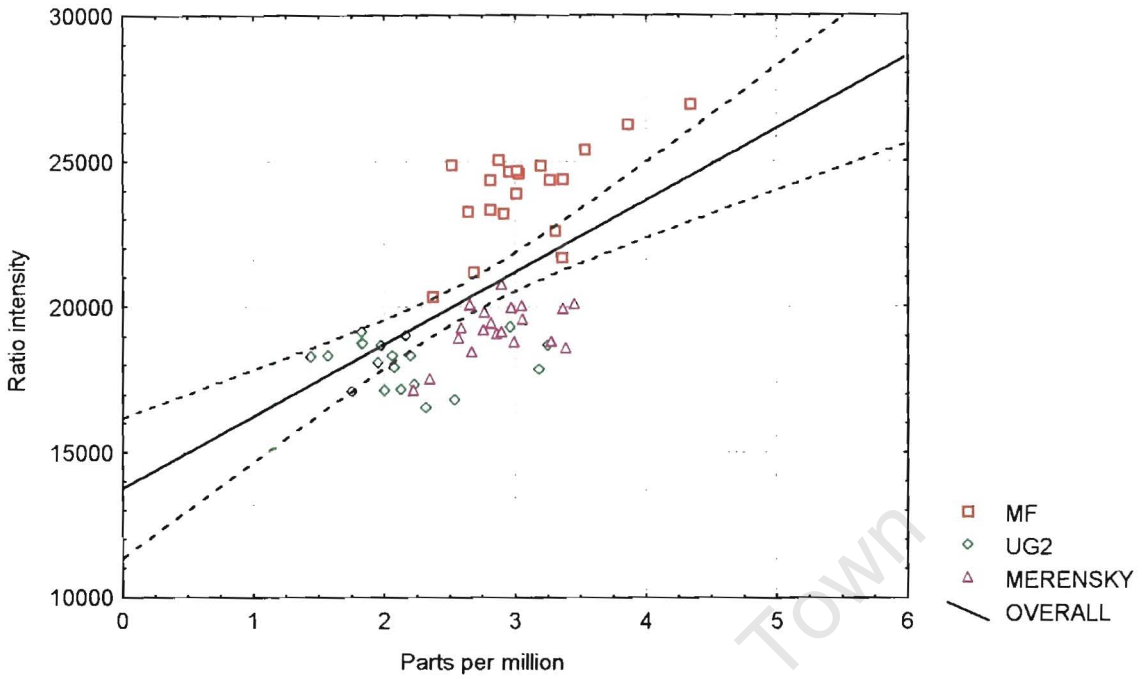

Fig 5.12. Calibration of Pt 299.797nm using the M5 spectrometer with ore tailing samples (MERENSKY, UG2 and MF) only. The regression analysis to describe the curve is r = 0.62, b = 2481, a = 13741.

5.4.1.2. Calibration of platinum using the M7 spectrometer.

The calibration of the two first order platinum emission wavelengths at 265.875nm and 299.797nm was carried out using the M7 spectrometer. At 265.875nm, platinum in the CONC SA standards appeared to fit reasonably closely to the line of least squares projected with the PURE SA standards, with the exception of a few outlying data points (Fig.5.13). The correlation coefficient was 0.97 indicating that this calibration was quite good compared to that obtained using the M5 spectrometer. If the standard addition samples are deleted from the calibration, the ore tailing samples are once again segregated according to type and a working calibration cannot be obtained (Fig.5.14).

At 299.797nm, the standard addition was shown to introduce bias using a y-residuals test (calibration shown in Fig.5.15). Deletion of the standards containing concentrate (CONC SA) and pure metals (PURE SA) produced the calibration (Fig.5.16). where there are only ore tailing samples. The different sample types are grouped, and the correlation coefficient for this population indicated that this calibration was, once again, not acceptable.

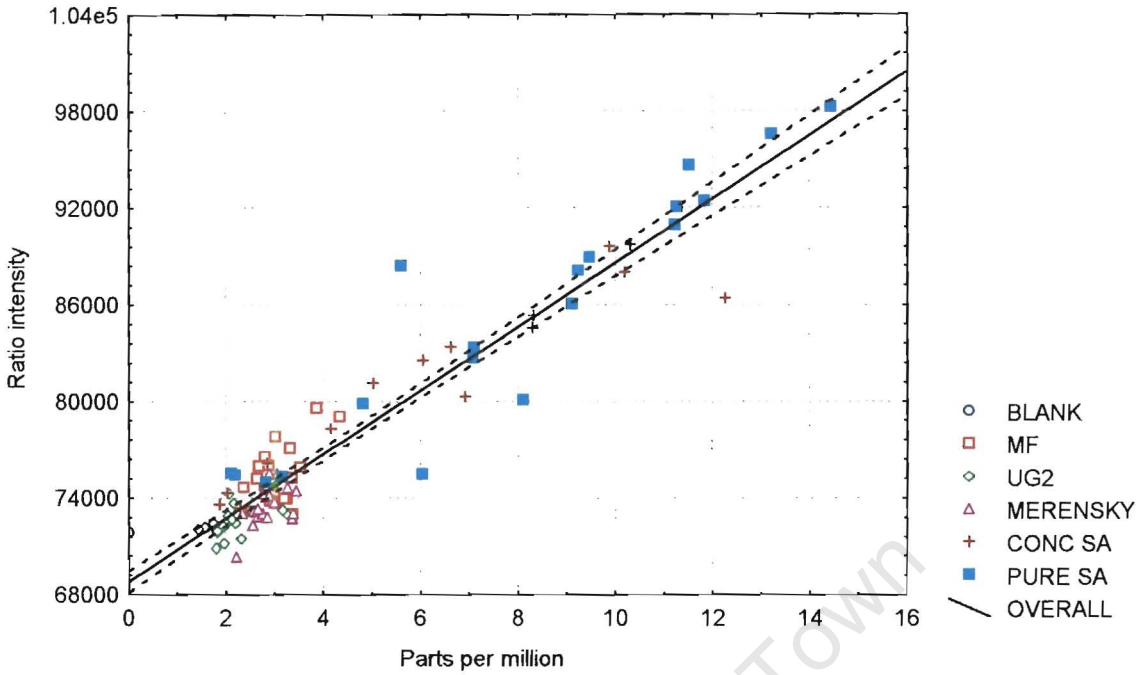

Fig.5.13. Calibration of platinum emissions at 265.875nm in the first order using the M7 spectrometer using ore tailing samples (MERENSKY, UG2, MF) and standard addition materials (CONC SA and PURE SA). The regression analysis to describe the curve to include all data pairs is r = 0.97, b = 1979, a = 68798.

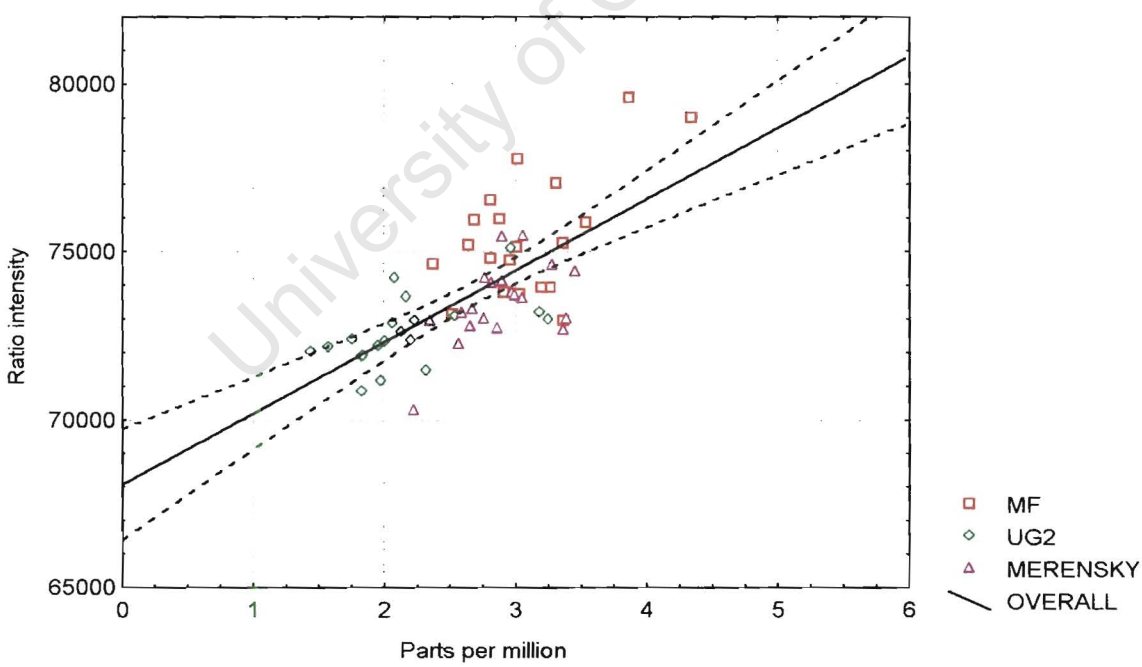

Fig.5.14. Calibration of platinum emissions at 265.875nm in the first order using the M7 spectrometer using ore tailing samples (MERENSKY, UG2, MF) only. The regression analysis to describe the curve to include all data pairs is r = 0.68, b = 2153, a = 67971.

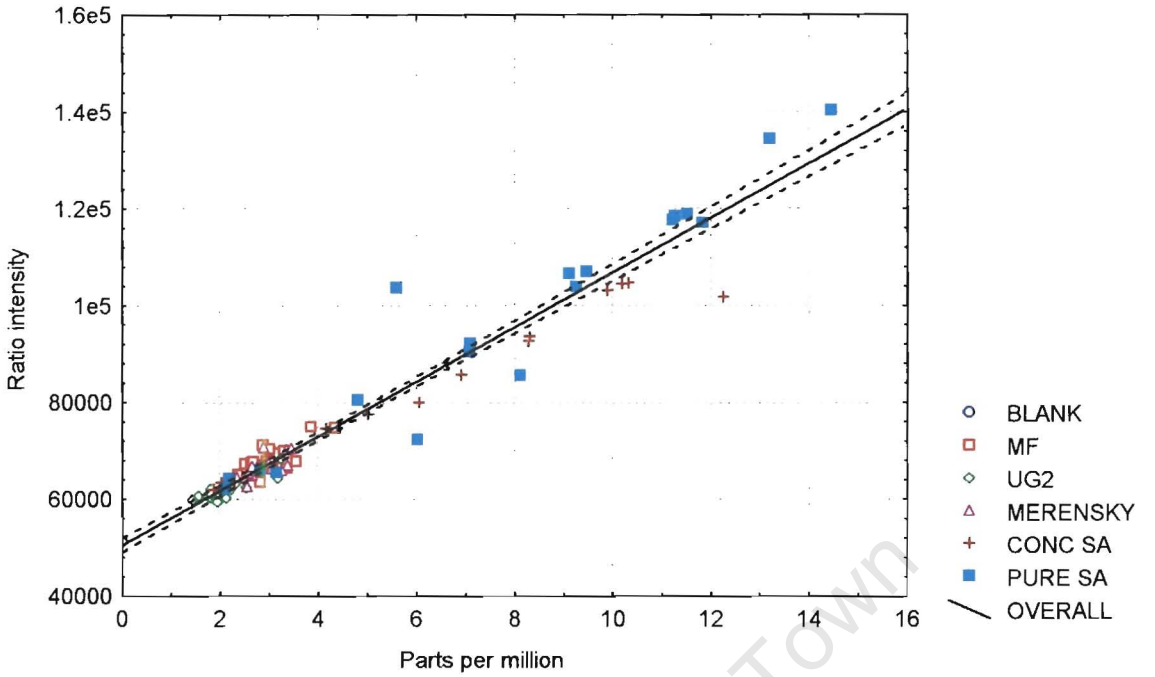

Fig.5.15. Calibration of platinum emissions at 299.967nm in the first order using the M7 spectrometer using ore tailing samples (MERENSKY, UG2, MF) and standard addition materials (CONC SA and PURE SA). The regression analysis to describe the curve to include all data pairs is r = 0.90, b = 5638, a = 50478.

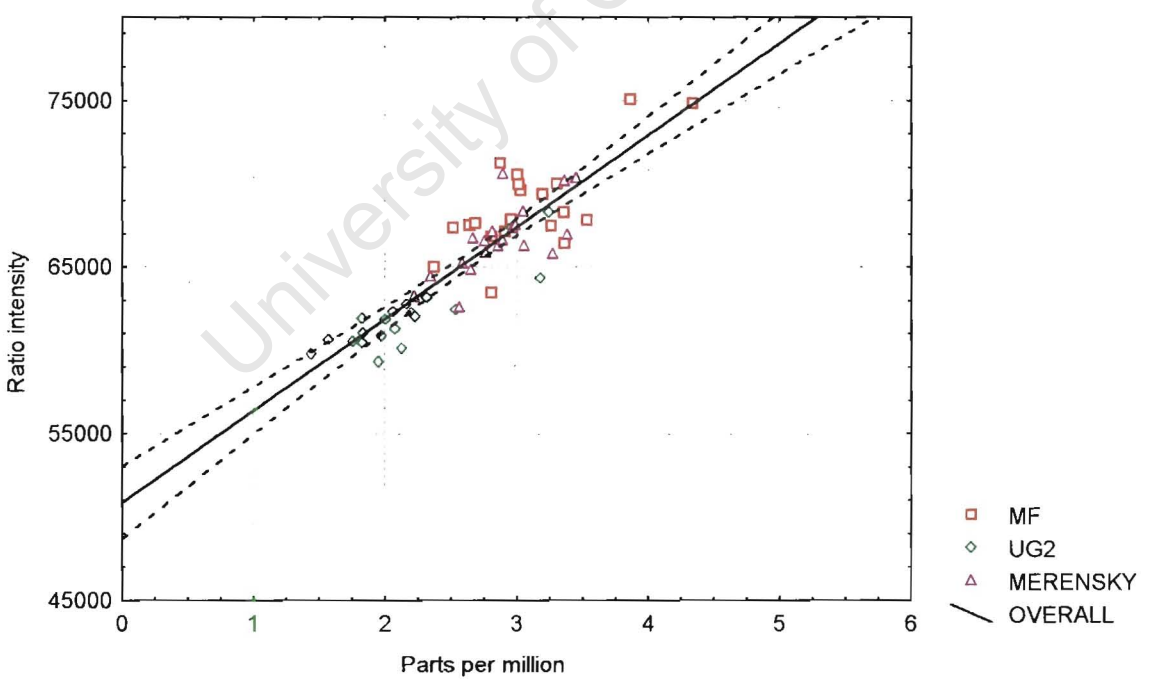

Fig.5.16. Calibration of platinum emissions at 299.967nm in the first order using the M7 spectrometer using ore tailing samples (MERENSKY, UG2, MF) only. The regression analysis to describe the curve is r = 0.88, b = 5532, a = 50794.

Calibrations for platinum emissions at their second order wavelengths (531.93nm and 598.81nm) were not improved, the reduced sensitivity being an additional negative aspect (Fig.5.17 to Fig.5.20).

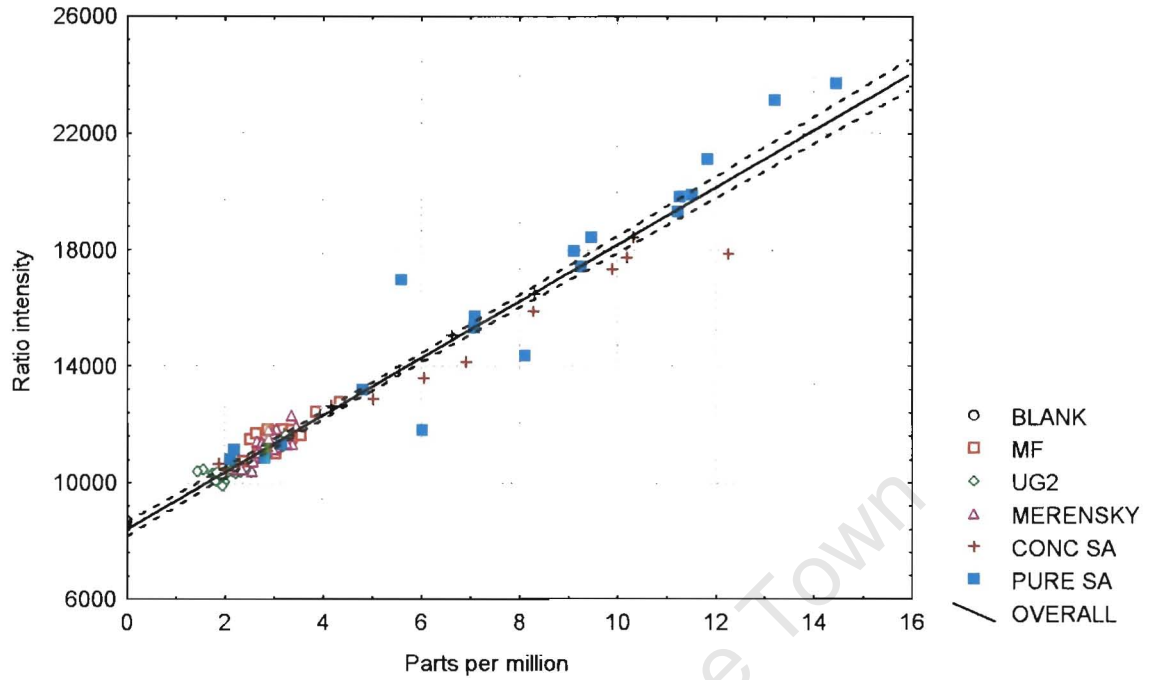

Fig 5.17. Calibration of platinum emissions at 531.93nm in the second order using the M7 spectrometer using ore tailing samples (MERENSKY, UG2 and MF) and standard addition materials (CONC SA and PURE SA). The regression anlaysis to describe the curve is r = 0.99, b = 979, a = 8413.

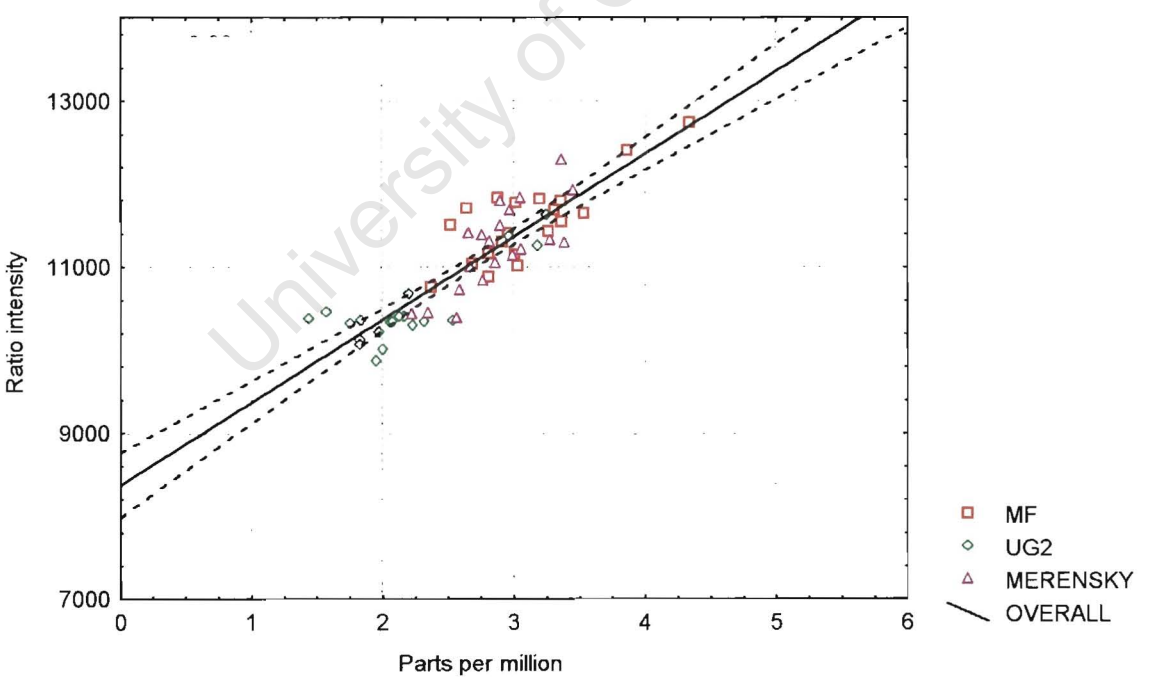

Fig 5.18. Calibration of platinum emissions at 531.93nm in the second order using the M7 spectrometer using ore tailing samples (MERENSKY, UG2 and MF) only. The regression anlaysis to describe the curve is r = 0.88, b = 998, a = 8374.

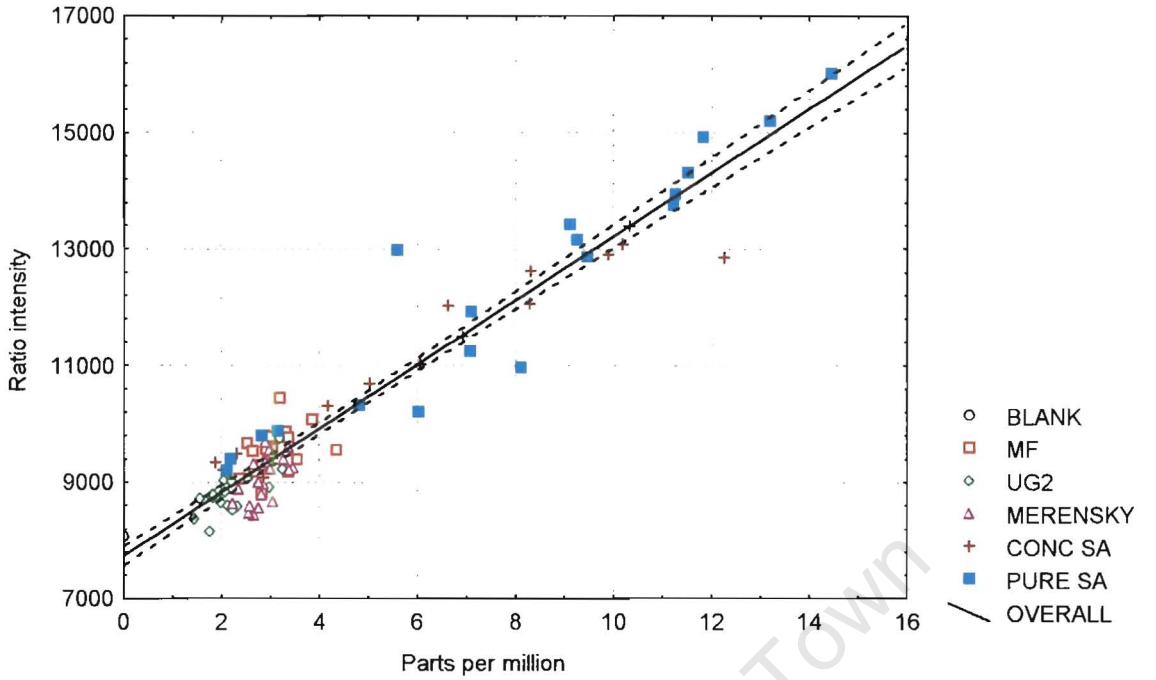

Fig 5.19. Calibration of platinum emissions at 598.813nm in the second order using the M7 spectrometer using ore tailing samples (MERENSKY, UG2 and MF) and standard addition materials (CONC SA and PURE SA). The regression anlaysis to describe the curve is r = 0.97, b = 548, a = 7737.

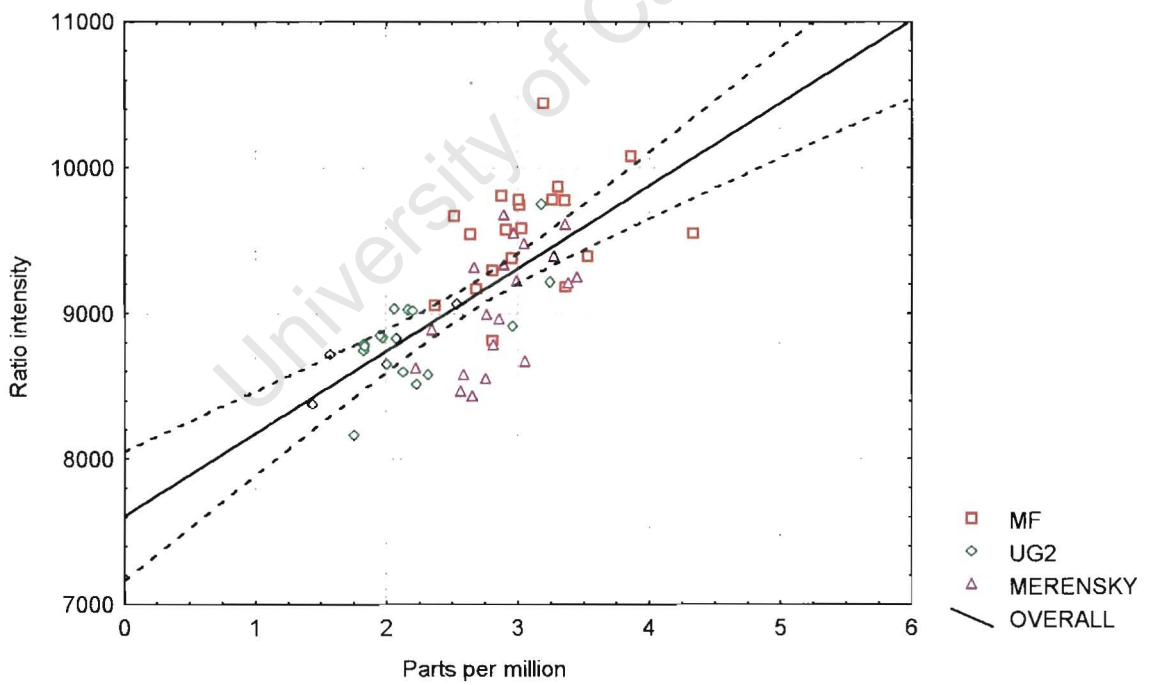

Fig 5.20. Calibration of platinum emissions at 598.81nm in the second order using the M7 spectrometer using ore tailing samples (MERENSKY, UG2 and MF) only. The regression anlaysis to describe the curve is r = 0.68, b = 569, a = 7602.

To obtain a general idea of the performance of the SAFT for measurement of platinum using both spectrometer versions, a comparison of the regression data obtained for each platinum wavelength was made. It was felt that there was more confidence in fitting the line of least squares over a greater concentration range, the instrument response being the critical factor rather than the accuracy. Keeping the data population the same for the regression analysis performed for each platinum wavelength for both spectrometers, a good comparison of the performance of each could be obtained. (The ore tailing samples and standards addition samples were included in the calibrations, but those data points where platinum was spectrally enhanced by nickel emissions were excluded.)

Table 5.2. Summary of the regression analysis of the calibrations carried out for platinum emissions at different wavelengths using the M5 and M7 versions of SAFT spectrometer.

Spectrometer	Emission λ (nm)	A	S_a	b	S_b	g	Sx_0 at 3.4ppm($^m/_m$)	$x_0 \pm tSx_0$
M7	299.967	51945	69.4	5092	18.2	0.00005	0.195	$x_0 \pm 0.38$
M7	265.87	68735	59.3	1990	15.6	0.0002	0.427	$x_0 \pm 0.84$
M7	598.81	7742	82.6	544	21.7	0.006	0.397	$x_0 \pm 0.78$
M7	531.93	8637	13.5	900	3.6	0.00006	0.215	$x_0 \pm 0.42$
M5	299.967	14667	92.1	2281	24.2	0.0004	0.579	$x_0 \pm 1.13$
M5	306.47	310475	4331	34602	1139	0.004	1.79	$x_0 \pm 3.51$

a = intercept,
b = slope,
S_a = standard deviation of the intercept,
S_b = standard deviation of the slope,
g = Sx_0 is an approximation that is only valid when the function g has a value less than 0.05. g is defined at the end of Section 4.1 of Appendix 3. For g to have low values, the slope and the sum of the differences of each concentration from the mean concentration squared must be large relative to the sum of the y-residuals squared.
Sx_0 = standard deviation of a single concentration derived from the instrument signal (y value),
tSx_0 = confidence limits of a single concentration derived from the instrument signal (y value) where t has been chosen at 95% confidence.

The level of confidence of low level platinum concentrations below 16ppm obtained using the M5 spectrometer was found to be very poor. For example, there could be an error of ±3.5ppm($^m/_m$) at a typical concentration of 2 to 3ppm($^m/_m$) platinum in lead from an ore tailing sample at 306.47nm, and ±1ppm($^m/_m$) error at the same sample concentration when measured at the 299.967nm platinum wavelength.

The best analysis that could be achieved using the M7 spectrometer could be expected at 299.967nm with a platinum concentration error of ±12% at 3ppm($^m/_m$). A graphical representation of the sensitivity of both SAFT spectrometer versions using the platinum wavelength at 299.967nm showed that the M7 spectrometer was more sensitive, however it suffered higher background emissions than the M5. A diagram showing the differences can be seen in Fig.5.21. The background equivalent concentrations and limits of detection for the platinum emissions at the different wavelengths were calculated to be as follows in Table 5.3 using the formulae applied in Appendix 3, Section 1.1.1 and 1.2.

Table 5.3. BEC and LOD for platinum at different wavelengths using SAFT.

Spectrometer	Wavelength (nm)	BEC (ppm($^m/_m$))	LOD (ppm($^m/_m$))
M7	299.967	10	0.04
M7	265.87	35	0.09
M7	598.81	14	0.46
M7	531.93	9	0.05
M5	299.967	6	0.12
M5	306.47	9	0.38

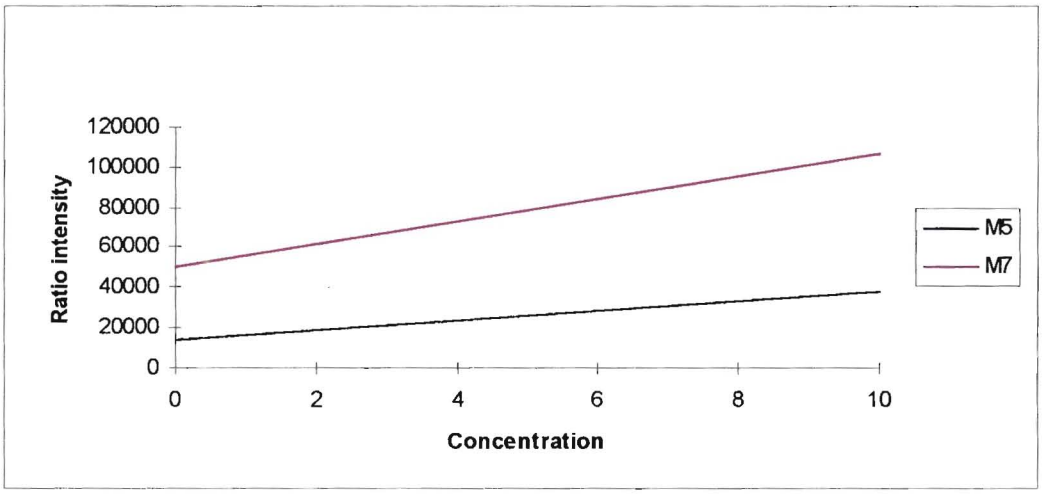

Fig.5.21. Comparison of sensitivity of both the M5 and M7 spectrometers for platinum emissions at 299.967nm.

A summary of the problems experienced with the platinum analysis in ore tailing samples by SAFT is as follows.

i) The concentration of platinum in lead is low and fairly close to the limit of detection of the SAFT.

ii) The insensitivity of the platinum wavelengths is a major problem; the most sensitive line at 306.47nm cannot be used because of an uncorrectable nickel spectral interference, the nickel being present in the lead together with the platinum that originates from the ore samples.

iii) The background emissions and hence the background equivalent concentration of platinum for all selected platinum wavelengths is high and therefore the precision of *concentrations* is very poor.

iv) Platinum in the ore tailing samples has a limited concentration range.

v) Platinum by SAFT is extremely sensitive to matrix effects.

vi) There is an inherent error of about 10%(rel) in platinum concentrations obtained from the nickel sulfide method of analysis, these values being used for SAFT calibration standard concentrations.

5.4.2. Calibrations for palladium and rhodium.

The wavelengths available for measuring emissions of palladium and rhodium were at 340.46nm and 343.49nm respectively using both the M5 and M7 SAFT spectrometers. Scatter diagrams were constructed for the SAFT emissions recorded as ratio intensities (ratioed to lead), and the corresponding concentrations of palladium and rhodium respectively.

The set of calibration standards that were used for platinum was also used for palladium and rhodium, the emission data obtained simultaneously. The calibration plots for the latter elements are shown in Fig.5.22 to 5.29. As with platinum, the graphs are presented in pairs showing, in the first instance, a plot of the combined effect of ore tailing samples and standards containing the added PGM material, and secondly, a plot of the ore tailing samples only.

It was found that there was still evidence of segregation of the three samples types although this was not as pronounced as it had been for platinum. There was still evidence though that if a line of least squares was fitted independently to each type of standard where PGM material had been added there would be two separate lines. This indicated that, as in the case of platinum, the use of standard addition should not be used to extend the concentration range as the accuracy of calibration is affected.

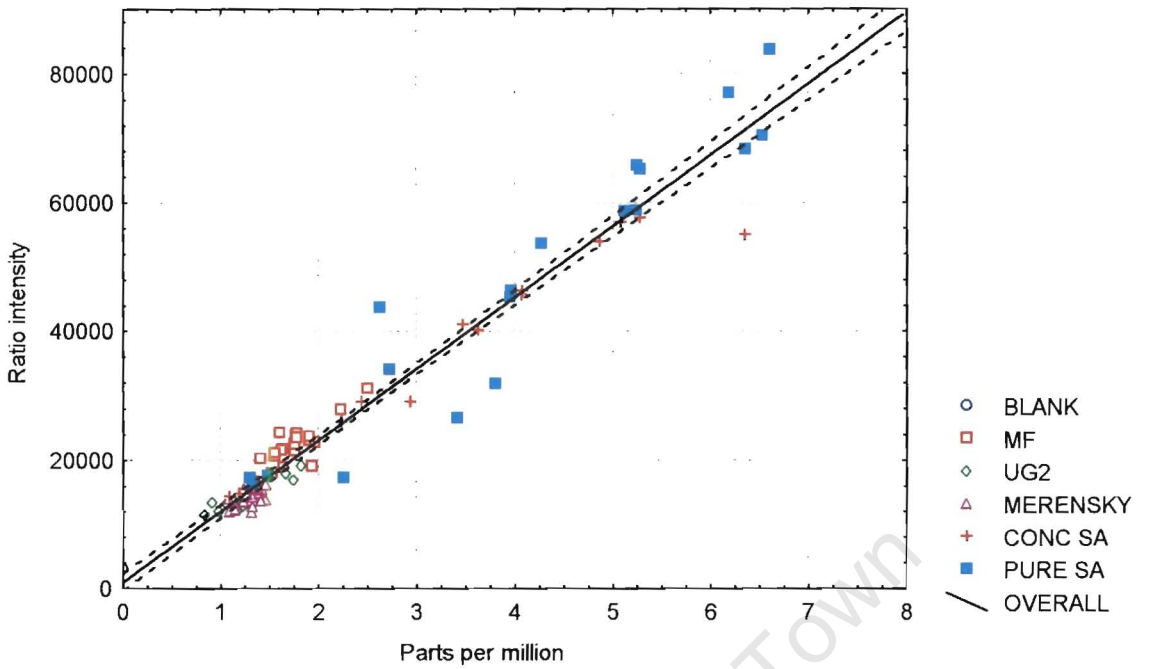

Fig. 5.22. Calibration of palladium at 340.46nm using the M5 SAFT spectrometer with ore tailing samples (MERENSKY, UG2, MF) and standard addition materials (CONC SA and PURE SA). The regression analysis to describe the curve is r = 0.98, b = 11079, a = 985.

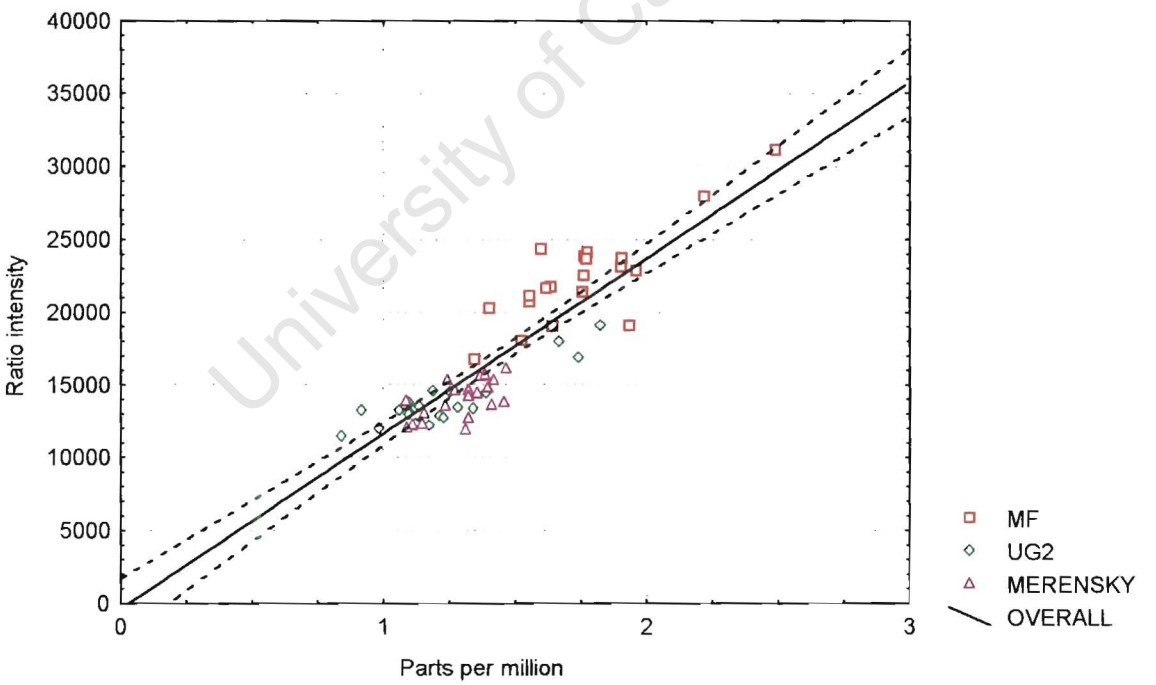

Fig. 5.23. Calibration of palladium at 340.46nm using the M5 SAFT spectrometer with ore tailing samples (MERENSKY, UG2, MF) only. The regression analysis to describe the curve is r = 0.91, b = 12868, a = −1637.

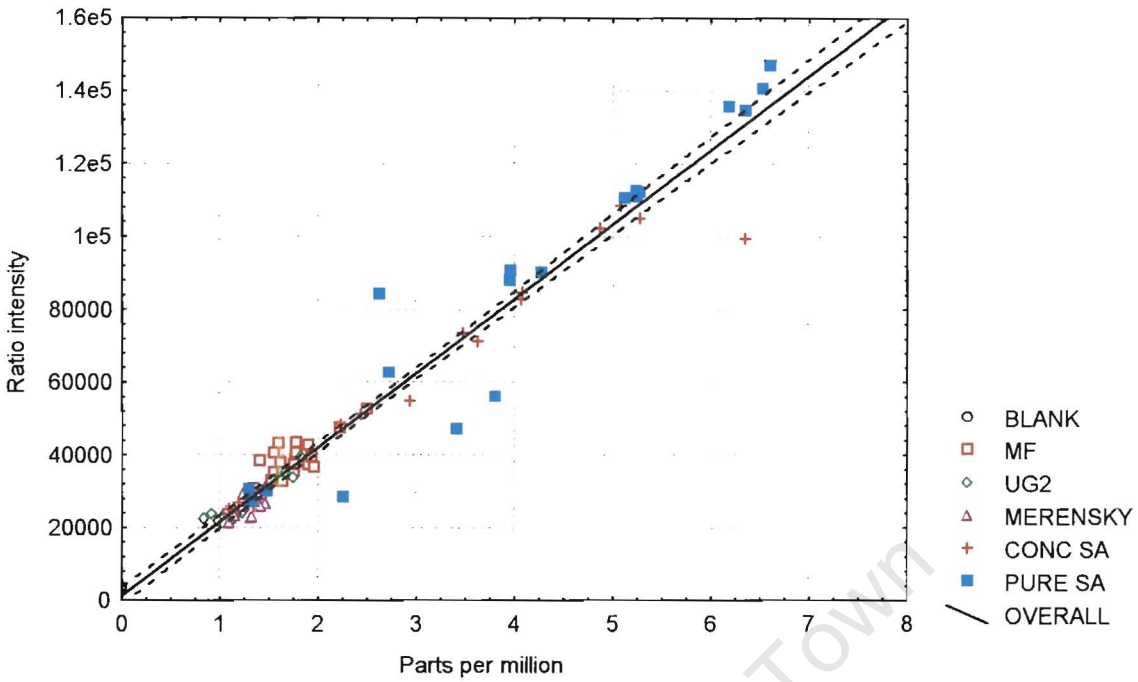

Fig. 5.24. Calibration of palladium at 340.46nm using the M7 SAFT spectrometer with ore tailing samples (MERENSKY, UG2, MF) and standard addition materials (CONC SA and PURE SA). The regression analysis to describe the curve is r = 0.98, b = 20400, a = 1315.

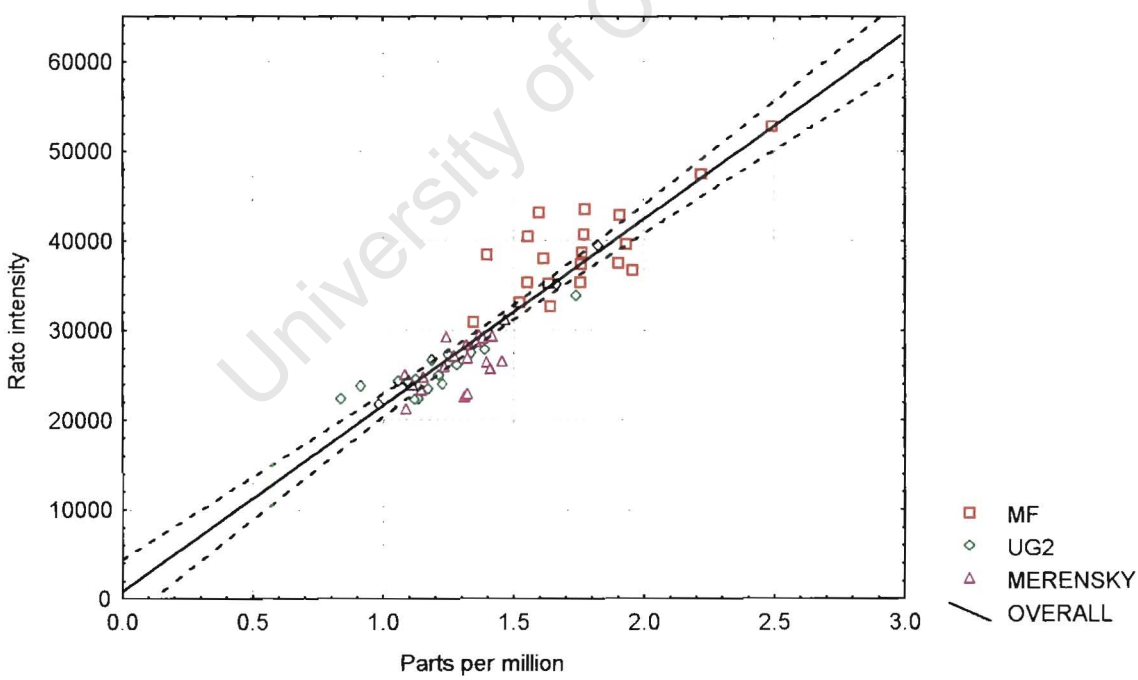

Fig. 5.25. Calibration of palladium at 340.46nm using the M7 SAFT spectrometer with ore tailing samples (MERENSKY, UG2, MF) only. The regression analysis to describe the curve is r = 0.91, b = 20832, a = 767.

It is interesting to note that a negative intercept was calculated for palladium when ore tailing samples only were measured using the M5 spectrometer (Fig.5.23). This was the only case recorded like this and is a clear indication there is something wrong with this calibration. The equivalent measurements taken using the M7 gave a positive intercept close to zero (Fig.5.25). The slope was of the order of 20 000 and intercept at about 800 intensity units, hence giving good sensitivity with low background. The unsatisfactory correlation coefficient (r = 0.91) was therefore partly due to either the applied concentration values (about 10%(rel) concentration error obtained due to the nickel sulfide method) or that the matrix of the standard samples derived from different ore tailing samples affected the palladium emissions adversely.

A similar situation to palladium existed with rhodium where high sensitivity and low background emissions were found using both instruments. See Fig.5.26 to 5.29. There was also an inherent error of about 10%(rel) due to the error of the nickel sulfide values assigned to the calibration standard concentrations.

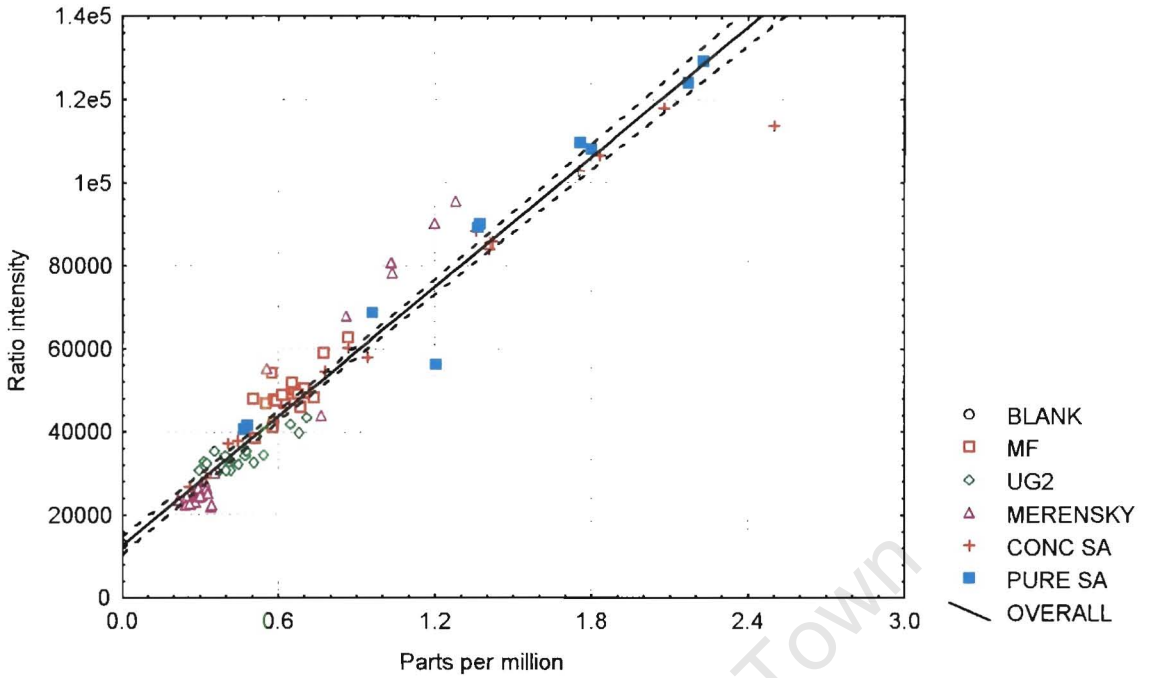

Fig. 5.26. Calibration of rhodium 343.49nm using the M5 SAFT spectrometer with ore tailing samples (MERENSKY, UG2, MF) and standard addition materials (CONC SA and PURE SA). The regression analysis to describe the curve is r = 0.97, b = 52009, a = 12610.

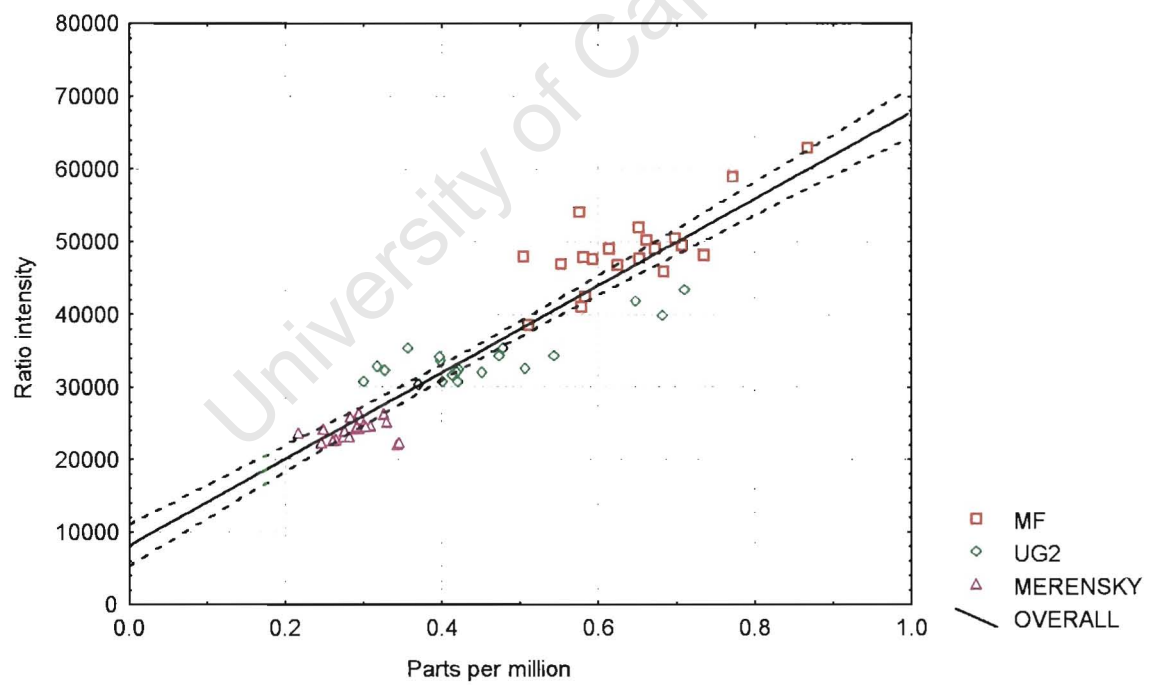

Fig. 5.27. Calibration of rhodium at 343.49nm using the M5 SAFT spectrometer with ore tailing samples (MERENSKY, UG2, MF) only. The regression analysis to describe the curve is r = 0.94, b = 60950, a = 7533.

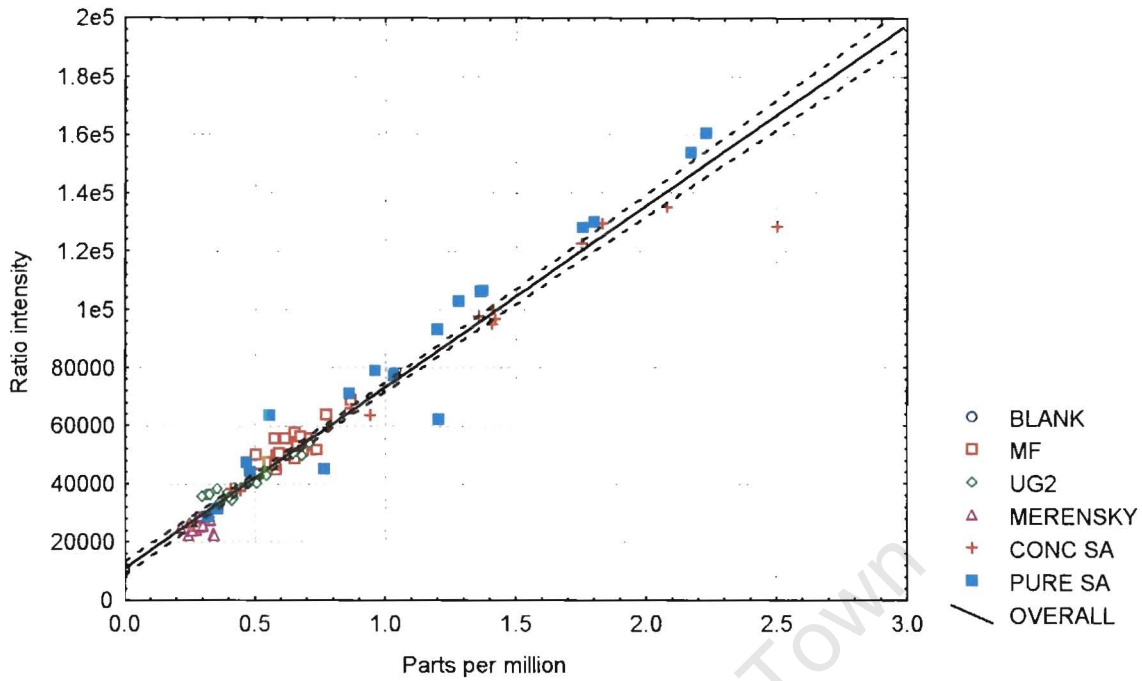

Fig. 5.28. Calibration of rhodium at 344.49nm using the M7 SAFT spectrometer with ore tailing samples (MERENSKY, UG2, MF) and standard addition materials (CONC SA and PURE SA). The regression analysis to describe the curve is r = 0.96, b = 62318, a = 11023.

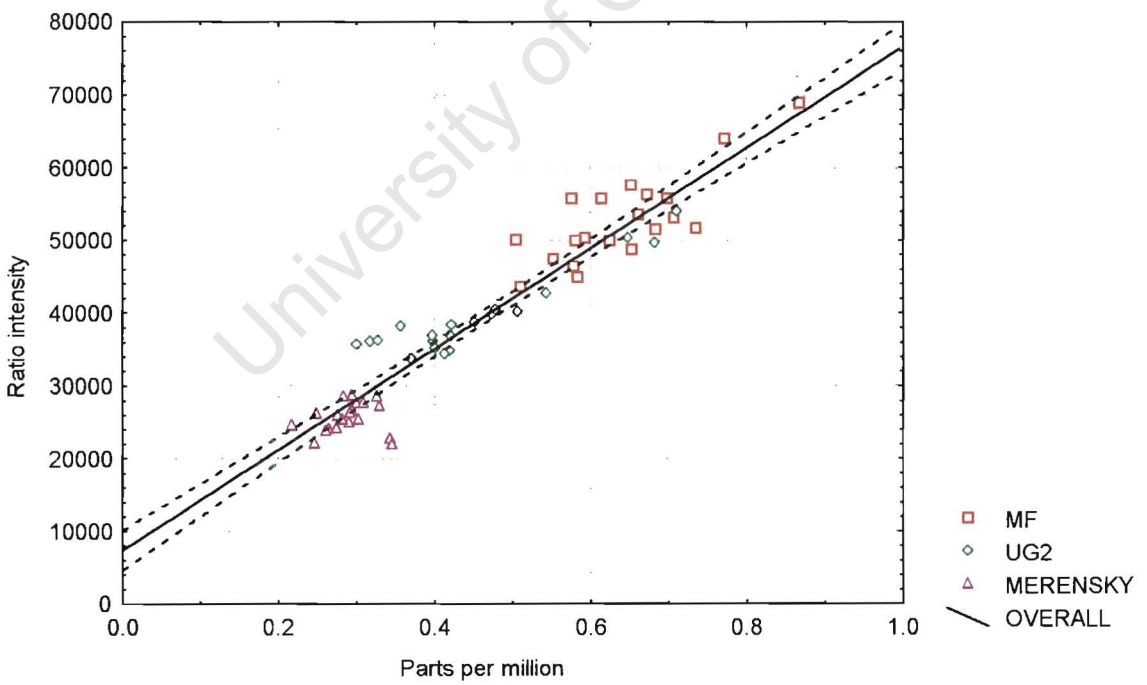

Fig. 5.29. Calibration of rhodium at 343.49nm using the M7 SAFT spectrometer with ore tailing samples (MERENSKY, UG2, MF) only. The regression analysis to describe the curve is r = 0.94, b = 69221, a = 7396.

A comparison of the calibrations obtained using the two spectrometer versions was made to obtain the overall concentration errors at typical concentrations of 1.3ppm($^m/_m$) and 0.5ppm($^m/_m$) for palladium and rhodium respectively in lead given by x_0 as shown in Table 5.4. It can be estimated that probably about half of the error can be attributed to the overall SAFT determination, while the rest is due to the error of the nickel sulfide values used for calibration.

Table 5.4 compares the performance of the two spectrometers for calibration of palladium and rhodium. (Details of the calculations can be found in Appendix 3, Section 4.1.) Ore tailing samples and standards with pure metal added (PURE SA) were included in the calculations. The final concentrate additions (CONC SA) were excluded from the calculations since these data points created a bias to the curves. Calculations for both elements were carried out using three SAFT sparks per lead sample.

Table 5.4. Summary of the regression analysis of the calibrations carried out for palladium and rhodium emissions at different wavelengths using the M5 and M7 versions of SAFT spectrometer.

Spectrometer & element	Emission λ (nm)	a	S_a	b	S_b	g	Sx_0 *	$x_0 \pm tSx_0$
M7 Pd	340.46	1776	319	19991	162	0.0003	0.106	$x_0 \pm 0.208$
M5 Pd	340.46	1229	193	10867	98	0.0003	0.118	$x_0 \pm 0.231$
M7 Rh	343.49	10166	728	63098	1065	0.001	0.035	$x_0 \pm 0.069$
M5 Rh	343.49	11302	770	53210	1127	0.002	0.043	$x_0 \pm 0.084$

*Sx_o is calculated for Pd at 1.323ppm($^m/_m$) and Rh at 0.507ppm($^m/_m$).

a = intercept,
b = slope,
S_a = standard deviation of the intercept,
S_b = standard deviation of the slope,
$g = Sx_0$ is an approximation that is only valid when the function g has a value less than 0.05. g is defined at the end of Section 4.1 of Appendix 3. For g to have low values, the slope and the sum of the differences of each concentration from the mean concentration squared must be large relative to the sum of the y-residuals squared.
Sx_0 = standard deviation of a single concentration derived from the instrument signal (y value),
tSx_0 = confidence limits of a single concentration derived from the instrument signal (y value) where t has been chosen at 95% confidence.

It was found that better sensitivity of both palladium and rhodium was achieved using the M7 spectrometer as shown in Fig.5.30 and 5.31 respectively, and that the background emissions of both metals was relatively low and close to zero (Table 5.5). Therefore when measured results are converted to concentrations the replicate values would be expected to have a low standard deviation and high confidence. However, with real ore samples, the error of analysis was calculated at ±15%(rel) for both palladium and rhodium at levels of 1.3ppm($^m/_m$) and 0.5ppm($^m/_m$) respectively. So although the analysis of palladium and rhodium appears superior to the analysis of platinum by SAFT, there are still problems which make these calibrations for ore tailing samples unsatisfactory, the reasons being as follows.

i) The limited concentration range of both palladium and rhodium in the ore tailing samples.
ii) Palladium and rhodium are both sensitive to matrix effects.
iii) The error (10%(rel)) coming from the nickel sulfide concentration values for these elements.

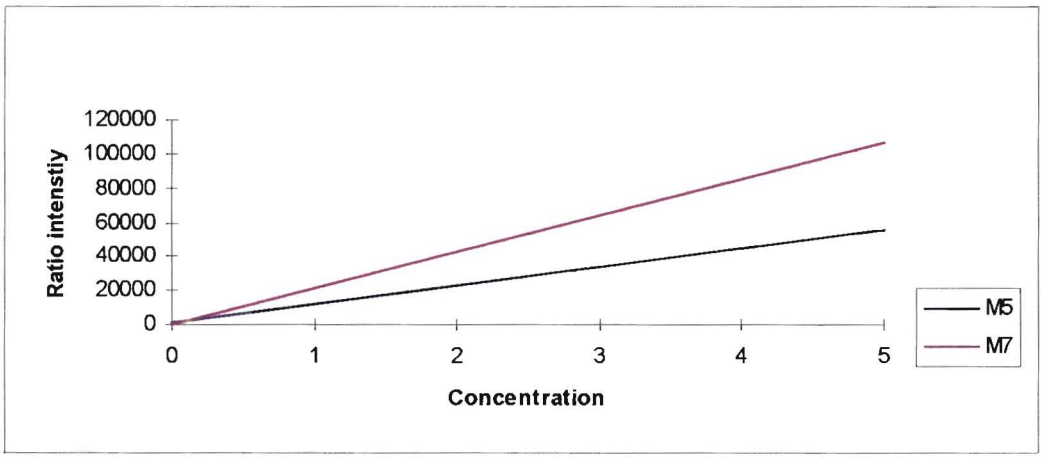

Fig.5.30. Comparison of sensitivity of palladium at 340.46nm for the M5 and M7 SAFT spectrometers.

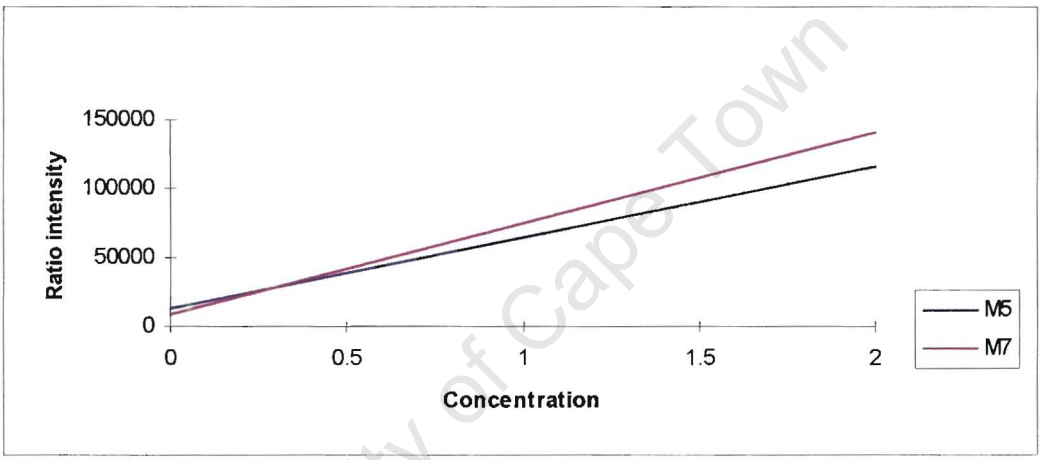

Fig.5.31. Comparison of sensitivity of rhodium at 343.49nm for the M5 and M7 SAFT spectrometers.

The background equivalent concentrations and limits of detection for palladium and rhodium are shown in Table 5.5.

Table 5.5. BEC and LOD for palladium and rhodium using SAFT.

Spectrometer & element	Wavelength (nm)	BEC (ppm($^{m}/_{m}$))	LOD (ppm($^{m}/_{m}$))
M7 Pd	340.46	0.09	0.05
M5 Pd	340.46	0.11	0.05
M7 Rh	343.49	0.16	0.03
M5 Rh	343.49	0.21	0.04

REFERENCES.

1. J.N. Miller, "Basic Statistical Methods for Analytical Chemistry Part 2. Calibration and Regression Methods", *Analyst*, 1991.

2. M.J. Adams, "Chemometrics in analytical Spectroscopy", The Royal Society of Chemistry, Cambridge, 1995.

3. A.G.W. Steyn, C.F.Smit, S.H.C.Du Toit, C.Strasheim, "Modern Statistics in Practice", second edition, J.L. van Schaik, Pretoria, 1996.

4. R.C. Mallet, "Precious Metals Analysis – A New Approach", International Conference on Applied Mineralogy (ICAM91), Symposium on the Platinum Group Metals, 6th September, 1991.

CHAPTER 6.

EFFECT OF SAMPLE MATRIX ON SAFT EMISSIONS IN LEAD BUTTONS.

6.1. Sample composition.

During litharge-based pyrochemical fusions sample decomposition occurs which results in the noble metals being collected by the lead while the rest of the sample components contribute to the formation of slag. In this way the noble metals are separated from the rest of the sample matrix. Most of the research into the chemical processes which occur has been to determine the efficiency of this method of separation and collection of the noble metals, and in identifying the sources of losses of noble metals during the fusion using techniques such as radioisotopic doping. Little interest has been shown in what happens to the other elements originating from the sample matrix other than to assume that all of it goes to the slag. In reality, these other elements could also partially be alloyed with lead, and certainly there was enough evidence from SAFT intensities obtained for base metal emissions in lead buttons to show that significant proportions of some base metals were being collected in the lead along with the noble metals.[1] Because the SAFT determination is spectrometric, the possibility existed that spectral emissions from these elements could interfere with the noble metal emissions at certain wavelengths,[2] or perhaps the physical properties such as hardness of the lead buttons due to the degree of base metal alloying with lead could affect the atomic emissions of the noble metals. It was therefore necessary to qualitatively and quantitatively determine elements other than the noble metals that may be present in the lead, and to assess the extent to which their presence could affect the spectrometric measurement of the coexisting noble metals.

In accordance with all other investigations, ore tailing samples originating from chemical flotation of milled Merensky and UG2 ores were used to generate lead buttons using the fire assay method. The total composition of the different *ore tailing samples* was determined and the base metal composition is shown in Table 6.1.

Table 6.1. Base metal composition of tailing samples originating from chemical flotation of Merensky and UG2 ores.

Tailing sample	%Cu	%Ni	%Fe	%Cr
Merensky ore	0.007	0.054	6.1	1.36
UG2 ore	0.004	0.093	13.1	21.6

Other elements such as total silicon, sulfur, calcium, magnesium and aluminium were also determined. These elements constituted the remaining proportion of the ore sample. Since they are refractory in nature, they collect in the slag during the pyrochemical fusion. The base metals on the other hand are likely to be present as either oxides or silicates and are expected to concentrate in the slag. Lead buttons that were prepared from tailing samples of Merensky and UG2 ores were sparked using SAFT to obtain emission data for platinum, palladium, rhodium, copper, nickel, iron and chromium. Wet chemical methods were then used to dissolve the lead buttons and atomic absorption or inductively-coupled plasma atomic emission spectroscopy (ICP-AES) used to determine the concentrations of impurities in the lead which originate from the ore samples (Appendix 4). Concentrations of platinum, palladium and rhodium in solution were lower than the detection limit of this technique and thus could not be determined concurrently. It was discovered that small quantities of the base metals copper, nickel and iron were alloyed with the lead in varying amounts suggesting that when base metal oxides and silicates are decomposed during the fusion some of these metals collect in the lead and some goes to the slag. Chromium was not found to collect in the lead and therefore must all go to the slag. The concentrations of copper, nickel and iron in lead were then correlated with the corresponding SAFT emissions to establish if a linear relationship existed. The extent to which the base metals would affect the SAFT emissions of the coexisting noble metals could then be assessed using lead buttons containing known amounts of base metals and platinum, palladium and rhodium.

6.2. The relationship between base metal concentrations in lead and their emissions obtained by SAFT.

6.2.1 The distribution of base metals in lead.

It was found that in most lead buttons the sample type could be identified by the unique trends of copper and nickel in the buttons prepared from tailings of either Merensky ore, UG2 ore, or a mixture thereof called MF ore. The SAFT emission data for copper and nickel obtained by sparking various lead buttons of these different ores is presented in Fig.6.1 and 6.2 respectively.

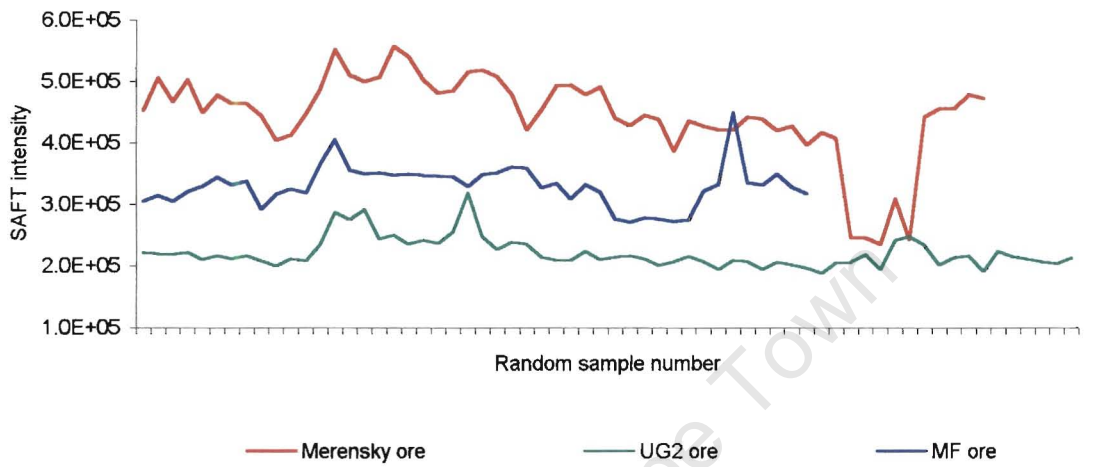

Fig.6.1. The proportion of copper in lead determined by SAFT in flotation tailing samples originating from Merensky, UG2 and MF ores.

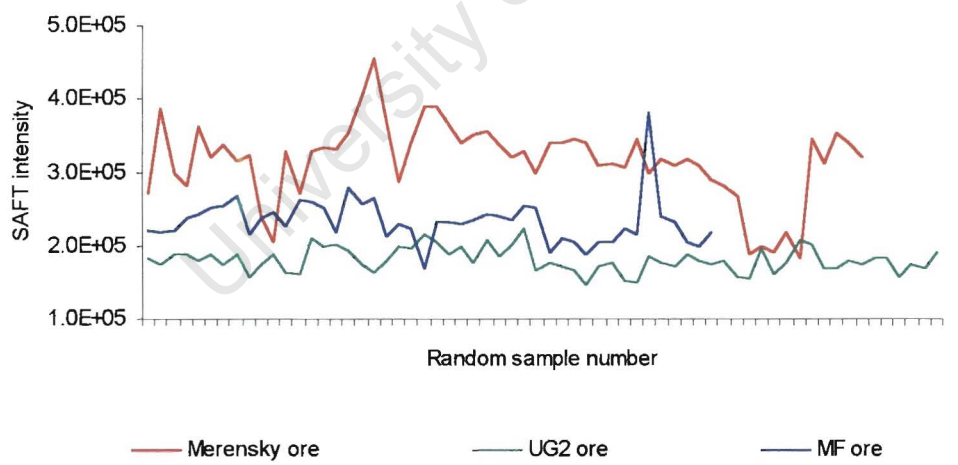

Fig.6.2. The proportion of nickel in lead determined by SAFT in flotation tailing samples originating from Merensky, UG2 and MF ores.

From the SAFT emissions for copper it can be seen that more was found in the lead buttons prepared from fusion of Merensky ore tailing samples than from UG2 ore tailing samples. This is reasonable since Merensky ore contains almost double the concentration of copper than UG2 ore (refer to Table 6.1). When the copper concentration in the lead was calculated in relation to the total copper present in the aliquot of tailing sample taken for analysis, it was found that copper is most probably quantitatively collected by lead for these sample

types. The third flotation tailing sample type referred to as MF ore was also prepared by fusion to produce lead buttons. Analysis for copper confirmed that it was also virtually all collected by the lead. The data pertaining to these tests is presented in Table 6.2.

Table 6.2. Details of concentration and SAFT emission measurements for copper in lead prepared from flotation tailing samples of Merensky, UG2 and MF ores.

Flotation tailing ore sample	Mean SAFT intensity for n	% RSD of intensities for n	Equivalent concentration ($ppm(^{m}/_{m})$)	Number of samples analysed n
Merensky	445862	15.7	355	58
UG2	221639	11.0	139	64
MF	330460	9.9	244	46

The %RSD of intensities is used to describe the range of variation of copper emissions obtained by SAFT for the total number of samples per sample type. Since the copper concentration within ore sample types is fairly constant, the variations in emissions seen in the lead buttons may in fact be due to occasional fusions where not all the copper is collected by the lead. Also there is a 6%(rel) variation in button mass which contributes to dilution error. This cannot be corrected for since emission intensities are used.

In the case of nickel (Table 6.3) the emission data indicates that more nickel is collected in lead from Merensky ore tailings than from UG2 ore tailings. The concentrations given in Table 6.1 shows the UG2 ore tailing to be richer in nickel than the Merensky ore tailing. Nickel emissions in lead samples prepared from mixed MF ore tailings were found to give expected intermediate concentrations.

Table 6.3. Details of concentration and SAFT emission measurements for nickel in lead prepared from flotation tailing samples of Merensky, UG2 and MF ores.

Flotation tailing ore sample	Mean SAFT intensity for n	% RSD of intensities for n	Equivalent concentration ($ppm(^{m}/_{m})$)	Number of samples analysed n
Merensky	315765	17.0	249	58
UG2	180865	9.2	208	64
MF	233682	13.5	224	46

The proportion of nickel found in the lead buttons after fusion in relation to the total nickel present in the analytical sample was calculated. It was found that approximately 10%(rel) of the total nickel present in the Merensky ore tailing sample and 7%(rel) from the UG2 ore tailing sample was taken up by the lead.

Since platinum group minerals are predominantly associated with base metal sulfides, ores that are processed by chemical flotation produce a concentrated portion of valuable sulfidic platinum group metals together with the associated base metals, and a separate proportion of waste gangue. The gangue or flotation tailing which is low in concentrations of *total* copper and nickel (Table 6.1) can be determined using wet chemical analysis for the *sulfidic* proportion in tailing samples originating from Merensky and UG2 ores. In the case of nickel, Merensky tailing samples were found to have about 0.03%(rel) sulfidic nickel, while the nickel in UG2 ore tailing samples was found to be almost entirely non-sulfidic. This means that the 250ppm($^{m}/_{m}$) of nickel determined in the lead represents only about 19%(rel) of the sufidic nickel typically present in tailings from Merensky ore. Therefore the quantity of nickel collected by the lead during the fusion cannot be related merely to the quantity of sulfidic nickel in the analytical sample.

However the mineralogical nature of the different sample types must have an influence the migration of nickel and copper into the lead since the quantities found in the lead are unique to each sample type. If this quantity is dependent purely on the alloy capability of lead and nickel then one would not expect to see characteristic trends of the different sample types.

The situation concerning iron was found to be different to copper and nickel as can be seen in Fig.6.3. The amount of iron extracted from the different sample types and collected by the lead did not show any characteristic trends. The UG2 ore tailing samples have approximately double the percent quantity of iron as the Merensky ore tailings (Table 6.1), yet the concentration of iron found in the lead was less than 100ppm($^{m}/_{m}$) and there were no characteristic trends relating concentration of iron to the sample type.

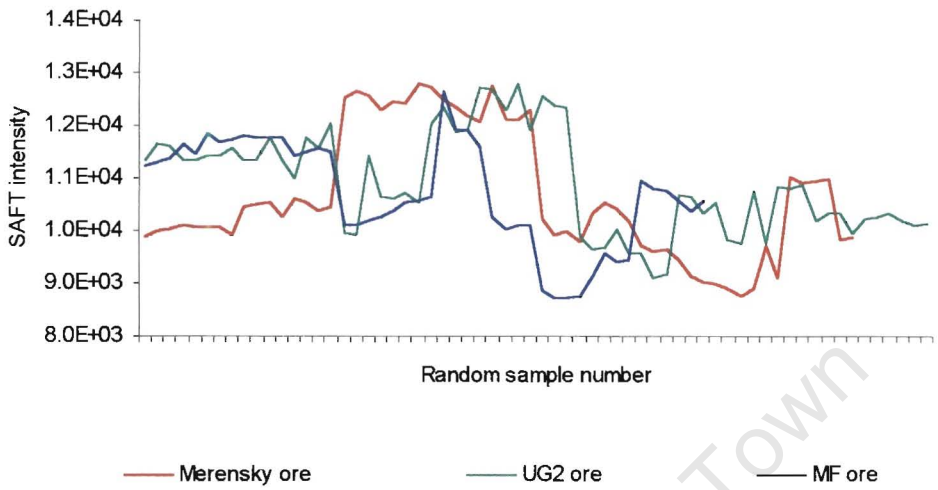

Fig.6.3. The proportion of iron in lead determined by SAFT in flotation tailing samples originating from Merensky, UG2 and MF ores.

Details of the iron concentrations determined using wet chemical methods and the corresponding SAFT intensities for iron emissions in the same lead buttons are shown in Table 6.4.

Table 6.4. Overall concentration and SAFT emission measurements for iron in lead prepared from flotation tailing samples of Merensky, UG2 and MF ores.

Flotation tailing ore sample	Mean SAFT intensity for n	% RSD of intensities for n	Equivalent concentration (ppm($^{m}/_{m}$))	Number of samples analysed n
Merensky	10674	11.2	93	58
UG2	10930	8.7	63	64
MF	10734	9.2	86	46

Occasionally the precision of iron emission intensities was found to be extremely poor. This suggested that there were localised areas of high concentrations of iron embedded in the lead.

6.2.2. Calibrations for copper, nickel and iron.

The atomic emissions for nickel, copper and iron were plotted against the concentrations obtained in the same lead buttons.

In the case of copper, all three sample types contributed to a linear calibration where the Merensky ore tailing samples ranged from about 250ppm($^{m}/_{m}$) to 420ppm($^{m}/_{m}$) and UG2 ore tailing samples between about 110ppm($^{m}/_{m}$) and 170ppm($^{m}/_{m}$), while copper in MF samples ranged as expected at intermediate concentrations. This is shown in Fig. 6.4.

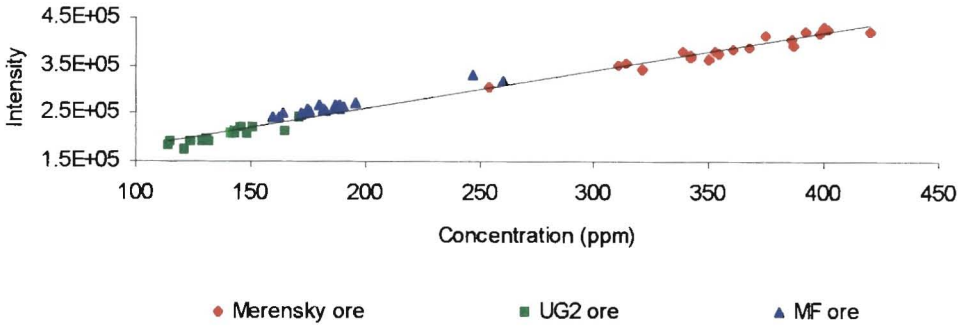

Fig.6.4. The calibration of copper in lead using SAFT. (r = 0.98).

The correlation of the concentrations determined by atomic absorption and the intensities obtained by SAFT emission is reasonably good. This indicates that the copper can be determined fairly accurately in lead and is homogeneously distributed.

Inspection of the emission intensities and concentrations of nickel in lead as shown in Fig.6.5, shows that the overall concentration range was from 150ppm($^{m}/_{m}$) to 340ppm($^{m}/_{m}$) and that the different sample types did not exhibit unique clusters as in the case of copper. The scatter of the data pairs (correlation coefficient r = 0.13) indicates that an acceptable calibration for nickel is not possible.

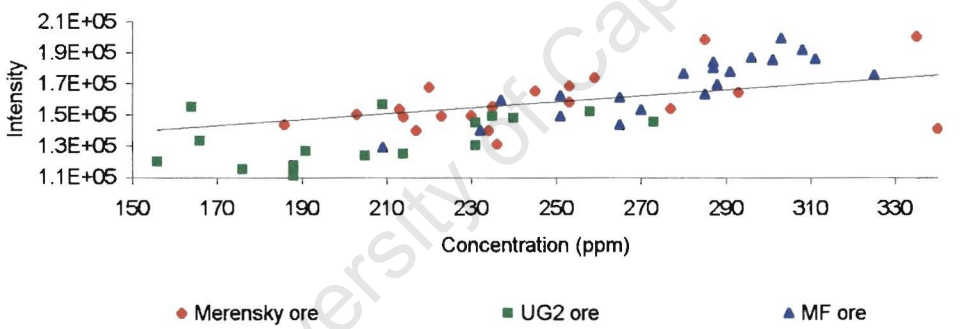

Fig.6.5. The calibration of nickel in lead using SAFT. (r = 0.13).

A comparison of Fig.6.4 and 6.5 shows that the relative proportions of nickel in lead buttons prepared from the three different sample types were different to the relative proportions of copper in the same lead buttons derived from the same samples.

The poor correlation of emission and concentrations for nickel suggests that there is variable collection of nickel by lead during the assay fusion. Also there was evidence of non-uniform distribution of nickel in the lead button matrix given by the poor precision (up to 18% RSD) of replicate determinations both for SAFT by emission and for ICP-AES for concentration measurements. The tailing samples themselves are considered to be reasonably homogeneous, and since 200g of Merensky ore and 150g UG2 ore tailing samples are taken as the analytical aliquot for fusion, it is acceptable that the contribution of error due to the nature of the sample is very small. Hence the problems experienced with the nickel in the lead can be directly related to what happens during the fusion of the sample, and each fusion can be expected to behave in a unique way where random amounts of nickel are collected in the lead.

The copper by contrast however is virtually totally collected by the lead. This proves that the chemical reactions that occur during the pyrochemical fusion are very complex and the theoretical explanations in literature where all base metals migrate to the slag may not apply in practice.

Fig.6.6 shows the variation of iron collected in lead, in concentrations less than 100ppm($^{m}/_{m}$) for the three sample types. It was found that there was poor precision at between 12 to 35% RSD of iron concentrations when determined by wet chemical methods which tends to indicate uneven distribution of iron in the lead. This was confirmed by the poor precision of SAFT emissions, which occasionally showed exceptionally high concentrations of iron for a particular spark. This problem must certainly contribute to not being able to find a linear relationship between the concentrations and emissions of iron in lead.

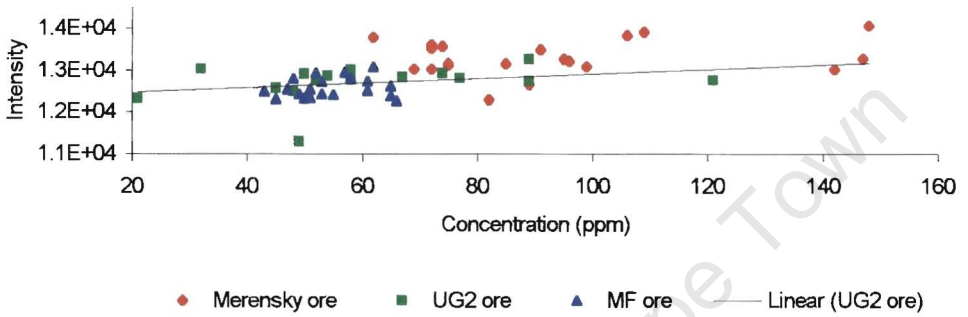

Fig.6.6. The calibration of iron in lead using SAFT. (r = 0.32).

6.3. Effects due to base metal content in lead on noble metal analysis by SAFT.

Literature could not be found concerning the collection of copper, nickel and iron at low concentrations of less than 1000ppm($^{m}/_{m}$) in lead. References are available for alloys of lead with higher levels such as 10%($^{m}/_{m}$) platinum and copper but these have no relevance to the trace level analysis of our research.

Our present investigations have clearly shown that besides the noble metals collecting in lead during pyrochemical fusions, variable amounts of copper, nickel and iron are also collected (Fig.6.1, 6.2 and 6.3). It is therefore important to assess the effects that these base metals have on the analysis of platinum, palladium and rhodium in lead by SAFT.

In order to do this a number of lead buttons were prepared containing various amounts of base metals. Each was then determined for physical hardness. This information was then related to the corresponding effects seen on the noble metal emission lines when each button was sparked using SAFT.

6.3.1. Method of preparation of lead containing an extended range of base metals.

Previous investigations had shown that there was limited variation in the concentration of base metals in lead when ore tailing samples were prepared (Tables 6.2, 6.3 and 6.4). Initial tests on a few of these buttons for variation in hardness relative to base metal content were inconclusive. To establish without doubt their possible effect on the hardening of the lead it was necessary to prepare lead buttons containing a much wider range of base metals.

Incremental amounts of fine powdered pure copper, nickel and iron were mixed with 150g aliquots taken from a single flotation tailing sample of UG2 ore. The maximum mass of each element added was 1750mg per 150g ore tailing sample. This is a relatively small quantity when one considers that the total content of flux and

sample in the crucible to be fused is about 500g, and that the resultant lead button after fusion weighs about 40g.

The SAFT emissions of copper, nickel and iron were determined by sparking each button and the intensity data obtained was compared to the original quantities added to the sample prior to fusion as can be seen in Fig.6.7.

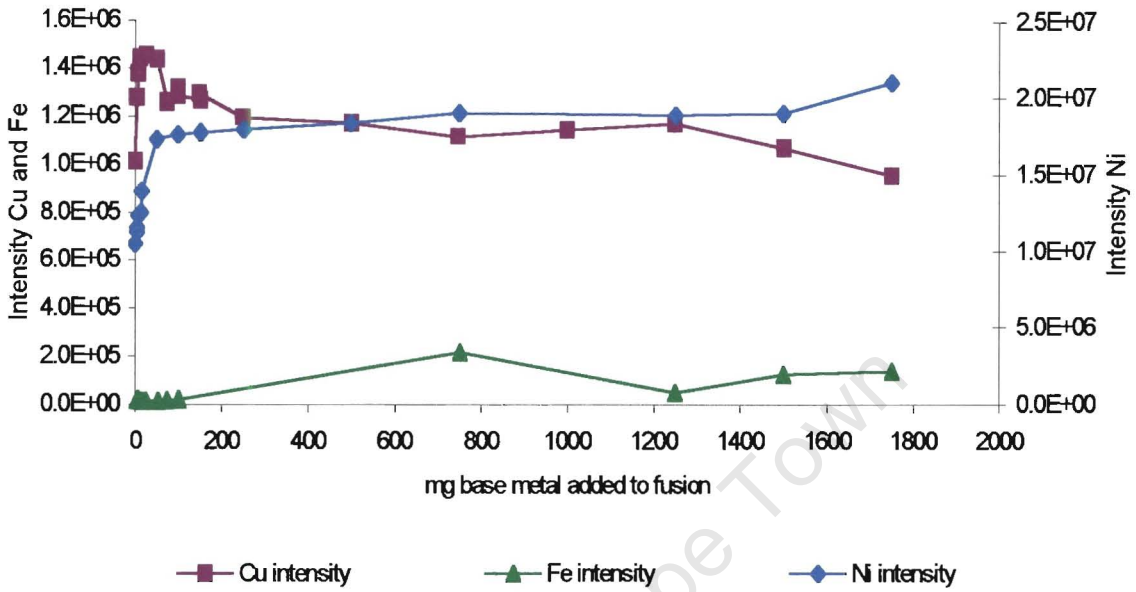

Fig.6.7. Co-collection of copper, nickel and iron with noble metals in lead during fusion.

There appears to be a rapid increase in the SAFT intensities when adding between zero and 200mg of metal, after which a levelling takes place. These intensities correspond to the concentration of base metals which are collected in the lead. Thus during the fusion process base metals may be collected to a certain limit after which no more is tolerated and the excess goes to the slag.

It was calculated that copper was almost entirely collected by lead for up to 25mg addition of pure copper to the flux. This corresponds to approximately 620ppm($^m/_m$) in the lead button taking into account that which will also have been naturally present in the ore sample itself. Similar trends for nickel addition were obtained, although the level of tolerance of nickel in lead was found to be considerably reduced. There was an increase in collection of nickel by lead where up to about 50mg had been added to the flux. Since there was a possible 2800ppm($^m/_m$) nickel which could potentially have been collected from the ore sample alone, most of the nickel must therefore end up in the slag. The tolerance of added nickel in lead was measured to be less than 350ppm($^m/_m$). It could be argued that when pure nickel was added to the flux in order to study its collection in lead, erroneous conclusions could be drawn because the nature and composition of the nickel ore in the sample may result in a different collection mechanism with the flux components compared to pure nickel metal during the fusion process.

From Fig.6.7 it is clear that virtually no additional iron is collected by the lead. The maximum amount of iron already present in the lead is presumably from the sample.

6.3.2. Effects of physical hardness of lead.

It could be postulated that the depth of penetration of the spark into a lead button containing different base metals could be influenced by the concentration of these metals. For example, pure lead could be expected to be

"softer" than an "alloy" of lead and nickel. Hence the SAFT spark characteristics could be affected to the extent where the emissions of the coexisting platinum, palladium and rhodium may be changed leading to erroneous concentrations of these analytes.

In order to prove or disprove this, an investigation into the relative hardness of lead samples containing separate amounts of copper, nickel and iron was carried out using Vickers' method. As can be seen in Fig.6.8, pure lead was found to be relatively softer than lead containing copper, nickel or iron. Copper appeared to impart the most hardening effect of the lead. Within the depth of each button type there was no significant change in hardness implying that the lead samples were fairly homogeneous.

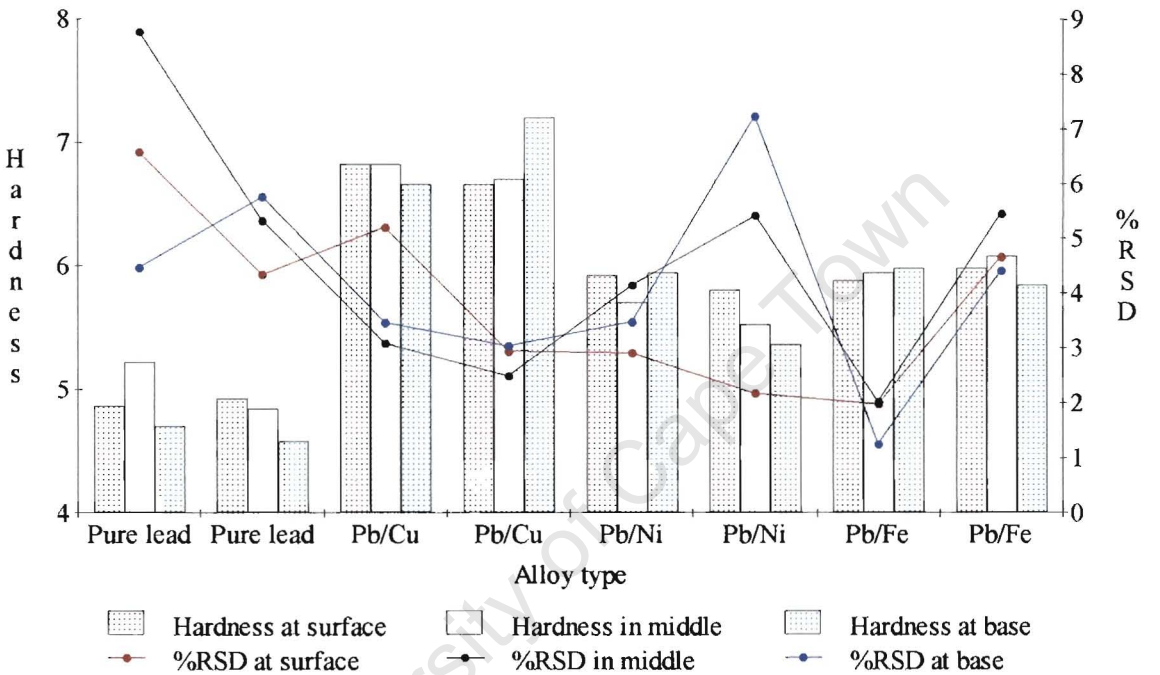

Fig.6.8. Hardness and precision of hardness measurements of lead when alloyed with copper, nickel and iron.

Clearly if uniquely different amounts of base metals were collected in lead from different sample types, the lead buttons obtained from real samples would therefore differ in hardness quality due to the effect caused by each base metal. Whether the combined effect on hardness would be significant was not established. Instead, each lead button was sparked using SAFT and the emission data for each base metal was correlated with the hardness of the lead. The results are shown in Fig.6.9, 6.10 and 6.11.

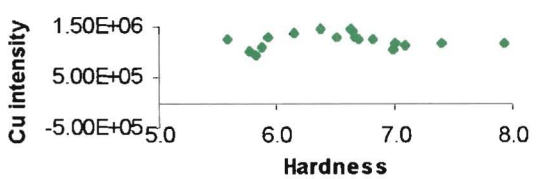

Fig.6.9 Hardness of lead containing copper.

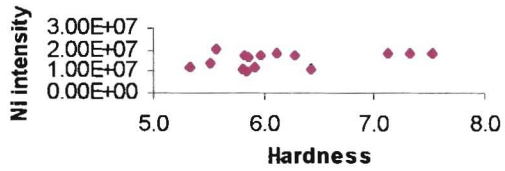

Fig.6.10. Hardness of lead containing nickel.

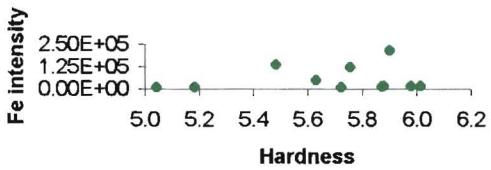

Fig.6.11. Hardness of lead containing iron.

No clear trends are evident and therefore since the lead does not really collect any more copper, nickel and iron it is essentially already "saturated" with these metals so trends cannot be expected.

There is however an effect on the platinum, palladium and rhodium SAFT intensities. The overall effect of increasing hardness of lead due to the combined presence of copper, nickel and iron was an apparent reduction in concentrations of platinum, palladium and rhodium (Fig.6.12) which is derived from relative intensity ratios where the calibration is from samples with unknown base metal content.

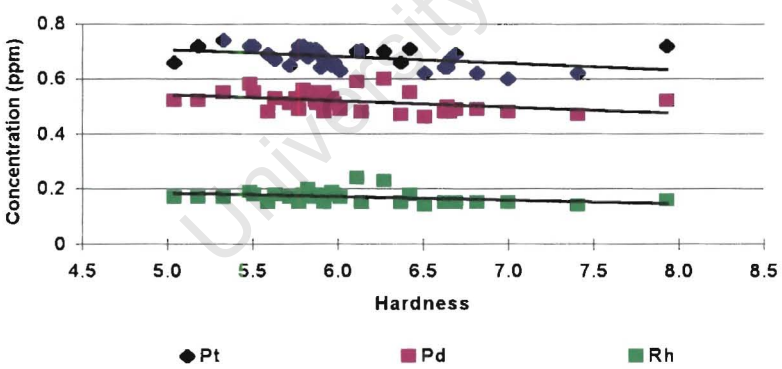

Fig.6.12. The effect of changing hardness of the lead samples on the concentrations of platinum, palladium and rhodium.

Since the SAFT technique uses the raw intensity of lead as a compensation for drift, it could be possible that as the base metal content increases in the lead the buttons become harder and this causes the lead emission intensity to be depressed more than the platinum, palladium, rhodium, copper, nickel or iron intensities, so resulting in wrong concentrations of platinum, palladium and rhodium.

It could also be possible that the degree of hardness influences the quantity of volatilised material immediately after the SAFT spark, implying that the harder the lead the less material will be atomised. The fact that the

atom cloud after the SAFT spark may contain different quantities of copper, nickel and iron could result in a change to the emission characteristics of platinum, palladium and rhodium.

6.4. Examination of lead buttons using an electron microbeam technique.

Electron beam techniques may be used to determine if noble metals are present as discrete particles or in solid solution in a specific phase using characteristic x-rays excited in the particle for qualitative and quantitative analysis, and secondary electrons and backscattered electrons for imaging purposes. Such methods of analysis are electron microscope techniques, and electron microprobe methods such as microprobe x-ray fluorescence (MXRF) and proton induced x-ray excitation (PIXE).[3] The electron microprobe methods are susceptible to errors due to relatively poor sensitivity and high background emissions where x-rays are used. Hence the noble metals that are present in lead buttons resulting from the fusion of platinum based ore samples were best determined qualitatively using scanning electron microscopy. In this respect references to scientific investigations could not be found concerning microscopic examination of lead buttons obtained from pyrochemical fusions.

Electron microscopes have a source that emits electrons that strike the specimen and create a magnified image. Magnetic "lenses" that create magnetic fields are used to direct and focus the electrons. A vacuum system ensures that electrons are not scattered by air molecules. A scanning electron microscope (SEM) creates a magnified image of the surface of an object. The SEM scans the sample by passing a tightly focussed electron beam over the sample surface which may be scattered directly off the sample or cause secondary electrons to be emitted from the surface of the sample. These scattered or secondary electrons are collected and counted by an electronic device located to the side of the sample. As the electron beam scans over the entire sample, a complete image of the sample is displayed on the monitor. Scanning electron microscopes can magnify objects 100 000 times or more. When an electron microscope is fitted with an x-ray spectrum analyser, the high energy characteristic x-rays that are emitted by the sample when it is bombarded by electrons may be used to identify different atoms or molecules providing information about the sample's chemical composition.

Special care must be exercised in sample preparation. A polished surface finish is required and the slightest degree of contamination can attenuate the intensities of the x-rays being detected. During the polishing process material from adjoining elements may be smeared on to the surface of the relevant particle and will be included in the analysis if not completely removed. Chemical polishing must be used with care as it can alter the composition of the sample surface.

Carbon build up can occur at the point of impingement of the electron beam on the sample surface owing to the breakdown of hydrocarbons in the vacuum of the instrument and thus attenuate the x-ray intensity. To prevent an electrostatic surface charge build up when exposed to the electron beam, a thin coating of carbon vacuum evaporated onto the sample surface prevents this problem.

The samples used in our investigation were lead buttons containing noble metals obtained by pyrochemically fusing various ore samples with a litharge based flux. The concentration of platinum was determined by SAFT spark to be approximately 5ppm($^{m}/_{m}$). Each button was then milled to expose a fresh surface and leached with dilute nitric acid (10 to 50%($^{v}/_{v}$)). After the surface was coated with a thin film of carbon, the button was ready to be studied using the electron microscope.

The morphology of lead ore samples indicated irregularly distributed darker areas over the button surface. Higher magnification at 2000 times showed that these dark areas consisted of clusters of tubular particles. Magnification at 5000 times resolved the area and the tubular particles were found to be randomly scattered within smaller crystals. See Photographs 1 and 2. Scanning these tubular particles using x-radiation determined the presence of nickel and copper interspersed in a lead matrix. There was also evidence of platinum as shown in the x-ray emission spectrum in Figure 6.13. When an area that had been sparked was studied, the lead did

not exhibit crystalline structure and Photograph 3 clearly indicates the change in lead form. But, there was still evidence under magnification of 10 000 times of small crystals in the craters even after the lead was exposed to extreme spark temperatures (Photograph 4).

Photograph 1. Electron micrograph of nickel and copper dispersed in lead at 2000 magnification.

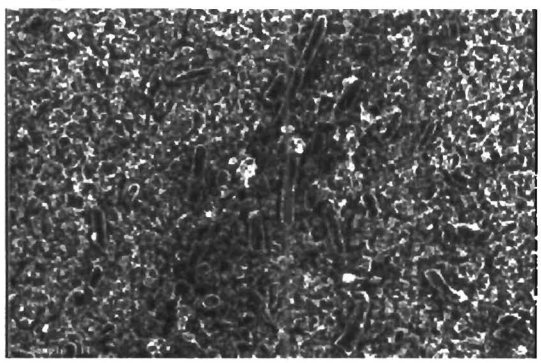

Photograph 2. Electron micrograph of nickel and copper dispersed in lead at 5000 magnification.

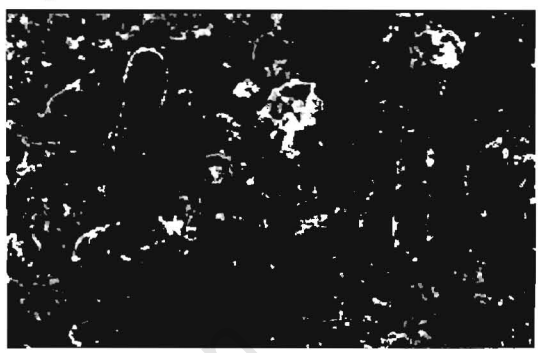

Photograph 3. Electron micrograph of area of lead that has been subjected to spark discharge. Magnification is 1000 times.

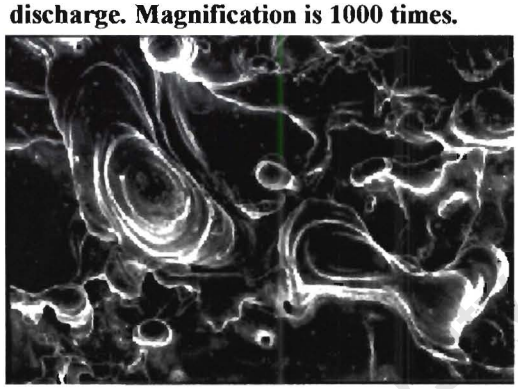

Photograph 4. Electron micrograph of crystal impurities in lead in area of spark discharge at magnification of 10.

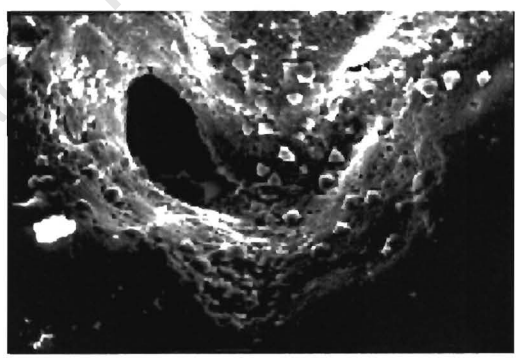

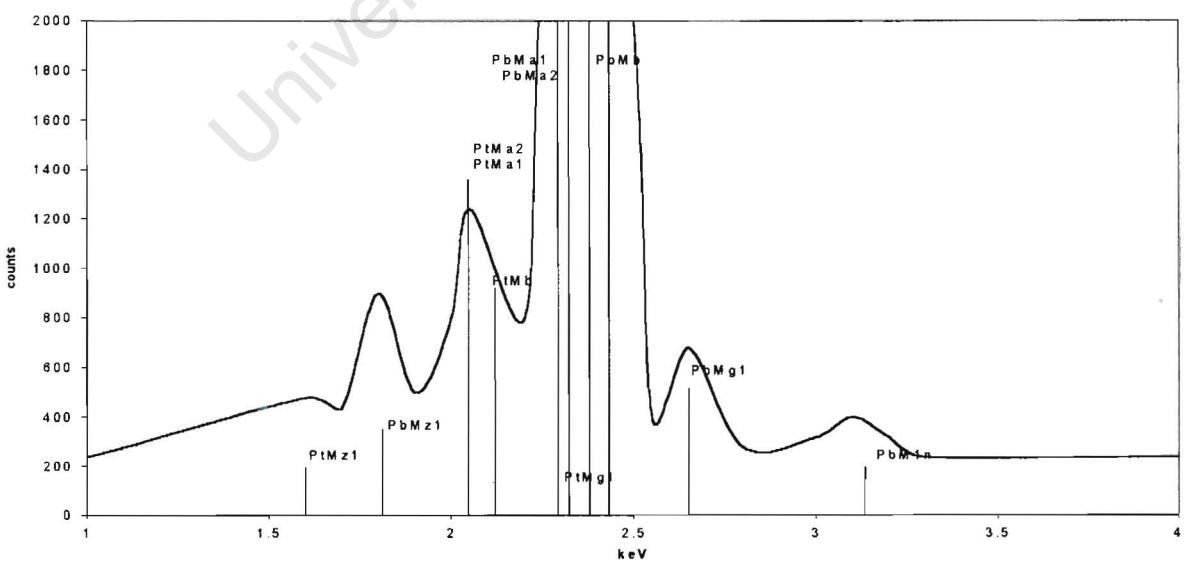

Fig.6.13. Section of x-ray spectrum showing trace levels of platinum in lead samples.

Photograph 5. Electron micrograph of occlusions in lead at 500 magnification obtained by fusing a different ore type.

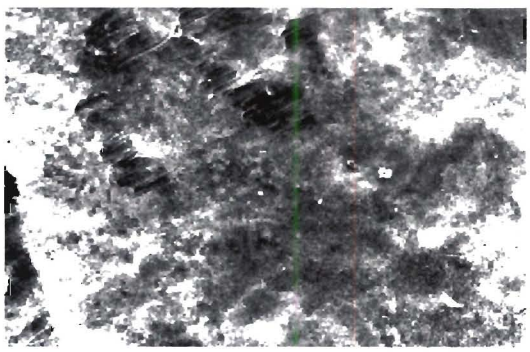

Photograph 6. Electron micrograph at magnification 6000 times of occlusions in lead as shown in Photograph 5.

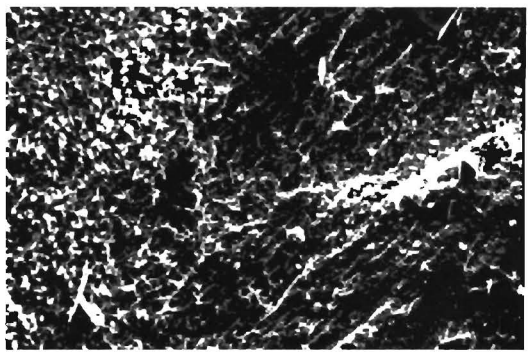

It was not possible to identify crystallites of platinum in any of the prepared lead buttons which was probably due to the low concentration of platinum in the lead. Nevertheless base metals could be detected and were non-homogeneously distributed.

A lead button obtained from fusing a different ore was examined. Similar rod-like structures were determined in the lead and were identified as nickel. Curiously no copper was identified. Either the particles of copper were not present at that particular area which was scanned, or alternatively there was insufficient copper to enable it to be detected. Photographs 5 and 6 depict the structure of occlusions at magnifications of 500 and 6000 times.

A comparison was made of the appearance of the lead obtained from the litharge fusion without the ore sample, and pure lead purchased as such and melted into a disc. It was found that the lead obtained from the fusion differed remarkably from the pure lead. The latter was evenly spread showing only mill contours. The lead extracted via the fusion was distributed as granular particles in the mass. It appeared that the acid treatment had possibly etched away grooves between each grain exposing distinct particles. The effect can be seen in Photographs 7 to 10.

Photograph 7. Electron micrograph of pure lead at 500 times magnification.

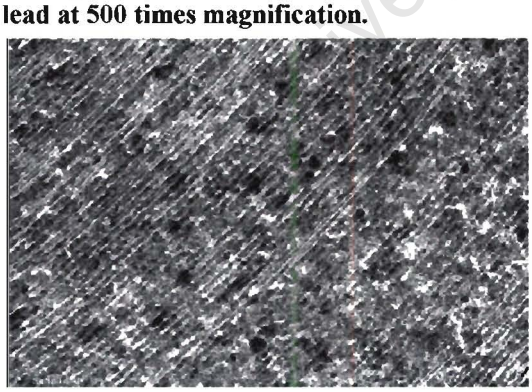

Photograph 8. Electron micrograph of pure lead at 2000 times magnification.

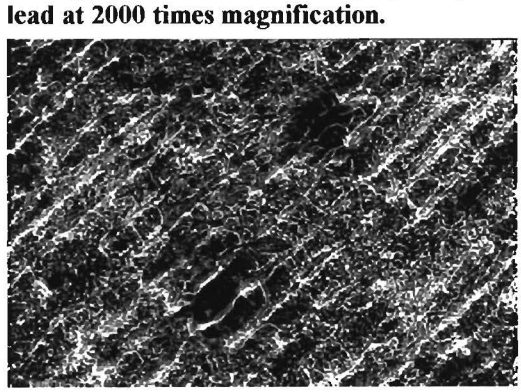

Photograph 9. Electron micrograph at 500 times magnification of lead from assay fusion of a litharge-based flux without ore .

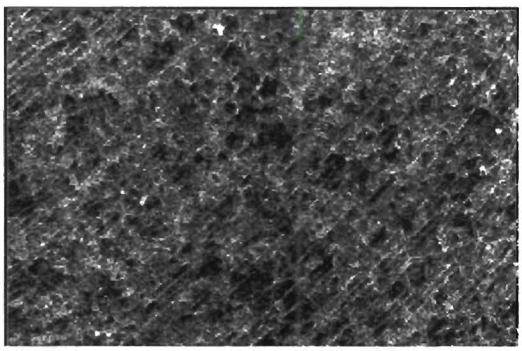

Photograph 10. Electron micrograph of Photograph 9 at 2000 times magnification.

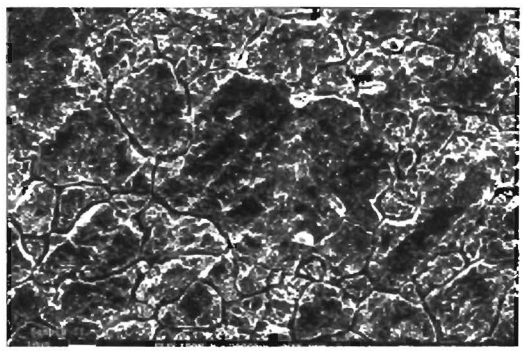

A lead disc that was considered to be of poor quality due to incomplete fusion was studied, the purpose being to indicate the effect on lead reduction and subsequent button formation when the sample preparation was not carried out optimally. The button surface had fractures which when magnified exposed large crystalline structures in a mass of small crystals and rod-like crystals. The large crystals were identified as being composed of chromium and oxygen, possibly originating from the mineralogical chrome in the sample. The phenomenon can be seen in Photographs 11 and 12. With good sample preparation techniques elements such as chromium would have been expected to go to the slag and not be retained by the lead.

Photograph 11. A lead button at 70 times magnification showing the typical surface characteristics resulting from the poor assay fusion of an ore sample.

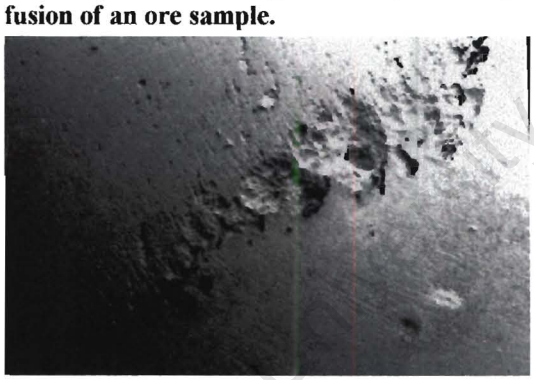

Photograph 12. Electron micrograph showing large crystalline structures occluded in lead obtained from a poor assay fusion of an ore sample. Magnification is at 2000 times.

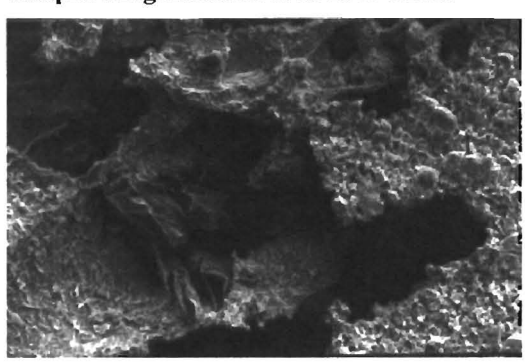

An independent investigation by C.C. Hamilton into the quality of the lead in question using electron microscope techniques was carried out.[4] It was recorded that there were no gross discernible differences between lead obtained from a Merensky and a UG2 ore sample. However, detailed microscopic inspection of the polished surface of the UG2 sample revealed extremely fine areas that were erratically distributed. The areas were ovoid in shape and comprised several sub-parallel, discontinuous veins between 3μm and 15μm in length and less than 1μm wide. Copper, and to a lesser extent chromium, were identified in these microscopic veinlets. This phenomenon was not observed in a button prepared from Merensky type ore. In Hamilton's opinion, the full extent and significance of the observed segregations were unresolved as it was unclear what the effect of the sample preparation such as lead smearing was on the microstructure. But if there may have been possible preparation problems, copper and chromium were a real inherent feature. Hamilton states that although the exact nature of the chromium was unresolvable due to the limitations of the microscope resolution and feature

size, it was possible that in whatever form chromium may act as a site for nucleation of a copper rich component with possible concurrent noble metal enrichment. The evidence for this was shown in the UG2 ore type button where the microstructural features may represent segregation products. Hamilton suggested if a significant elemental partitioning accompanies copper segregation, erratic noble metal distribution may result.

REFERENCES.

1. K.A. Slickers, "Reproducibilites for alloyed elements in Pb-base with the Spectrolab optical emission spectrometer", Application report No. 25/2, SPECTRO, Kleve, Germany.

2. G. Harrison, "Massachusetts Institute of Technology Wavelength Tables with intensities in arc, spark, or discharge tube of more than 100, 000 spectrum lines", 1969 edition, M.I.T., Cambridge, Massachusetts and London, 1969.

3. J.M. Cowley, "Electron Microscopy", *Analytical Chemistry*, Vol.54, No.5, 1982.

4. Confidential report, "A mineralogical investigation of two SAFT lead-collection buttons", Gencor Laboratories, DL1631, Johannesburg, 1994.

CONCLUSION.

Several problems were experienced with the analysis of platinum, palladium, and rhodium at trace levels in lead from ore tailing samples when measured by SAFT.

Our investigations have shown that the background emissions for platinum are too high to be able to determine platinum at trace levels in the lead matrix, since the ratio of the platinum atomic emission signal to the background emission is unacceptably low. The SAFT technique is thus inherently insensitive for platinum analysis in lead buttons, so that reliable calibrations cannot at present be prepared.

The five platinum emission wavelengths that were investigated revealed that the most sensitive platinum emission at wavelength 306.47nm experienced a nickel emission interference. Since nickel was found to be present in all lead samples prepared from mining ores, measurement of platinum emissions at this wavelength was useless since attempts at correcting for the interference failed because suitable matrix matched standards could not be prepared and the nickel was not quantitatively extracted into the lead.

SAFT calibrations for platinum at 265.87nm, 299.967nm, 531.93nm and 598.81nm were unfortunately not successful, partly as a result of the poor signal to background ratios, but also because these emissions were found to be extremely sensitive to changes in the matrix of the lead samples. These changes were directly related to the type of ore sample used in the preparation of the lead samples using the fire assay collection technique.

Palladium and rhodium emissions at 340.46nm and 343.49nm respectively were found to give relatively high atomic emission sensitivity and low background emissions with no spectral interferences from coexisting base metals. Nevertheless at trace levels, the SAFT calibrations for palladium and rhodium were far from ideal, with both element assays also being affected by changes in the matrix of the lead due to the type of sample used to prepare the lead buttons.

Finally this study illustrates an important point. A promising technique developed using synthetic standards prepared from precious metals and lead, can sometimes fail to be useful if subject to severe matrix effects due to sample variation, as was found for real ore tailing and other samples collected in lead. Neglect of such effects can lead to expensive inaccuracies, and bring a technique into serious disrepute.

The SAFT technique for platinum, palladium and rhodium as applied to lead button collection in its present form is not easily applicable, particularly for low levels of platinum in real ore samples.

Suggestions for further work.

1. Use of an internal standard to use as a ratio element with similar characteristics to the PGM's.
2. Other fusion methods to eliminate or reduce uptake of base metals.
3. Automation of techniques to provide better control of the fusion process and possibly make the interferences constant.
4. Improve spark technology to provide a more definite cut-off of the current flow. This would enable a more accurate switching of the "seeing time" of the photomultiplier. It could improve signal to background.

APPENDIX 1.

EXPERIMENTAL DETAILS OF SAMPLE PREPARATION FOR PLATINUM GROUP METALS ANALYSIS.

The following is an account of the experimental details of the methods of sample preparation used to determine platinum group metals as PGM, and the individual metals platinum, palladium and rhodium, for the purpose of this research.

1. Experimental details of preparation of calibration standards for SAFT analysis of platinum, palladium and rhodium in lead samples.

1.1. Sample preparation for determination of platinum, palladium and rhodium in lead using fire assay as the collection medium and SAFT spectroscopy.

Sample aliquots added to flux :

	Merensky	UG2
Concentrate	5g	2g or 5g
Feed	125g	125g
Tailings	200g	150g

Flux components per charge for fusion of tailing samples:

Litharge	74.7g
Sodium carbonate	150g
Silica	37g
Charcoal	2.2g
Borax	112g

An aliquot of powdered sample is accurately weighed and mixed thoroughly with a preweighed amount of litharge based flux. The mixture is put into a large fireclay crucible. This is loaded into a furnace at 1100°C. At this temperature the mixture melts and the sample components react with the flux chemicals pyrochemically. The chemical reaction which may occur between the sample and the flux chemicals during the fusion process can be found in Appendix 1, Section 2. The noble metals are collected by tiny globules of lead which form from reduction of litharge by the acidic portion of the mixture. The gangue of the sample also reacts with the flux and reports to the slag which lies as a lighter phase above the molten lead. The crucible is removed from the furnace after 55 minutes and the melt poured into an iron mould. The phases separate so that the slag floats above the lead. The mould is allowed to cool during which time the contents solidify. The cone shaped core is tipped from the mould, and the lead separated from the slag by hammering the interface of the two phases. The bulk of the slag is discarded and the small amount of residual slag adhering to the lead is removed by rotating and vibrating the lead button in a steel container with two small steel balls for about 10 seconds. The "clean" button is then weighed to enable the dilution factor to be calculated. The button must then be melted at 625°C to 700°C (depending on the type of ore being analysed) and poured into a copper cooling mould to produce a solid disc of diameter either 35mm or 42mm, the size depending on the mass of the lead button. The surface of the resultant disc (also referred to as a button) is then cut with a lathe to give a smooth horizontal finish. The button may be measured using spark emission and SAFT for platinum, palladium and rhodium.

200g of ore tailing sample is the maximum quantity that may be added to the flux without noble metal losses either to the slag or spilling out of the crucible during fusion.

Merensky and UG2 ore tailing samples were fluxed in the same flux type even though they are of different composition. The reason for this is that the traditional fire assay method of analysis (Appendix 1, Section 1.3) where prills are obtained as the measured quantity has been used historically on the assumption that the pyrochemical reactions which occur during the lead collection are not affected by the slightly different ore compositions since problems were not experienced with prill formation and PGM recovery for either type of ore.

1.2. Preparation of ore tailing calibration standards for determination of platinum, palladium and rhodium using SAFT spark emission spectroscopy.

1.2.1. Standards from ore tailing samples.

Merensky and UG2 ore tailings samples were selected for calibration of the SAFT emission spectrometers for determination of platinum, palladium and rhodium. The concentrations of these metals was determined using the nickel sulfide technique. Selection of individual samples was made for as wide a concentration range as possible.

For the preparation for SAFT calibration standards, 200g each of Merensky and MF ore tailing samples, and 150g of UG2 tailing samples were weighed and fluxed to produce lead buttons. Residual slag adhering to the lead was removed and the button mass obtained. The buttons were then remelted and cast into disc shape, and one of the faces was cut with a lathe to give a finished surface suitable for spark analysis. Each button was sparked to obtain the SAFT emissions for the precious metals of concern. The concentration values obtained from the nickel sulfide method were used to calculate the concentration of platinum, palladium and rhodium in the lead buttons. Sixty buttons were prepared from thirty flotation tail samples in this way. Hence the emission data and the concentrations for each lead button may be paired and a calibration prepared.

1.2.2. Standards from addition of PGM material to ore tailing samples.

In order to extend the calibration range the method of standard additions was used. Merensky and UG2 ore tailing samples were mixed with

a) final concentrate , 0 to 4g in increasing amounts of one gram,
b) synthetic solutions containing platinum, palladium and rhodium, 0 to 300μg in increasing additions of 100μg.

Each ore sample plus the additive was mixed with a litharge-based flux and fused as described in Appendix 1, Section 1.1 to produce lead buttons for spark analysis. The concentration of the noble metals present in the lead was calculated from values determined using the nickel sulfide method of preparation.

A total of 95 buttons consisting of samples and standard addition samples were each sparked in triplicate using the M5 spectrometer to obtain emission data for the calibration of platinum at wavelengths 299.967nm and 306.47nm, and palladium and rhodium at 340.46nm and 343.49nm respectively.

The same buttons were also sparked on the M7 spectrometer for platinum channels at the wavelengths 299.967nm, 531.93nm, 265.87nm, and 598.81nm. The 599.81nm line is the second order wavelength of platinum 299.967nm, and 531.93nm is the second order wavelength of platinum 265.87nm. Palladium and rhodium wavelengths on the M7 were the same as those on the M5. Lead was measured at 322.05nm. The emission data obtained was converted to ratio intensities by dividing the intensity of the noble metal by the intensity of the lead obtained simultaneously at the plasma directly after the spark for the duration of the SAFT measurement time. The ratio intensities were paired with the calculated noble metal concentrations present in the lead buttons to obtain a calibration.

The details of statistical calculations performed for calibration and related information is explained in Appendix 3.

1.3. Sample preparation for the determination of PGM using the fire assay lead collection method.

Sample aliquots added to flux :

	Merensky	UG2
Concentrate	5g	5g
Feed	125g	125g
Tailings	2 x 150g	2 x 150g

Flux components per charge for fusion of tailing samples:

Litharge	74.7g
Sodium carbonate	150g
Silica	37g
Charcoal	2.2g
Borax	112g

The required mass of sample is mixed thoroughly with flux in a fire assay crucible in the same way as for the SAFT preparation and 10mg of silver as silver nitrate solution is added. The contents of the crucible are fused under the sane conditions as described for the SAFT preparation. Once the button is obtained from the fusion, the bulk slag is removed and the lead button hammered into a square while removing residual slag. The PGM is separated from the lead by low temperature cupellation at 1000°C, the lead being absorbed as lead oxide into the refractory cupel matrix. The resultant prill is then treated by high temperature cupellation at 1360°C for 6 hours during which time three lead washes are made two hourly. This allows residual lead and other impurities such as silver to be separated by volatilisation or absorption into the cupel. The final prill is cleaned and weighed in micrograms. The prill mass is related to the mass of powdered sample originally weighed into the flux to obtain the grade of the PGM of the ore in gram per tonne or parts per million.

Tailing samples contain trace concentrations of PGM that may be too small to weigh at the final prill stage. The error margin at below 40μg becomes too large for the required levels of accuracy for a PGM assay. As the mass of ore sample that can be added to the flux is at its maximum, in order to increase the size of the prill the ore sample is weighed in duplicate and the lead buttons obtained after fusion combined at the cupellation stage. Once the lead is removed, the size of the prill is effectively doubled and can be weighed accurately.

Silver is added to the flux in order to produce a low cupellation prill of a certain size which is easy to handle. The control of the cupellation process depends to a large extent on the experience of the worker to be able to see the colour changes which indicate when the prills are to be removed from the furnace. Consistent combined concentrations of PGM and silver are conducive to better control at the furnaces.

1.4. Sample preparation for the determination of platinum, palladium and rhodium using the nickel sulfide collection method of fire assay and inductively-coupled plasma atomic emission spectroscopy (ICP-AES).

Sample aliquots :

	Merensky and UG2
Concentrate	25g
Feed	200g
Tailings	2 x 200g (combine NiS buttons)

Flux components per charge for fusion of tailing samples:

	Primary fusion	Secondary fusion
Nickel carbonate	32g	7g
Sodium carbonate	67g	10g
Borax ($Na_2B_4O_7$)	135g	30g
Sulfur	12g	3g

The required mass of sample is mixed with the flux in a crucible and fused at 1100°C for 55 minutes. The melt is poured into an iron mould and after cooling the slag is detached from the nickel sulfide button. The button is reserved while the slag is refused with a second charge of flux resulting in a second smaller nickel sulfide button. This procedure is carried out in duplicate so that in the case of tailing samples there are four buttons that are weighed accurately. The combined mass is digested on a waterbath in 400ml of hydrochloric acid to which 10g of ammonium chloride as added. After digestion for 4 hours the residual gases are boiled off and the solution allowed to cool. It is then filtered through a 0.2μm cellulose acetate membrane so that the undissolved PGM residue is retained quantitatively. The residue is then transferred to a pyrex glass ampoule and 5ml of hydrochloric acid added. The acid is then frozen using solid carbon dioxide and about 0.5ml of chlorine is carefully added. The glass ampoule is then sealed and transferred to a steel pressure vessel. The digestion of the PGM residue takes place during the 16 hours it is subjected to the pressure which builds up at 170°C in a rotary furnace. The pressure vessel is allowed to cool before the ampoule is carefully removed. The content of the ampoule is frozen to reduce the pressure within. It is then opened with a glass-cutter and the solution washed into a beaker. After gentle heating to remove residual gases the cooled solution may be analysed for the individual metals by atomic emission spectroscopy. Calibration standards are prepared using solutions prepared from the pure metals and are matrix matched for acid content. The emission of nickel, copper, iron and chromium are monitored for spectral interferences of the platinum group metals, corrections being applied where necessary. All solutions also contain an internal correction standard to account for viscosity changes between solutions and any fluctuations caused by the radio frequency generator drift which may occur when using ICP-AES.

2. Chemical reactions occurring during litharge fusions.

As the ore samples are already in fine powder form, it can be weighed directly into the flux. The chemicals constituting the fluxes are litharge, sodium carbonate, silica, borax and charcoal. The reactions that occur are very complex because of the mineralogy of the samples. All references concerning chemical reactions taking place with ores are similar in theory.[1,2,3,4] A simple explanation follows outlining the purpose of each flux component.

2.1. Sodium carbonate.

Sodium carbonate is added to the flux because it readily forms alkali silicates. It is a powerful basic flux. In the presence of air some sulfates are formed, and is therefore considered an oxidising and desulfurising reagent.

Sulfates are produced more readily in the presence of an oxidising agent such as litharge.

$$FeS_2 + 7PbO + 2Na_2CO_3 \rightarrow FeO + 7\,Pb + 2Na_2SO_4 + 2CO_2$$

Sodium carbonate melts at 850°C and dissociates partially at 950°C liberating some free alkali and evolving carbon dioxide.

$$Na_2CO_3 + Na_2SiO_3 \rightarrow Na_4SiO_4 + CO_2$$

2.2. Silica.

Silica is a strongly acidic flux reagent. It reacts with metal oxides to form silicates, which are fundamental to most slags. Silica forms five different classes of silicate slag, classified according to the ratio of oxygen in the metal oxide (base) to oxygen in the silica (acid). A metasilicate slag is the most desirable with a ratio of 1:2 because of its stablility.

$$PbO + SiO_2 \rightarrow PbSiO_3$$

When there is a deficiency of silica in the sample, it must be added to the flux to produce a fluid slag and also to protect the crucible from corrosion of litharge and borax.

2.3. Borax.

Borax is a strongly acidic reagent and readily dissolves all metal oxides. Its rational formula, $Na_2O.2B2O_3$, indicates an excess of acid radical. The dissolution of metal oxides during the fusion process takes place in two stages. The borax melts first to form a viscous glass consisting of sodium metaborate and boric anhydride. It also lowers the fusion temperature of the slag appreciably as it melts at 741°C to form a glass.

$$Na_2B_4O_7 \rightarrow Na_2B_2O_4 + B_2O_3$$

Then the boric anhydride reacts with the metal oxide to form the metal borate. For example, copper will report to the slag by reacting with boric anhydride.

$$CuO + B_2O_3 \rightarrow CuB_2O_4$$

2.4. Litharge.

Litharge is a readily fusible basic flux reagent. Also it acts as an oxidising and desulfurising agent. It melts at 883°C and is reduced by the addition of the reductant charcoal providing the metallic lead which collects the noble metals.

2.5. Charcoal.

Carbon is an effective reductant. In the flux it reduces litharge to lead, with the evolution of carbon monoxide and carbon dioxide. Flour and charcoal may also be added to the flux as a carbon substitute.

$$PbO + C \rightarrow Pb + CO \text{ at high temperatures}$$

$$2PbO + C \rightarrow Pb + CO_2 \text{ at lower temperatures}$$

REFERENCES.

1. W.C. Lenehan and R. de L. Murray-Smith, "Assay and Analytical Practice in the South African Mining Industry", The South African Institute of Mining and Metallurgy, Johannesburg, 1986.

2. J. Lurie, "South African Geology for Mining, Metallurgical, Hydrological and Civil Engineering", 4th edition, McGraw-Hill, Johannesburg, 1984.

3. V.S. Dillon, "Assay Practice on the Witwatersrand", Transvaal and Orange Free State Chamber of Mines, Cape Town, 1955.

4. E.E. Bugbee, "A Textbook of Fire Assaying", John Wiley and Sons Inc., New York, 1940.

APPENDIX 2.

OPTIMISATION OF THE REMELT TEMPERATURE FOR PREPARATION OF LEAD SAMPLES FOR SAFT ANALYSIS.

Lead buttons obtained from the pyrochemical fusion of litharge and ore samples are cleaned of residual slag. After weighing the button to ascertain the dilution factor, the lead must be remelted and cast into a suitable form which can be presented to the spectrometer for spark discharge and SAFT analysis. The remelt stage is important since the final button must be homogeneous if a successful analysis is to be obtained.

Numerous buttons were prepared from the same tailing sample of Merensky and UG2 ores at different remelt temperatures and then sparked to obtain SAFT determinations for platinum, palladium and rhodium. The temperature range selected was between 600 °C and 700 °C. Temperatures outside of these limits proved to be either too cool to allow microscopic quantities of slag to float to the surface of the molten lead or too hot as there is risk of loss of lead through volatilisation. It also becomes more hazardous working at higher temperatures.

A plot of the concentrations of platinum, palladium and rhodium in the ore sample, thereby taking dilution into account, and the precision of SAFT measurements which indicates the homogeneity of the buttons for each remelt temperature was made. These are presented in Fig.1 to Fig.3 for Merensky ore tailing samples and Fig.4 to Fig.6 for UG2 ore samples.

In Merensky ore tailing samples, the SAFT emissions of platinum were closer to 0.49ppm($^{m}/_{m}$) more often, and the precision of SAFT measurements most reduced at the remelt temperature of 625 °C. The SAFT emissions of palladium and rhodium were not affected in the same way as platinum, and it would seem that a remelt at any temperature between 600 °C and 700 °C would produce a suitable analytical sample for analysis of palladium and rhodium.

In UG2 ore tailing samples, platinum emissions were more precise at the higher temperatures 675 °C to 700 °C. The emissions of palladium and rhodium were relatively unaffected by the remelt temperature with the precision measured as %RSD being less than about 2% in most test determinations.

Since all three elements are present together in a button it would thus probably be better to remelt Merensky ore tailing samples at 625 °C and UG2 ore tailing samples at 675 °C.

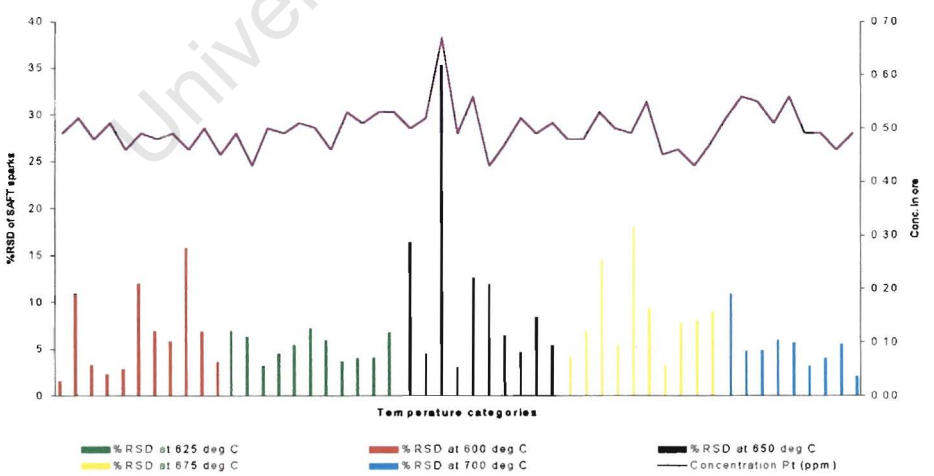

Fig.1. Lead samples of Merensky ore tailing samples remelted at different temperature to cast buttons which were analysed by SAFT for platinum.

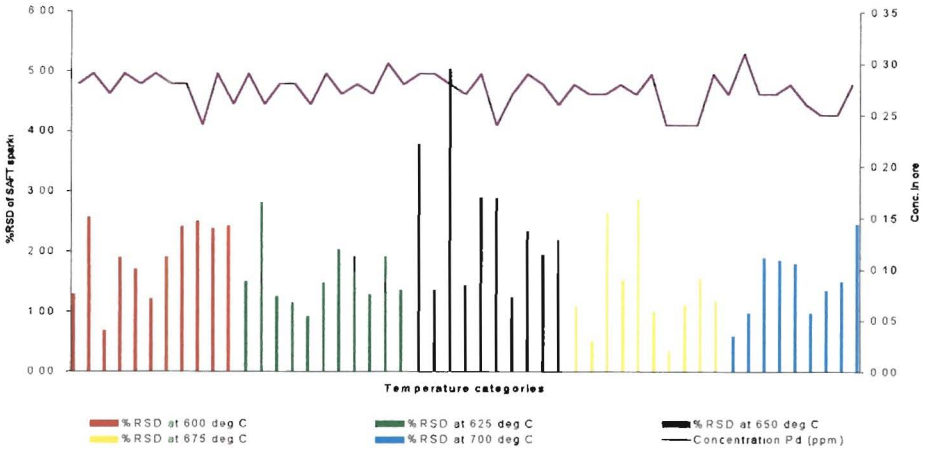

Fig.2. Lead samples of Merensky ore tailing samples remelted at different temperature to cast buttons which were analysed by SAFT for palladium.

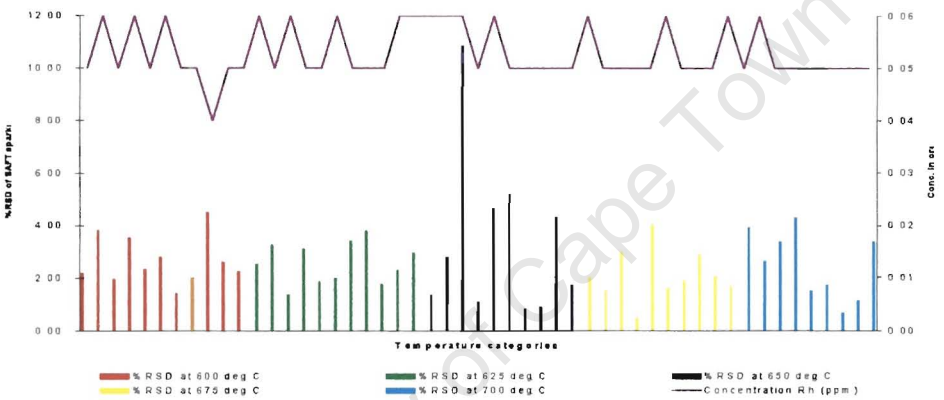

Fig.3. Lead samples of Merensky ore tailing samples remelted at different temperature to cast buttons which were analysed by SAFT for rhodium.

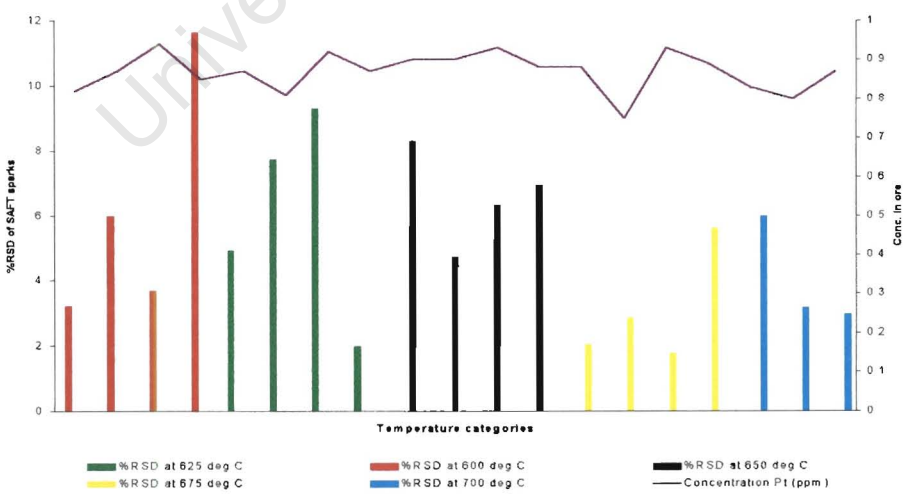

Fig.4. Lead samples of UG2 ore tailing samples remelted at different temperature to cast buttons which were analysed by SAFT for platinum.

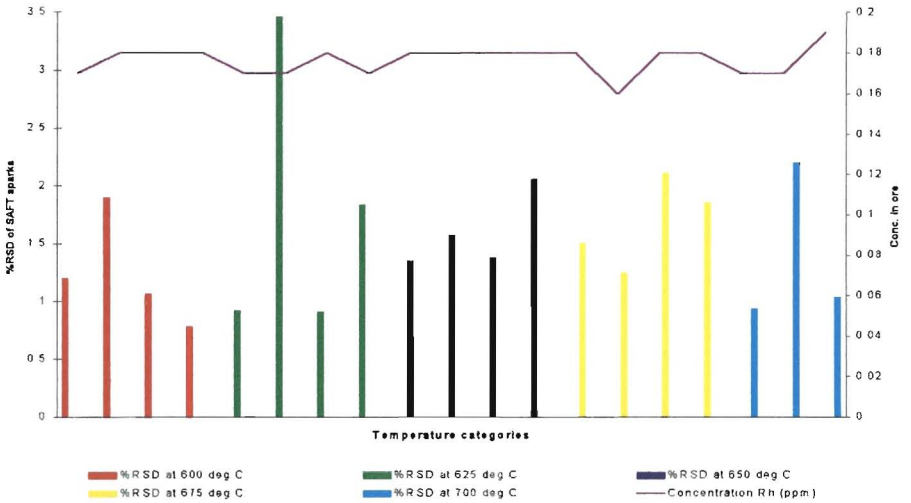

Fig.5. Lead samples of UG2 ore tailing samples remelted at different temperature to cast buttons which were analysed by SAFT for palladium.

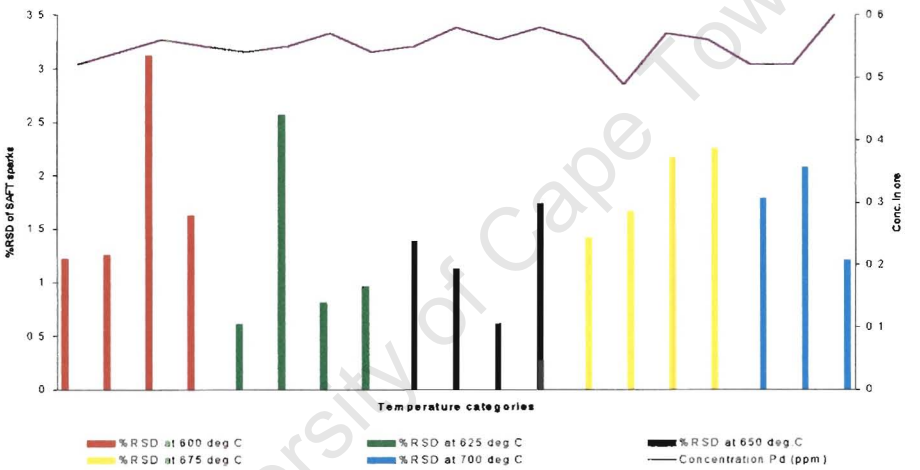

Fig.6. Lead samples of UG2 ore tailing samples remelted at different temperature to cast buttons which were analysed by SAFT for rhodium.

APPENDIX 3.

DEFINITION OF TERMS AND DETAILS OF REGRESSION ANALYSIS RELATED TO SAFT CALIBRATIONS.

1. Definition of terms.

1.1. Limit of detection.

1.1.1. Definition using the *International Union of Pure and Applied Chemistry method.*

The quantitative determination of the ability of an analytical method to determine low concentrations is termed limit of detection (LOD).

For the purpose of this thesis the following calculation was applied.

$$y_L = y_B + k\,s$$

y_L = lowest detectable instrument signal

y_B = blank signal

s_B = standard deviation of the blank signal

k = constant

Any sample yielding a signal $>y_L$ implies that the sample contains some analyte.

Any sample yielding a signal $<y_L$ implies that the sample contains no detectable analyte.

The constant k is at the discretion of the analyst, but is generally accepted as having a value of 3. This recommendation has been reinforced by the International Union of Pure and Applied Chemistry (IUPAC).[1]

Once y_L has been calculated, it is converted to concentrations, c_L.

$$c_L = \frac{k\,s_B}{b}$$ where b = slope of the graph.

1.1.2. Definition and calculations applied using the *Spectro* software.

The definition and calculations applied using the *Spectro* software, which is also explained by Slickers, is as follows.

The LOD is that equivalent concentration of the standard deviation s_0 of the precision of the spectral background.

$$LOD = 3 \times \sqrt{2} s_0$$

Slickers explains his reasons for using such a simple formula in considerable detail and refers to not only the precision of the spectral background, but also to parameters such as electrical resolution and relative standard deviation of individual spark discharges.

1.2. Background equivalent concentration.

Slickers explains that the background equivalent concentration (BEC) is the concentration in the sample which produces the same line intensity as the spectral background.

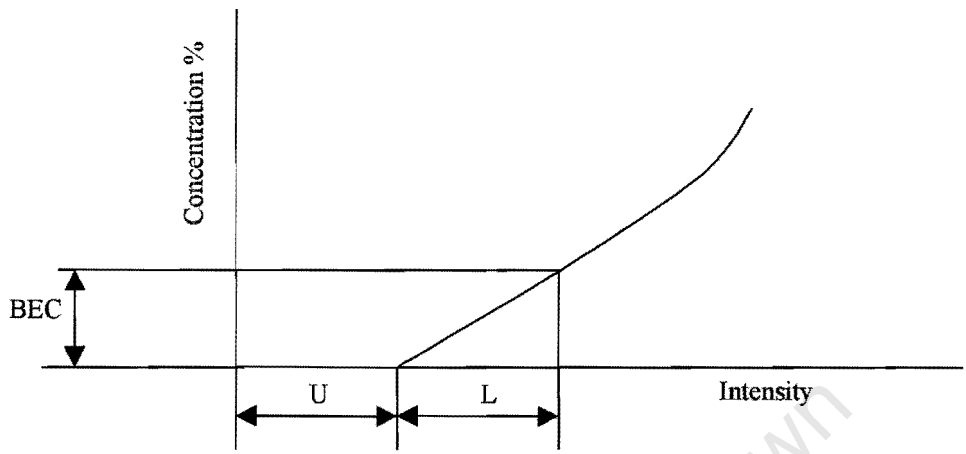

When the analyte concentration is zero, an intensity U which is the same as the spectral background, is already present. If U is doubled and plotted along the intensity axis (x) and this point (U + L) is projected on the concentration axis, the BEC is obtained.

1.3. Limit of detection and background equivalent concentration.

The relationship between the LOD and the BEC is described by Slickers as follows:

$$LOD = 3 \times RSD_0 \times BEC/100$$

where RSD_0 is the relative standard deviation of the blank as a percentage in terms of concentration.

1.4. Standard error.

Std. Err. is the abbreviated term used for standard error. This is defined by Slickers as SR and is a measure of analytical accuracy. To calculate SR, a plot is made of the concentrations against the intensities, then the sum of the squares of the deviations (Δ_i^2) of each data point is calculated such that these are at a minimum for the best fit calibration curve.

$$1\ SR = \pm \sqrt{\frac{\sum \Delta_i^2}{n - a}}$$

where a = 2 for a straight line, a = 3 for a second order curve, a = 4 for a third order curve, and n is the number of samples. Slickers has used ± 1 SR for the accuracy of the calibration which includes 67% of values.

Normally analytical accuracy is calculated using ± 2 SR where 96% of all values are used.

1.5. Calibration function.

The calibration function can be represented mathematically in various ways. A linear calibration function is expressed as

$$\text{Intensity} = f(c) = a_0 + a_1 c$$

A non linear calibration function is expressed as

$$\text{Intensity} = f(c) = a_0 + a_1 x + a_2 x^2 + a_3 x^3 + \ldots.$$

For the particular example above, f_0, f_1, f_2 are the factors used to describe the least squares fit second order polynomial equation. Depending on the relationship between the two variables $y = f(x)$ where y is the concentration and x is the measured value, the calibration function can be estimated by an nth degree equation of the form $y = a_0 + a_1 x + a_2 x^2 + a_3 x^3 + \ldots.$

1.6. Breakpoints.

The non-linear calibration function can be divided into support sections over the entire calibration range in which linear (polygons) or non linear (polynomial) functions can again be formulated. The extent to which the regression approaches the true course of any particular section of the curve is determined from the residual scatter.

1.7. Ratio intensity.

$$\text{Ratio intensity} = \frac{\text{intensity of analyte}}{\text{intensity of reference}} \times \text{typical intensity reference}$$

"Reference" indicates reference to lead analytical line.

2. Normalisation.

Spectro have used the term recalibration for the process more commonly known as normalisation. This is where an adjustment is made for the changing measured sensitivity within the spectrometer instead of creating regular new calibrations to ensure accurate analysis.

The recalibration samples are measured during the calibration of the spectrometer. The calibration samples are no longer required for analytical work, and the recalibration samples are measured to make a comparison between the actual and nominal states of the spectrometer. The nominal values of the recalibration samples are stored in a data file together with the latest data measured for the recalibration samples. Two samples are chosen with a high and a low concentration for a two point recalibration. The actual measured values are calculated back to the nominal state of the spectrometer from the factor which is the ratio of the nominal to actual values. An additional quality, the offset, shows changes in the zero point.

Nominal Low = (factor x Actual Low) + offset
Nominal High = (factor x Actual High) + offset

The factor and offset for each analysis channel are stored in the data file and are used to correct subsequent measured values with respect to the nominal state of the spectrometer.

Example of calculations for two point recalibration:

Element	Nominal Low	Actual Low	Nominal High	Actual High	Factor	Offset
Platinum	28785	26705	57656	54109	1.05	650
Palladium	38034	39670	135396	143239	0.940	741
Rhodium	60229	61566	194752	197803	0.987	-563

The formula for calculating the recalibrated intensity ratio from the measured intensity ratio is

Recalibrated intensity ratio = factor x Measured intensity ratio + offset

3. Conversion to concentration after normalisation.

To calculate the analyte concentration c, the recalibrated intensity ratio of the analysis channel (IR) is applied to the polynomial function

$$c = a_3 \times (IR)^3 + a_2 \times (IR)^2 + a_1 \times (IR) + a_0$$

where a_3, a_2, a_1 and a_0 are the coefficients of the third order polynomial function.

Working with linear series (polygon) gives the same results as the polynomial function. But for second and third order calibration curves, the quality of conversion to concentration depends on the number and location of support points. It is therefore recommended by Slickers that the polynomial function be used preferentially.

4. Regression analysis.

The approach that is used by K. Slickers which is applied using the *Spectro* software which operates with the SAFT spectrometer is different to the universally accepted method of representing spectrographic calibration data. Details of both techniques are described in the following sections.

4.1. The regression analyses performed for the purpose of this thesis.

Once the intensities have been generated by the SAFT analyses, these signals can be represented on the y axis of a calibration graph, with the standard concentrations on the x axis. In order to accommodate slight unevenness of the disc surface at which the spark strikes, the analyte intensity is ratioed to the simultaneously measured lead intensity. It is these ratios which are actually plotted against the concentrations.

The linearity of the calibration may be tested using the correlation coefficient, r.

$$r = \frac{\sum_i [(x_i - \bar{x}) (y_i - \bar{y})]}{\{ [\sum_i (x_i - \bar{x})^2] [\sum_i (y_i - \bar{y})^2] \}^{1/2}}$$

where $(x_1, y_1), (x_2, y_2) \ldots\ldots (x_i, y_i) \ldots\ldots (x_n, y_n)$ are the points on the graph.

$\bar{x}$ and $\bar{y}$ are the mean values of x_i , the concentrations, and y_i, the ratio intensities respectively.

The ideal spectrographic calibration would have the data pairs in a perfect linear relationship so that r = 1.

If r = 0 then the fit of the least squares is so poor that the knowledge of,x will not help in the prediction of y.

The strength of the linear relationship between the (x, y) observations can be tested. The deviations of the y values from the least squares line $\hat{y} = a + bx$ can provide information that can to a large extent explain the situation. A graphic representation of the residuals $y - \hat{y}$ against x enables a visual study of these deviations.

A linear plot may be generated using the unweighted method of least squares to obtain the best straight line. One assumes that all the errors occur in the y direction (namely instrument signals), that they are normally distributed, and that the variation in the y direction errors is the same at all values of x. The linear equation y = a + bx describes the relationship between the two variables x and y. The least squares method is described by $\hat{y} = a + bx$.

The slope b, and the intercept a, of the unweighted least squares line are found from

$$b = \frac{\sum_i [(x_i - \bar{x})(y_i - \bar{y})]}{\sum_i [(x_i - \bar{x})^2]}$$

$$a = \bar{y} - b\bar{x}$$

Once the slope has been determined, then the intercept may be calculated using the fact that the fitted line passes through the centroid ($\bar{x}$ and $\bar{y}$). Once a regression line has been established which has a good fit and this is confirmed by r being close to +1, the degree of deviation of the observed y values from the sample regression line must be established. This is defined by

$$s_{y/x} = \left[\frac{\sum_i (y_i - \hat{y})^2}{n - 2} \right]^{1/2}$$

The coefficient of determination R^2 provides an indication of how well the least squares curve fits the observed data, so that

$$R^2 = 1 - \frac{\sum_i (y_i - \hat{y})^2}{\sum_i (y_i - \bar{y})^2}$$

The correlation coefficient r which is a measure of the linear relationship between two variables x and y, is defined as

$$r = \frac{\sum_i [(x_i - \bar{x})(y_i - \bar{y})]}{\left[[\sum_i (x_i - \bar{x})^2][\sum_i (y_i - \bar{y})^2] \right]^{1/2}}$$

$$\text{or} \qquad r = \frac{bs_x}{s_y}$$

where s_x and s_y respectively represent the standard deviation of the x and y observations.

If we wish to calculate a 95% confidence interval for the intercept a, then

$$(a - t_{n-2,\,0.025} \times s_a ,\ a + t_{n-2,\,0.025} \times s_a)$$

applies where

$$s_a = s_{y/x} \left[\frac{\sum_i x_i^2}{n \sum_i (x_i - \bar{x})^2} \right]^{1/2}$$

We can also calculate a 95% confidence interval for the slope b, so that

$$(b - t_{n-2,\,0.025} \times s_b ,\ b + t_{n-2,\,0.025} \times s_b)$$

applies where

$$s_b = \frac{s_{y/x}}{\left[\sum_i (x_i - \bar{x})^2 \right]^{1/2}}$$

In order to calculate a confidence band for the regression line $\hat{y} = a + bx$, the 95% confidence interval for $a + bx$ in which x is specified is given by

$$(a + bx - t_{n-2,\,0.025} \times d_x ,\ a + bx + t_{n-2,\,0.025} \times d_x)$$

with d_x the observed deviation of $a + bx$, namely

$$d_x = s_{y/x} \left[\frac{1}{n} + \frac{(x - \bar{x})^2}{\Sigma [x^2 - 1/n (\Sigma x)^2]} \right]^{1/2}$$

The confidence interval for an x value results from the uncertainty in the measurement of the instrument signal, the y value, combined with the confidence interval for the regression line at that y value. The standard deviation s_x is given by

$$s_{x0} = \frac{s_{y/x}}{b} \left[\frac{1}{m} + \frac{1}{n} + \frac{(y_0 - \bar{y})^2}{b^2 \sum_i (x_i - \bar{x})^2} \right]^{1/2}$$

where n is the number of test sample observations. Typically a value for y may be obtained as the mean of m

observations of a test sample, rather than a single observation (n). The previous equation is only an approximation that is valid when the function g has a value less than about 0.05.

$$g = \frac{t^2}{\left[b \div \left[\frac{s_{y/x}^2}{\sum_i (x_i - x)^2} \right]^{1/2} \right]^2}$$

After s_{x0} has been calculated the 95% confidence limits for x_0 can be determined as

$$(x_0 - t_{n-2,\,0.025} \times s_{x0},\ x_0 + t_{n-2,\,0.025} \times s_{x0})$$

4.2. The regression analysis as generated by the *Spectro* software.

Slickers' approach to regression analysis is put into practice using *Spectro* software which drives the spectrometer. An example of a typical calibration follows. The intensity ratio of the analytical line to the reference line, in this example platinum and lead respectively, is plotted against the concentration ratio of the analyte to the reference. Since the platinum is present as microgram quantities in virtually 100% lead, the reference analyte concentration is taken as 1.

Name of programme	PB-BASE 2			Date 09/19/91 11:25
Channel	Pt s (299.80nm)			Polynomial
Reference	Pb s (322.05nm)			f_0 = -1.07180E-03
No. of samples	13			f_1 = 2.57571E-04
Matrix correction	N	B.E.C.	= 12.51 ppm	f_2 = 6.15092E-06
Relative min.	N	L.O.D.	= 0.416 ppm	
I.E. Corrections	N	Std.Err.	= 0.564 ppm	(.00005 - 2.00)

Breakpoints

Conc.	Ratio
.00004	3950
.00059	5675
.00177	7399
.00179	9123
.00245	10847
.00314	12572
.00358	13625

Sample	Weight	Ratio			Concentrations		Deviation	
	Raw	Corr.	Chem.	Corr.	Raw		Abs.	Rel.
*-RPB11	1	3725	3725	.00001	-0.000	-0.000	-.00004	-370 %
S-1	1	8613	8613	.00159	.00160	.00160	+.00001	+0.556 %
S-2	1	10002	10002	.00208	.00212	.00212	+.00004	+1.76 %
S-3	1	11275	11275	.00264	.00261	.00261	-.00003	-1.06 %
S-4	20	3854	3854	.00001	.00001	.00001	+.00000	+22.64 %
S-5	1	3984	3984	.00005	.00004	.00004	-.00001	-21.53 %
S-6	1	4478	4478	.00021	.00020	.00020	-.00000	-1.95 %
S-7	1	5464	5464	.00052	.00052	.00052	-.00000	-0.535 %
S-8	1	7062	7062	.00105	.00105	.00105	+.00000	+0.0830%
SARM 7 1	1	5797	5797	.00055	.00063	.00063	+.00007	+13.16 %
SARM 7 ½	1	4756	4756	.00027	.00029	.00029	+.00002	+7.78 %
SARM 7a	1	4749	4749	.00037	.00029	.00029	-.00008	-22.43 %
SARM 7c	1	4584	4584	.00037	.00024	.00024	-.00014	-36.32 %

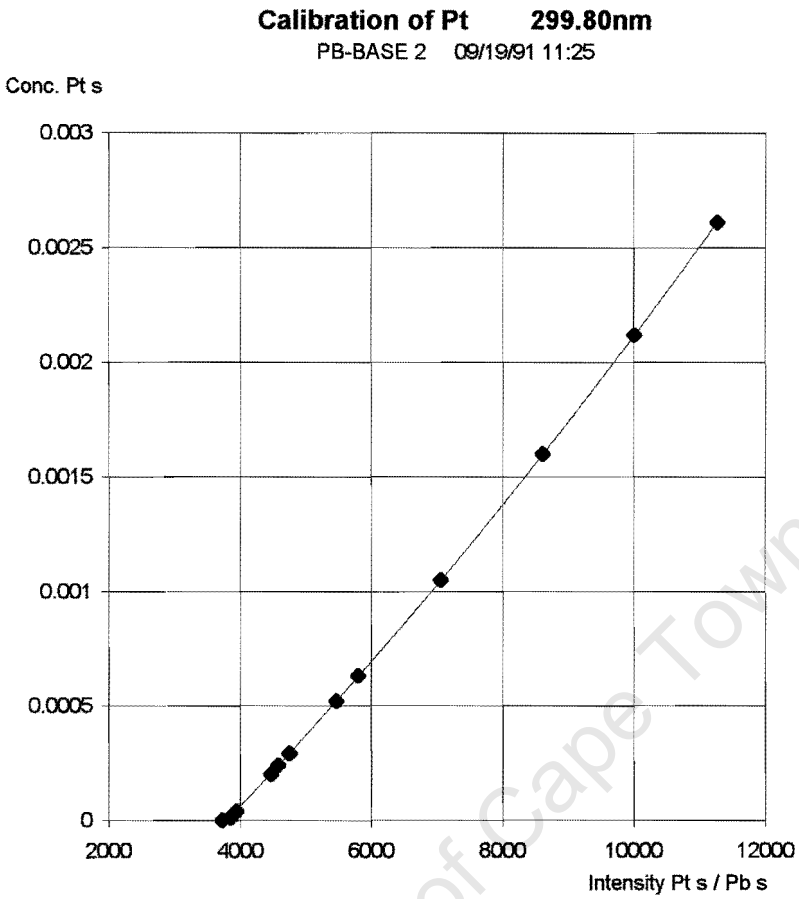

The approach taken by the instrument software is to plot the ratio intensities of the analyte versus the concentrations in the lead as a percentage. The ratio intensities are plotted on the y ordinate, while the concentrations are on the x ordinate.

REFERENCES.

1. IUPAC, Nomenclature, Symbols, Units and Their Usage in Spectrochemical Analysis - II, *Spectrochim, Acta*, Part B, 1978, 33, 242.

APPENDIX 4.

DETERMINATION OF NICKEL, COPPER AND IRON IN LEAD USING WET CHEMICAL DISSOLUTION AND ATOMIC SPECTROSCOPY.

1. Method.

The lead buttons obtained from fire assay collection of ore tailing samples that were measured by SAFT were drilled with a tungsten bit to produce small representative portions of lead in the form of drillings. Sub-samples were weighed (1g) accurately and dissolved in 1:1 nitric acid using gentle heat and the resultant solutions made to volume in 100ml flasks[1]. Appropriate standards containing a range of concentrations for nickel, copper and iron and matrix matched for 100%(^{m}/v) lead were prepared for measurement by atomic absorption spectroscopy using an air-acetylene flame to obtain calibration curves for each element[2]. The lead ore tailing samples were then measured and the atomic absorbances obtained converted to concentrations by interpolation of the calibration. Dilution correction was applied to obtain the concentration of nickel, copper and iron in the lead buttons for each fire assay collection of different ore tailing samples.

REFERENCES.

1. A.I. Vogel, "A Textbook of Quantitative Inorganic Analysis", 4th edition, Longmans, London, 1978.

2. Varian Techtron, "Analytical Methods for Flame Spectroscopy", Varian Techtron, Springvale, Australia, 1978.